UCRL-1680(Del.)

UNIVERSITY OF CALIFORNIA

Radiation Laboratory

Contract No. W-7405-eng-48

Photostat Price $ 1.80
Microfilm Price $ 6.30
Available from the
Office of Technical Services
Department of Commerce
Washington 25, D. C.

MTA QUARTERLY PROGRESS REPORT

September, October, November 1951

February 29, 1952

LEGAL NOTICE

This report was prepared as an account of Government sponsored work. Neither the United States, nor the Commission, nor any person acting on behalf of the Commission

A. Makes any warranty or representation, express or implied, with respect to the accuracy, completeness, or usefulness of the information contained in this report, or that the use of any information, apparatus, method, or process disclosed in this report may not infringe privately owned rights; or

B. Assumes any liabilities with respect to the use of, or for damages resulting from the use of any information, apparatus, method, or process disclosed in this report.

As used in the above, "person acting on behalf of the Commission" includes any employee or contractor of the Commission to the extent that such employee or contractor prepares, handles or distributes, or provides access to, any information pursuant to his employment or contract with the Commission.

Berkeley, California

270 001

TABLE OF CONTENTS

1.	Cavity Design	4
2.	X-ray and Sparking Tests in a Mercury Pumped System	7
3.	X-ray Monitored Vacuum RF Sparks	15
4.	D-C Drain and Breakdown Phenomena for Uncutgassed Metals	22
5.	Ion Pump Development	52
6.	Mark I Injector	70
7.	Injector Electrical Equipment	75
8.	High Frequency Program	76
9.	Mark I Electronics Studies	78
10.	Drift Tube Magnet Tests	79
11.	M.T.A. Mechanical Design	81
13.	A-12 Target and Lattice Development	90
	Target Design	91
	Target Development	92
	Materials Research	94
	Target and Lattice Calculations	99
	Nuclear and Engineering Physics	101
	Calculation of Target Neutron Leakage	104
	Calculation of Internal Neutron Flux Distribution for Solid Uranium Target	104
	Nuclear Chemistry	106
	Fission and Capture in Mark II Targets	106
	Isotopic Composition of Product in Primary and Secondary Targets	107
	Fission Yields as a Function of Neutron Energy	108
	Deuteron Produced Activities in Coolants	109
	Diffusion and Corrosion Introduced Activities	109
	Instrumentation	110
14.	MTA Chemical Processing	117
	Process Research	117
	Process Development	119
	Process Design	121
15.	Theoretical Studies	125
16.	Electron Model Thomas Cyclotron	127
17.	20-inch Cyclotron Project	132

276 -2

DECLASSIFIED

1. CAVITY DESIGN

S. W. Kitchen
UCRL

As previously reported, methods for improving accelerator efficiency were being considered. One of these methods made use of acceleration on every half cycle, obtained by inserting diaphragms for cell isolation and feeding power to successive cells 180° out of phase. The other method was to change the drift tube contour from a thick cylinder to a thin one with a bulge in the middle to contain the magnet. For a 1500 foot accelerator operating at 12.1 mc/sec with optimum cavity diameter, the calculated rf skin losses are as follows.

RF Skin Loss for Optimum Cavity Shape

	"Normal" Thick Cylinders	Diaphragms Thick Cylinders	Bulbous Pipes
350 Mev	54 Mev	47 Mev	40 Mev
600 Mev	200	110	100

Furthermore, when the bulbous pipes were fitted for a final energy of 350 Mev to a cavity shape which had been prepared for and which had undergone engineering studies by CRD (See UCRL-1252), the increase in power consumption was only two megawatts. This data led to the adoption of bulbous pipes for the drift tube shape.

The decision to use bulbous pipes enabled the cavity contour, which had previously been indeterminate in total length and diameter for the first two hundred feet, to be completely specified. (See Fig. 1). It also required that detailed resonance and transit time coupling factors be determined for the new drift tube shape as a basis for the final drift tube table. These measurements are being made.

Since gap-splitters or "washers" will be placed in mid-gap for several reasons, including fine tuning adjustment, a study of the effectiveness of gap splitter tuning along the design curve of A-12 was made. The results are shown in Fig. 2. Because 0.1 percent accuracy in the resonance field maps is desired, a similar study of the frequency perturbing effect of the insertion of the gap-splitters and of drift tube and gap splitter support stems was made. The insertion of the gap splitters in the gap causes a decrease of over one-percent in frequency at low β's with no perceptible effect at high β's. The drift tube stems have no effect at low β's but at high β's increase the frequency by almost one percent. The gap splitter stems have no perceptible effect at any point. As a result, the new resonance data being obtained includes the effects of both the gap splitters and the drift tube stems.

During this period the cavity design group consisted of D. B. Cummings, B. V. Hill, S. W. Kitchen, J. Levinthal, D. Moore, A. D. Schelberg, A. J. Schwemin, R. G. Smits and S. P. Stone.

276 293

DECLASSIFIED

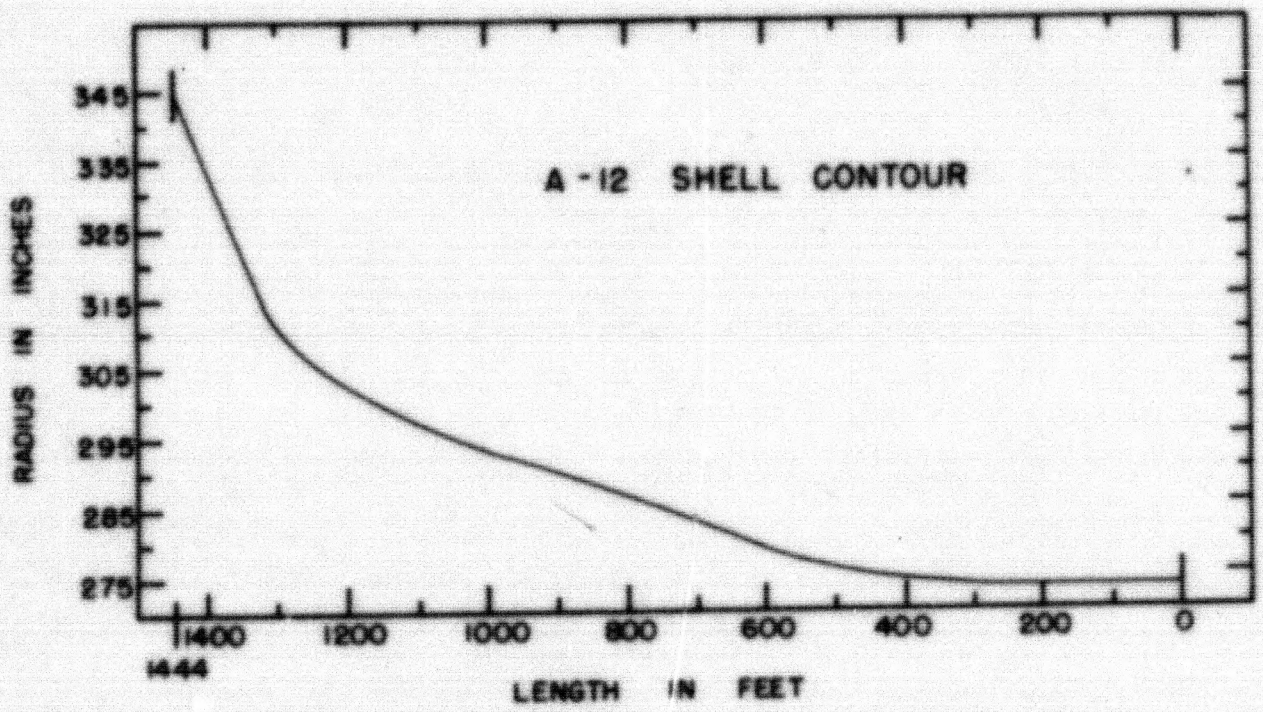

FIG. 1

MU3226

276 C04

DECLASSIFIED

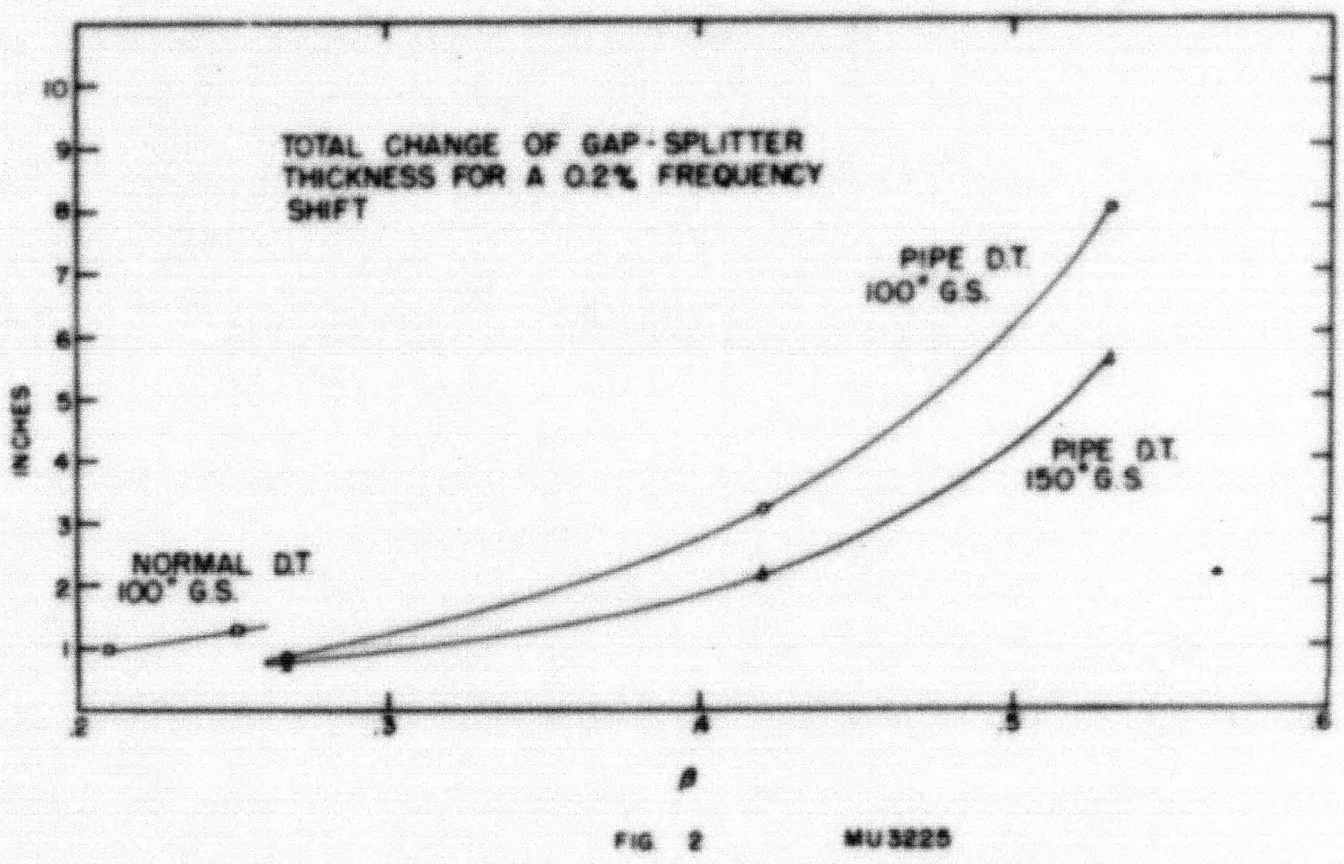

FIG. 2 MU3225

DECLASSIFIED

2. X-RAY AND SPARKING TESTS IN A MERCURY PUMPED SYSTEM

Wallace Kilpatrick
UCRL

X-ray and sparking measurements at 202 mc and constant 1-3/4 ± 1/16 inch gap have been continued in the same mercury pumped system (B-3) along the same lines as previously reported.

"Stove pipe" drift tubes were compared with the previous hemisphere type for x-rays and sparking. There was essentially no difference observable (Fig. 1) when the best phosphoric acid deplating was used in both cases. The "stove pipe" dimensions were:

Outside diameter = 3.227 in.
Inside (aperture) diameter = 2.151 in.
Gap = 1-3/4 ± 1/16 in.
Maximum nose radius of curvature = 0.267 in.

Note that the x-ray intensities are not as low as previously reported on hemispheres with phosphoric acid deplating in spite of all efforts and technique, but that a comparison was made.

Using "stove pipe" geometry, a gap splitter in the form of a flat copper annulus (8" OD, 4" ID) was biased with d.c., while the cavity cell was excited with rf. A small but noticeable increase in the general x-ray level was observed when the bias was positive, and inversely a small decrease in x-rays with negative bias. This effect, for $0.5 \times 10^6 < V(rf) < 0.75 \times 10^6$, as shown in Fig. 2 could not be explored over a greater range at the time. Other experiments with biased elements placed inside and outside the drift tube bore changed the x-ray level slightly, but the results were too irregular for summation.

An attempt was made to draw ions (possibly existing in the gap) through a 1/4 inch diameter hole drilled in the nose of one hemisphere, and then analyse the resulting beam with a magnet and a phosphor screen. Two focusing anodes and magnet bias (for a field-free trajectory) up to 30 kv showed nothing positive or negative for normal rf up to 1.0 Mv. Sparks, however, displayed a continuous spectrum of inferred electron energies from 1.0 Mv (maximum peak rf) to less than 0.25 Mv, but accurate measurements were difficult. A hot filament placed opposite the "ion" hole gave an electron beam with deflection energy sensibly in agreement with other rf peak voltage calibrations.

Figure 3 shows the comparative similarity of minimum x-ray levels obtainable with clean metal and best glow discharge for copper, tantalum, chrome on copper, and gold on copper. Oxygen glow discharge raises the low x-ray levels consistently, irrespective of base metal as shown in Fig. 4. Also note the characteristic hump in the curve. This oxygen effect may be erased by simply glow discharging in nitrogen.

Mark I drift tubes were to be cleaned with phosphoric acid deplating in accordance with previously reported findings. However, samples of the deplating process failed to reach the expected minimum by a factor of between 10^3 and 10^4 which was still acceptable on grounds of extrapolation. No phosphoric acid de-

DECLASSIFIED

plating looked very good--in fact, simply sanding with a buffing wheel seemed just as effective for x-rays but gave enormous sparking rates. Sample tubes for B-3 were deplated along with Mark I Nos. 0 and 8. The results after glow discharge in nitrogen are shown in Fig 5.

In looking for a better surface, oxided copper (chemically bonded oxygen) was found to be very good and more consistent. A particularly good method of oxiding the surface, developed by H. R. Ahrens and K. W. Ehlers, that employs an oxy-acetylene torch can be used outside of the vacuum system. Whether the oxide, the cleaning action of the oxidising flame or both is responsible for the favorable results is yet to be determined. Low temperature (100°C) oxiding using this method is so encouraging that peak rf gradients of 450 kv/cm or more are required to investigate cold emission and sparking. These gradients should be available shortly in B-4.

There are several errors in the graph on page 10 of the Quarterly Report, UCRL-1573, and more points are now available. See Fig. 6 for a complete tabulation of x-ray loading vs sparking rate data.

UNCLASSIFIED

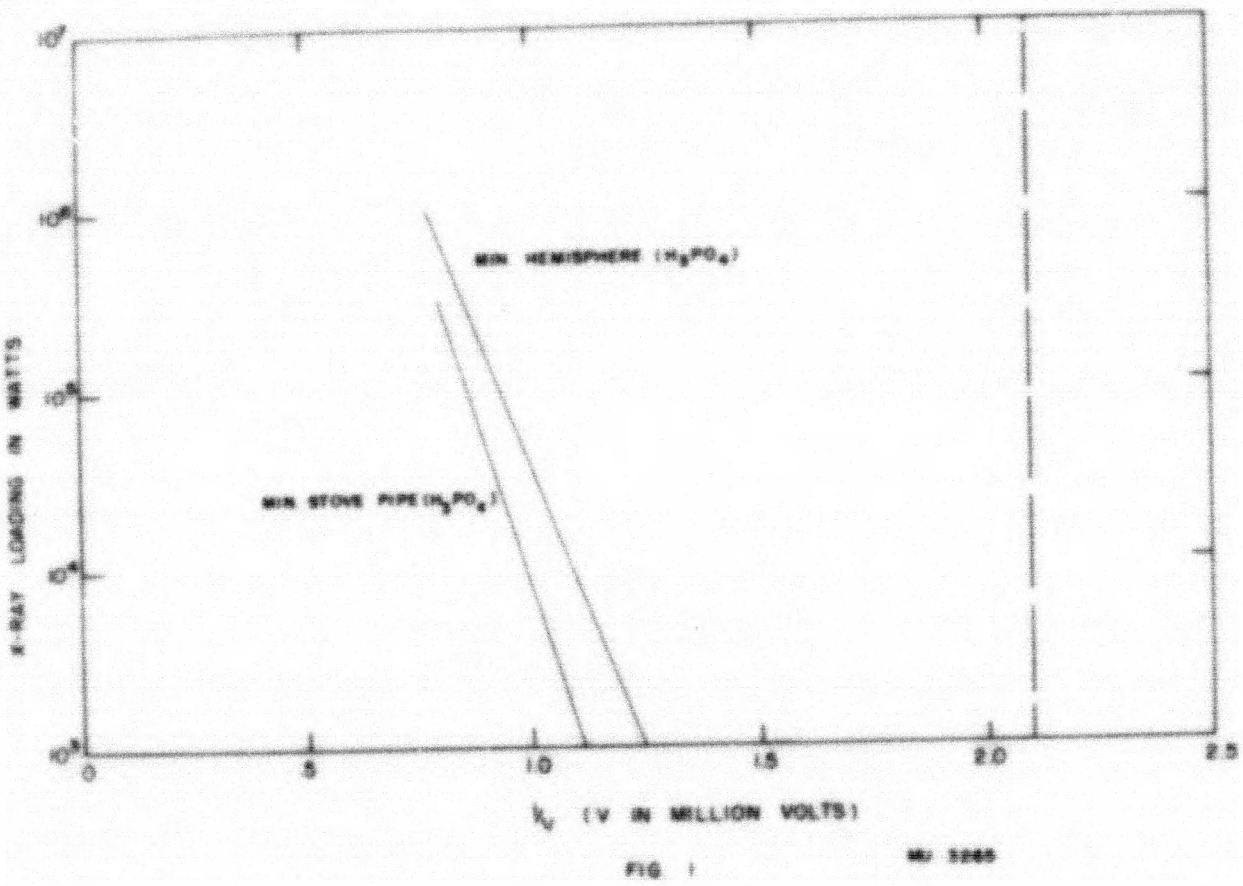

MU 5265

FIG. 1

DECLASSIFIED

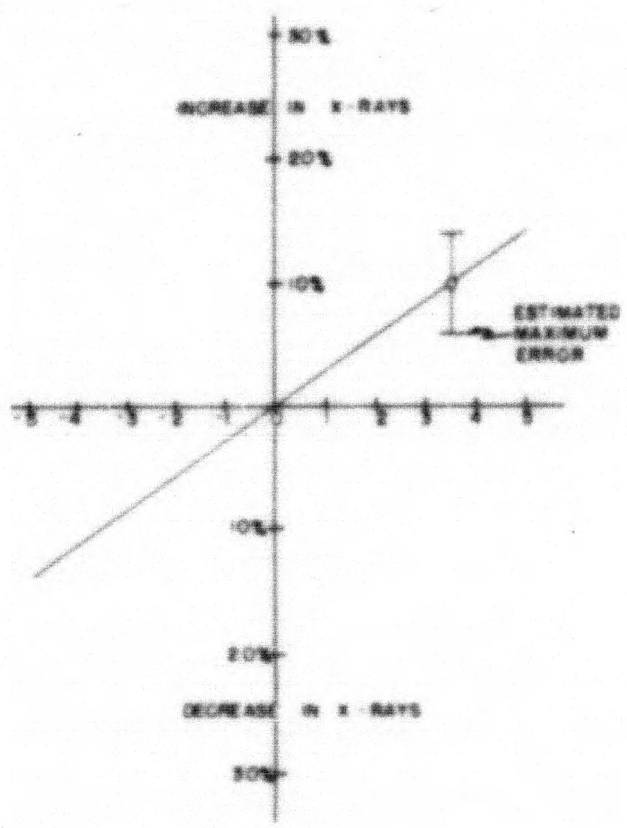

FIG 2

MU 5266

DECLASSIFIED

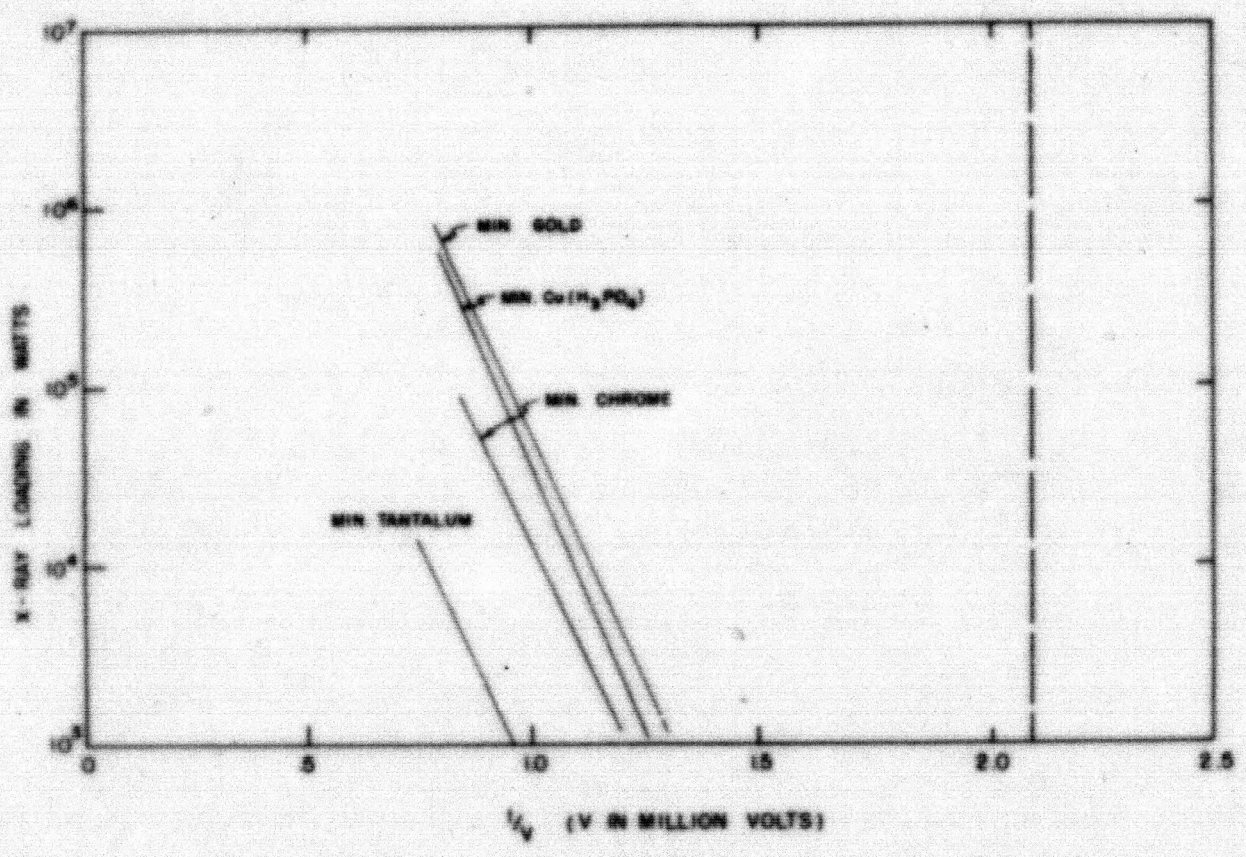

FIG. 3 MU-3267

276 -1D

DECLASSIFIED

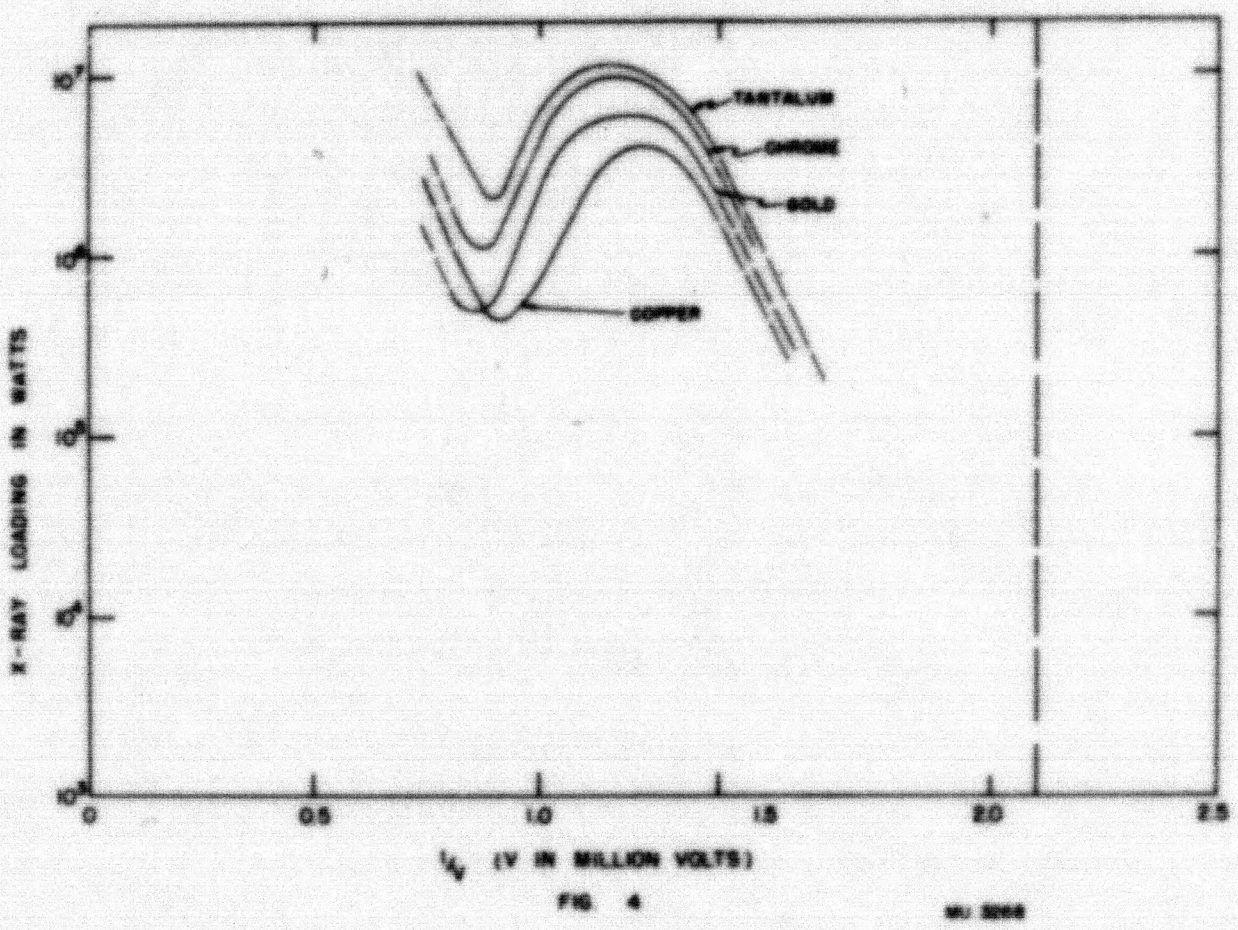

FIG 4

276 11

DECLASSIFIED

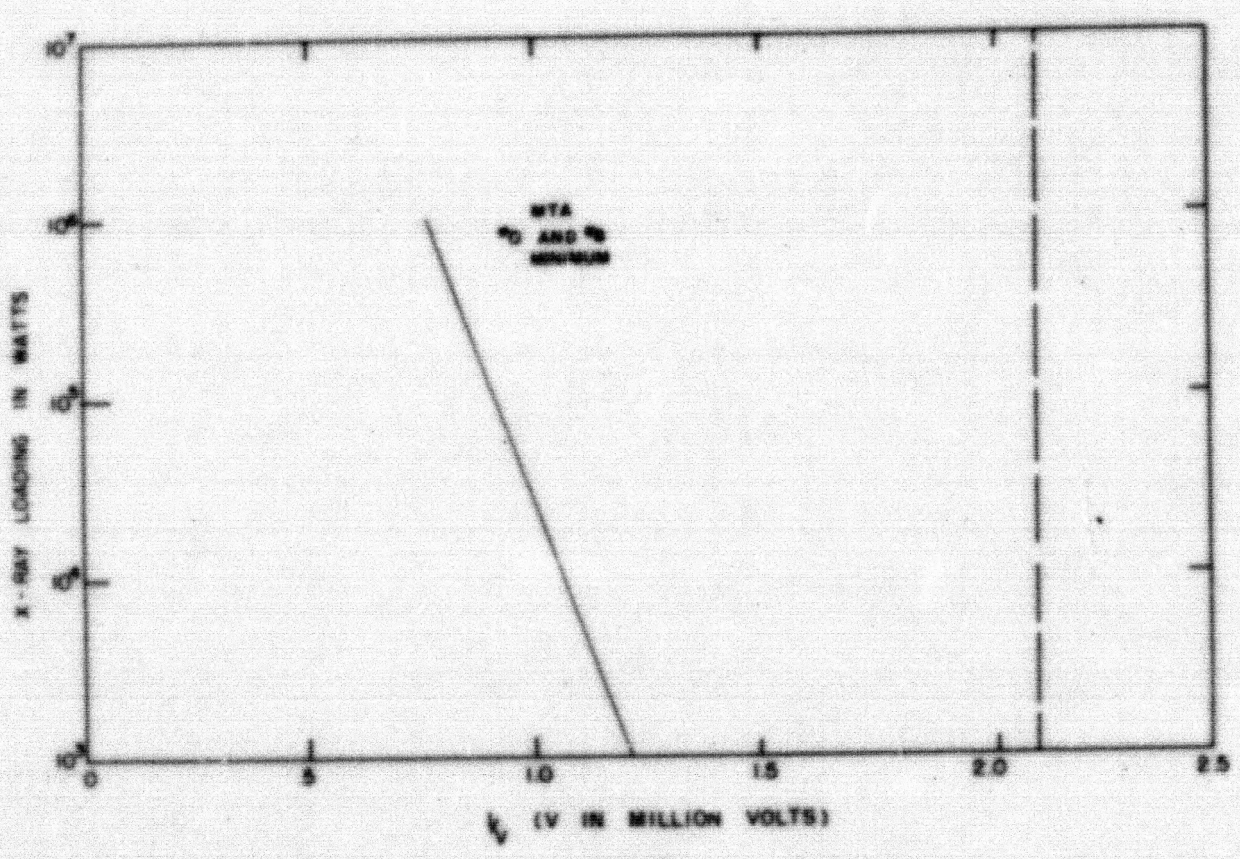

FIG. 5

MU 3269

27[illegible] 012

DECLASSIFIED

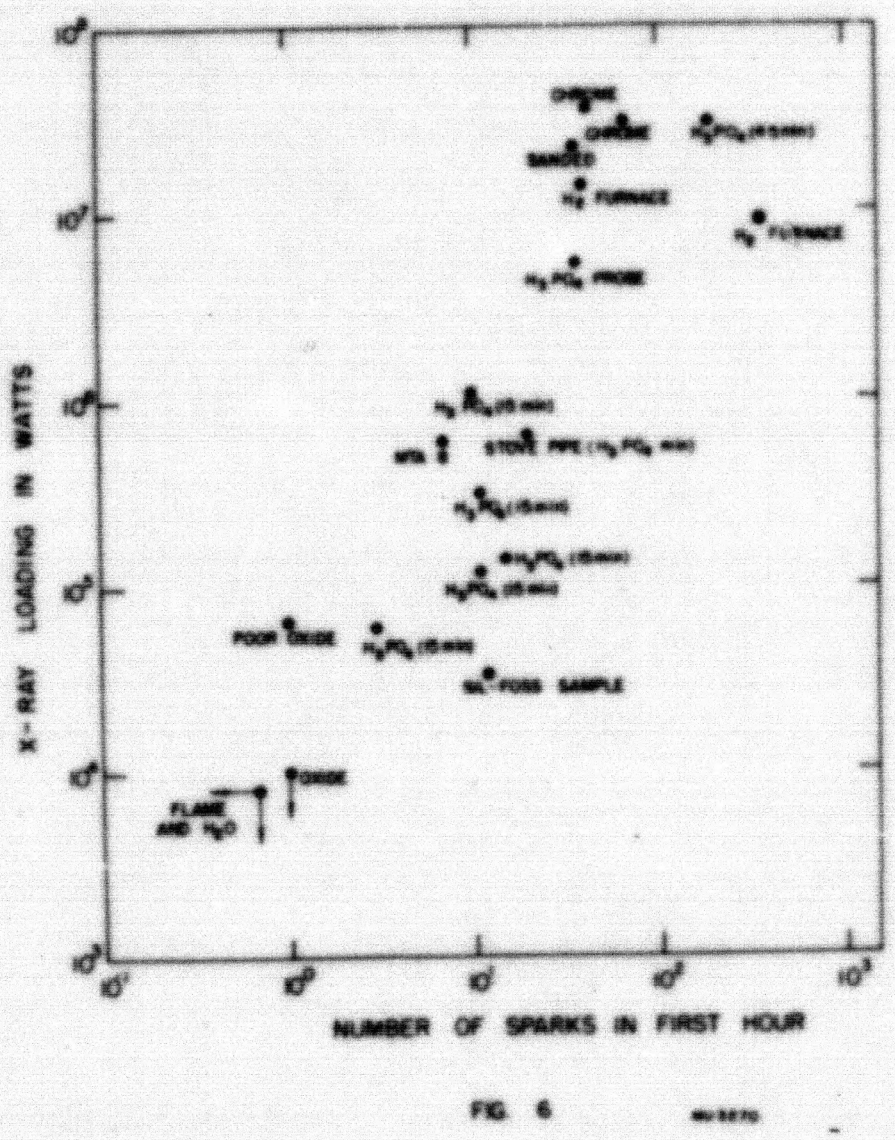
X-RAY LOADING IN WATTS
NUMBER OF SPARKS IN FIRST HOUR
FLAME AND H_2O
FURNACE
FURNACE
FURNACE

3. X-RAY MONITORED VACUUM RF SPARKS

R. Birge, E. J. Lauer, and E. J. Lofgren
UCRL

The x-rays from rf sparks have been monitored using a photomultiplier tube connected to fast amplifiers and thence to an oscilloscope. (See Fig. 1). The output of the amplifiers was divided into two parts: One part was used to trigger the sweep and the other part was delayed about 0.5 μ sec and put on the vertical plates of the oscilloscope. A camera photographed the resulting trace.

With the equipment described, the sparks in two different systems have been observed. The first system makes use of the XC cyclotron tank which has the geometry shown in Fig. 2a. A quarter-wave line (axis normal to the paper) ends between two flat planes. A magnetic field can be applied perpendicular to the planes. This system is usually run between 700 kv and 1000 kv. The other electrode system (Baker's Ball) consists essentially of concentric hemispheres (Fig. 2b). It resonates at about 12 mc and has between 2 and 3 Mv on the center electrode.

A few remarks about the response of the monitoring system might be in order. The rf in the XC tank is 14.3 mc/sec and a timing signal of this frequency is put on each of the pictures above the spark trace. (The timing signal is not synchronized with the rf in the tank). The amplifiers are Hewlett-Packard 100 mc/sec distributed circuits having a rise time of about 5×10^{-9} sec when three are put in series. A shorted line is used to differentiate the pulses in 10^{-8} seconds. The input line from the phototube to the amplifer is terminated at the amplifier to eliminate reflections. The signal lead to the scope is left open to get more amplitude and a reflection of the signal from this end, reflected again from the amplifier appears about 15 rf cycles later with opposite polarity. This reflection can be seen on some of the pictures where slower sweep speeds were used. (Note: The original pulses are negative.) The trigger cable is also terminated, but a small reflection from this appears about 0.5 rf cycles after each pulse. The amplitude linearity of the whole system is very poor. The height of the signal on most of the pictures is a measure of amplifier saturation. To get a large signal, the grids of the last amplifier are driven positive, and to get enough drive, the next to the last amplifier must go to cutoff. The overall effect is to give about a factor of two change in response for a factor five change in signal. The rf voltage on the electrodes in the XC tank could be set so that sparks occured every 5 or 10 seconds apart on the average. The procedure was then to hold the camera shutter open until a spark occured. Examples of the x-ray signals are shown in Figs. 3,4,5 and 6. Fig. 3 shows typical spark signals from the XC tank and Fig. 4 is a spark signal from Baker's Ball. That these signals are actually due to x-rays coming through the lead collimator to the crystal and phototube and not just electrical pick up was checked by closing the collimator with a lead brick which stopped the signal on the scope even though the sparks were still occuring as indicated by the peak rf voltmeter. It is known that these pulses represented a "pile up" of many photons by comparing them with the signal due to single x-ray quanta.

The two important characteristics of these spark signals are:

(1) The x-ray pulses in a spark group occur on alternate half cycles

DECLASSIFIED 276 014

of the rf even when the phototube can see both electrodes. This suggests that the sparks are rectified, with all of the x-rays coming from one electrode. That most of the x-rays come from the wall (low field) electrode in the XC tank was shown by directing the lead collimator separately at the wall and center electrode. An exception to this rectifying action is discussed later in this report.

(2) The x-ray pulses are never observed to build up or stop suddenly (in one cycle) but usually take a few, about three, cycles to build up and continue once started until (apparently) the energy and voltage in the tank have been reduced.

It is also interesting that the spark signals from two different systems (XC tank and Baker's Ball) are very similar.

The first characteristic is confirmed by x-ray pinhole camera pictures which showed the x-rays to be coming from only the walls in XC and from only the outer shell in Baker's Ball. We believe this to be due to the geometry of the electrodes. Thus, the high fields on the center electrodes may cause more electron emission, or the larger rf heating may drive out more gas.

That the build up takes a few cycles is characteristic of proton transit times, not copper or photons. Also positive ions would account for the memory of the spark from one cycle to the next. However, a numerical calculation done by the theoretical group indicates that a proton cannot travel from the outside to the center electrode in Baker's Ball. The non-uniform field causes the proton to change phase and walk back to the outside after four or five cycles and after traversing only half the gap.

An exception to the rectifying action in the XC tank is shown in Fig. 5. The collimator was directed at the center electrode and no sparks were detected. The gain was then increased and rectified sparks were seen, presumably due to x-rays from the wall electrode scattering into the counter from the rear. However, as shown in Fig. 5, some x-rays came from both electrodes during the last few cycles of this spark's duration. This was a rare occurance as no such event was seen when looking at both electrodes even when the gain was set at a comparably high level.

Turning the magnetic field on has no signficant effect upon the x-ray monitored sparks in the XC tank (except that they occur at lower voltages).

The sparks in the XC tank were also monitored by looking at the visable light with the phototube. Here "visible light" is defined as light that could be reflected by a mirror and stopped by black paper. The signal was not significantly different from that due to x-rays.

The "background" x-rays that came from the XC tank when there were no "sparks" were detected by increasing the solid angle and gain. The sweep was triggered randomly. Small, relatively constant amplitude x-ray pulses are seen on alternate half cycles (Fig. 6). These pulses are due to single x-ray photons.

276 013

DECLASSIFIED

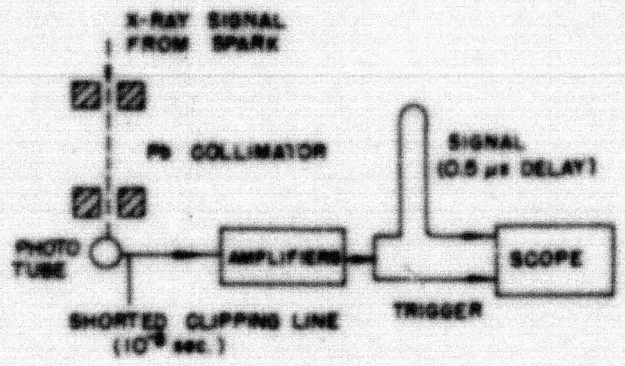

FIG. 1

CIRCUIT USED TO MONITOR X RAYS FROM R.F. SPARKS

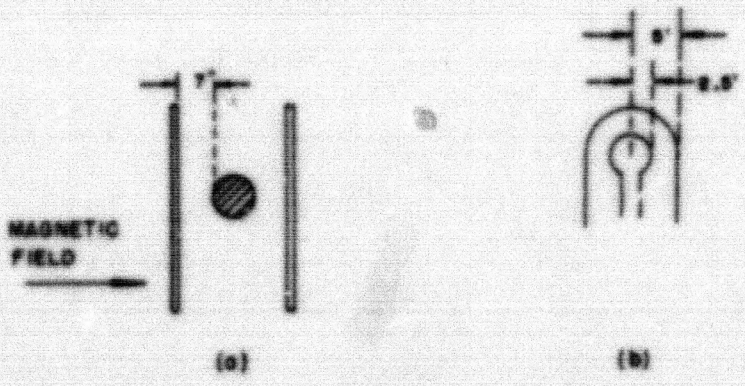

FIG. 2

TWO SYSTEMS IN WHICH SPARK HAVE BEEN MONITORED

(a) X C TANK, 14.3 m.c., 0.7 TO 1.0MV

(b) BAKERS BALL, 12 m.c., 2 TO 3 MV

MU 3271

DECLASSIFIED

27C 016

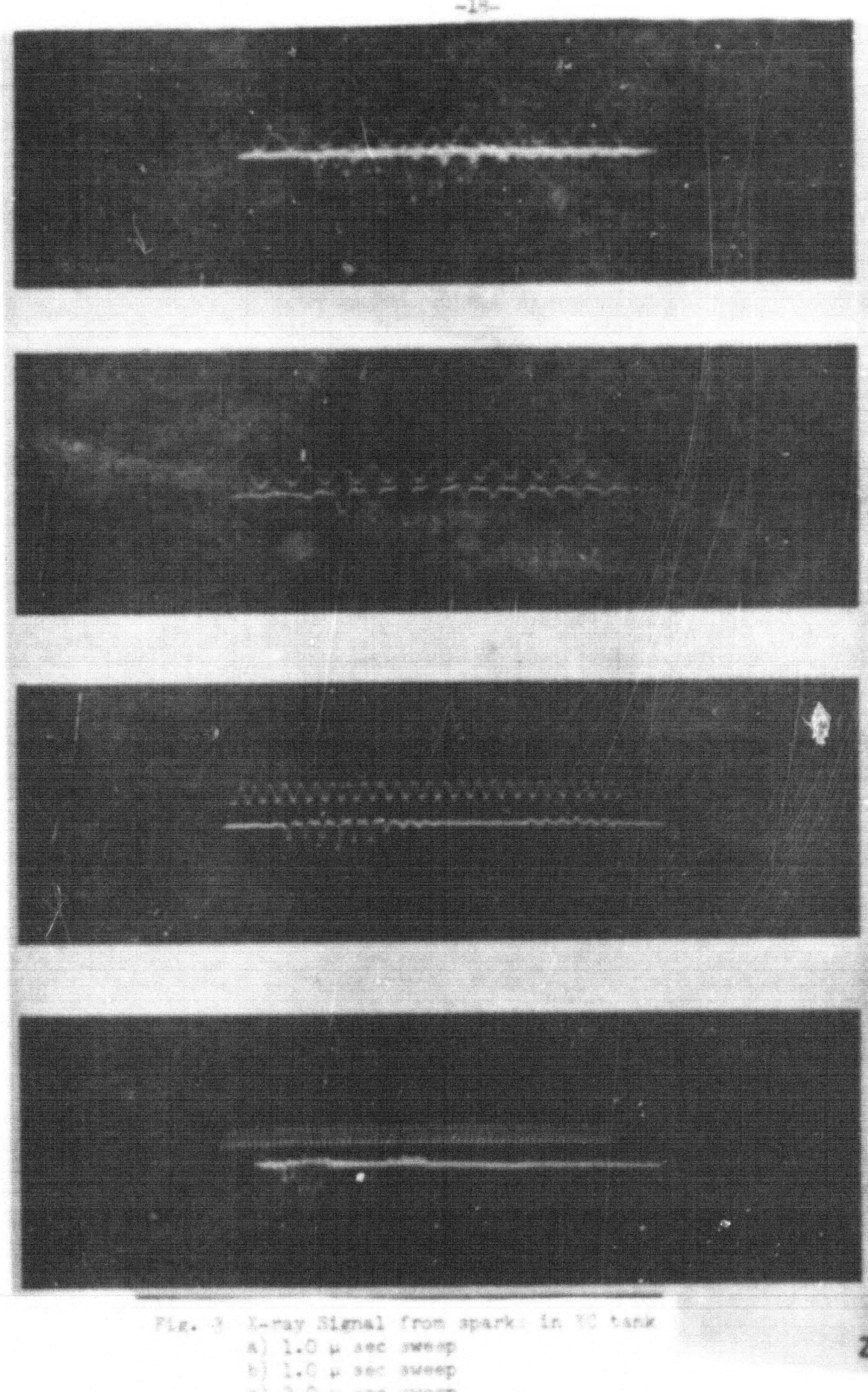

Fig. 3 X-ray Signal from sparks in XC tank
a) 1.0 μ sec sweep
b) 1.0 μ sec sweep
c) 2.0 μ sec sweep
d) 5.0 μ sec sweep

ZN 20

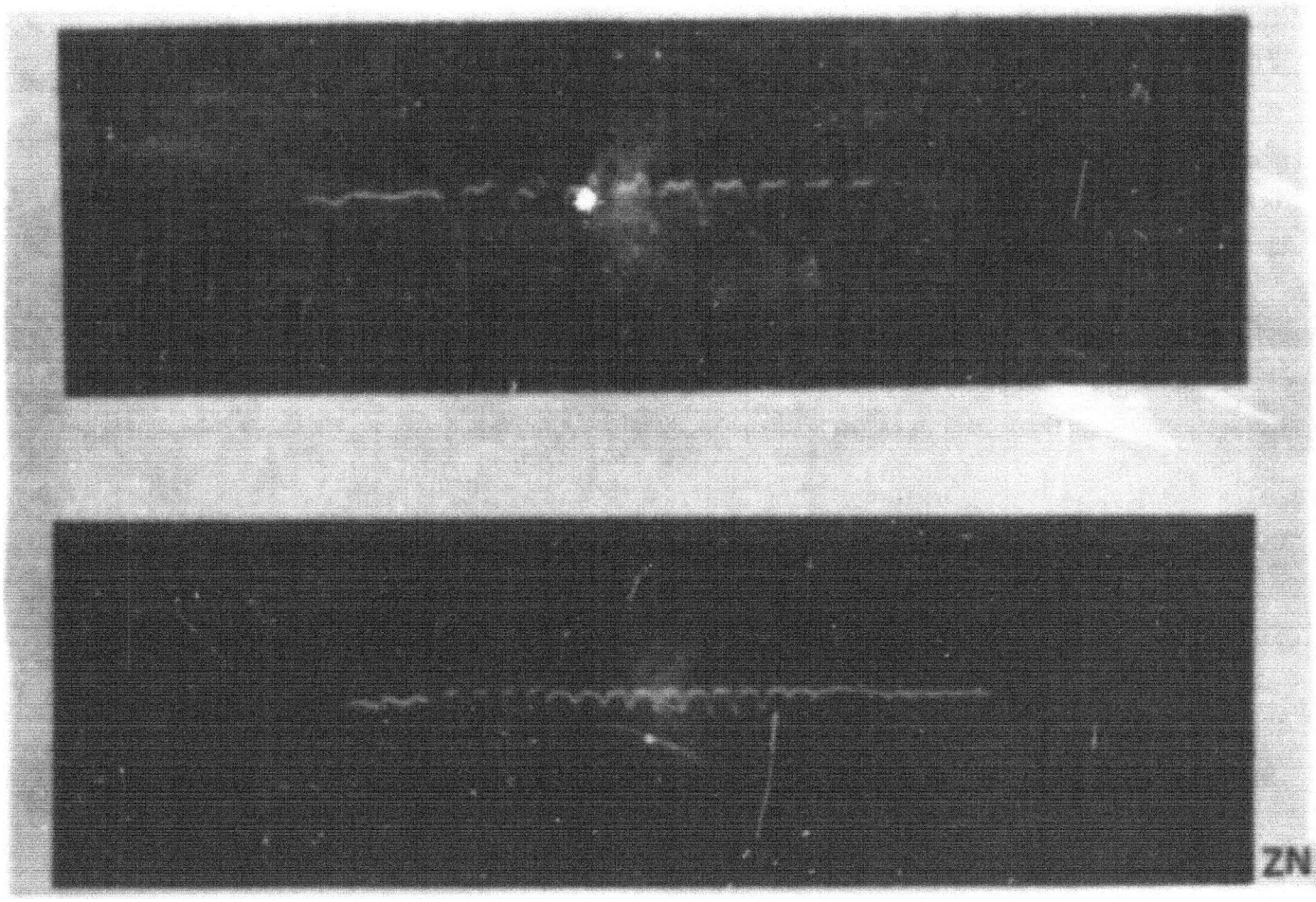

Fig. 4 X-ray signal from spark in Baker's Ball
a) 1.0 μ sec sweep
b) 2.0 μ sec sweep

270 013
DECLASSIFIED

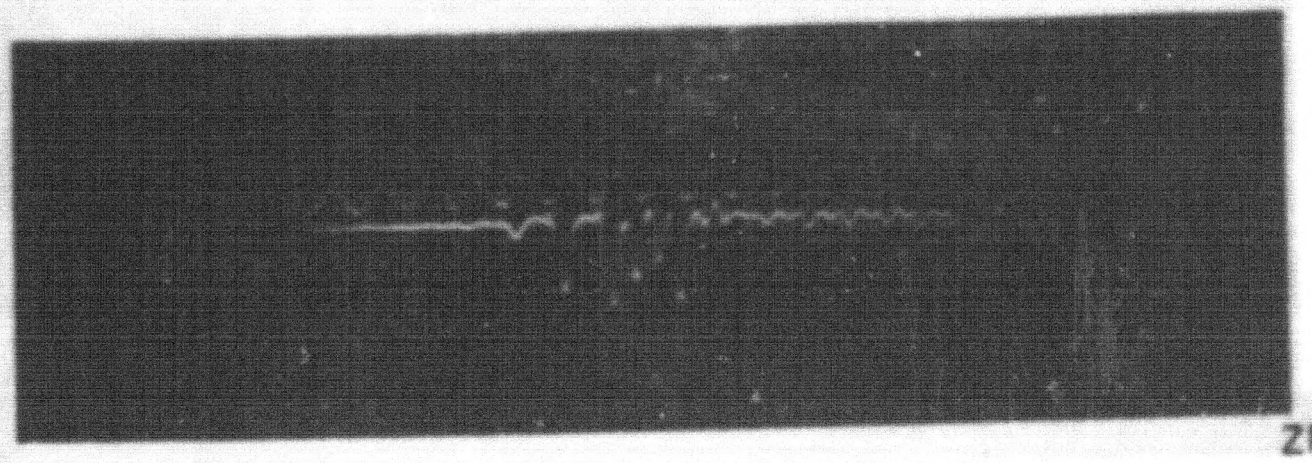

ZN203

Fig. 5 Collimator location at center electrode in KC tube
1.6 μ sec sweep
The pulse at the beginning are x-rays from the walls scattered into the collimator, but where are two pulses of x-rays from the center electrode

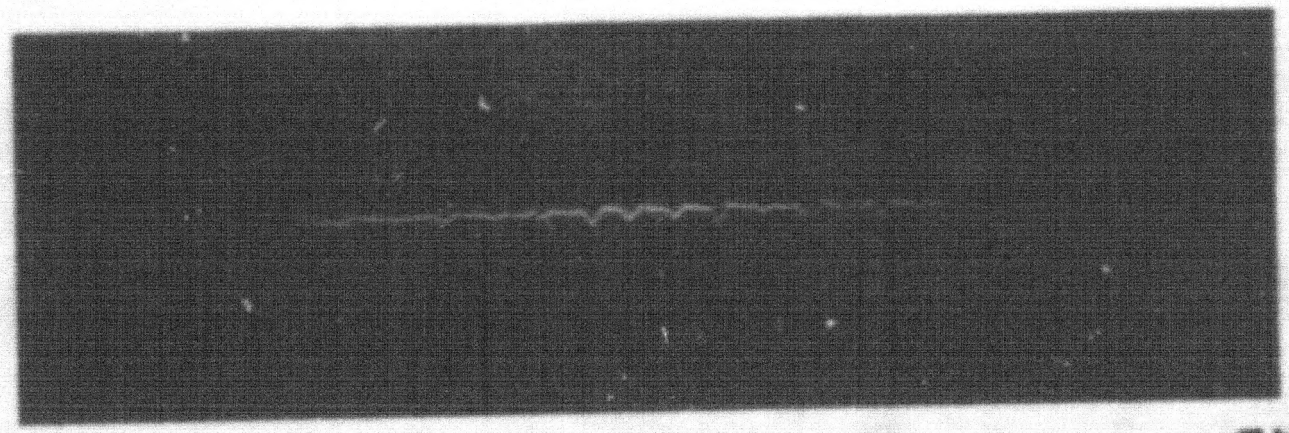

ZN204

Fig. 6 Background (non-sparking) x-rays in HC tank
1.0 μ sec sweep
The solid angle and gain are greater than in Figs. 3 and 4. Manually triggered sweep

4. D-C DRAIN AND BREAKDOWN PHENOMENA FOR UNOUTGASSED METALS

H. G. Heard and E. J. Lofgren
UCRL

Introduction

A desideratum in high-power linear accelerators is the availability of the largest fraction of the input power for increasing particle energy. Because of the large surface areas exposed to high voltages and moderate gradients, the dark current (cold emission) drain and resulting x-ray load may consume an undue fraction of the stored energy of the machine. While voltage breakdown in a linear accelerator is important, the x-ray loading usually represents a more serious problem. In contrast, cyclic accelerators require the utilization of the maximum breakdown voltage for a restricted volume; the total drain is less important.

When applied to the Fermi-Sommerfeld picture of a metal, the concept of wave mechanical penetration by electrons of a surface potential barrier lowered and thinned by an externally applied intense electric field leads to the celebrated Fowler-Nordheim equation[1-3]. For the simple triangular potential barrier this equation reduces to

$$J = 6.2\times10^{-6}\ \frac{\mu^{1/2}}{(\mu+\varphi)\varphi^{1/2}}\ E^2\ \exp\left(\frac{-6.85\times10^{7}\varphi^{3/2}}{E}\right)$$

When the image force effect is included the expression becomes

$$J = 1.55\times10^{-6}\left(\frac{E^2}{\varphi}\right)10^{-2.98\times10^{7}\ \left(\frac{\varphi^{3/2}}{E}\right)}\ f(y)$$

where J = amps/cm^2
E = volts/cm
φ = work function of the electrode material
$y = 3.62\times10^{-4}\ \frac{E^{1/2}}{\varphi}$

$f(y)$ = functions of two elliptic integrals which have been tabulated for values of y from 0-1 by Nordheim[2].

The correctness of the above relations has been established for well outgassed electrodes[4]. Careful work has shown that breakdown between metals occurs when the applied electric field is sufficient to lower the surface potential barrier to the level of the top Fermi electrons[5]. The experimentally observed fact that electrode drains are orders of magnitude higher and that critical fields are orders of magnitude lower for unoutgassed metals in vacuum of the order of 10^{-6} mm Hg requires a reinvestigation of these phenomena in this range.

DECLASSIFIED

Because of the size and construction of high energy accelerators, one cannot resort to the desirable approach of high temperature outgassing of metal parts. Previous attempts to construct very high voltage machines from unoutgassed metals have been hampered by large dark current drains and destructive breakdown which occurs when potentials of the order of a million volts are applied between electrodes[5-8].

In order to reduce the skin effect losses attendant with rf excitation, electrode materials are chosen for high conductivity. It turns out that the materials which are suitable in this respect are notably poor in holding voltage. It is therefore necessary to determine the specific drain for a given voltage and spacing for copper and to investigate those techniques by which the drain may be minimized. The limits in design imposed by the maximum voltage which can be applied to electrodes for a given spacing in high vacuum are also of primary importance.

A study of electrode drain and breakdown phenomena was undertaken at dc voltages up to 100,000 volts. The effects of pumping fluids and trapping agents on the total drain between electrolytic copper electrodes was investigated. Radioactive tracer experiments have shown that anode metal is transferred to the cathode in a non-sparking discharge. Simultaneous observations of total cavity pressure and electrode drain as a function of electrode voltage serve to clarify the breakdown problem.

Description of Apparatus

Vacuum System. The all-metal vacuum system used in these experiments was continuously evacuated with a special two-stage mercury pump, designed by Warren Chupp*. Interposed between the test cavity and the metal diffusion pump was a "multiple bounce" - type liquid nitrogen baffle having an effective pumping speed for condensables of approximately 1,000 ℓ/sec. The high-vacuum section of the system was purposely built without a shut-off valve to eliminate the possible contamination of the system by the gasket material of the valve plate. The intake of the mercury pump was covered with a simple water-cooled baffle designed to reduce the load on the liquid nitrogen trap. An additional cold trap placed between the mercury pump and the forevac pump, prevented the oil vapors of the mechanical pump from reaching the test cavity. The general arrangement of units is shown in Fig. 1.

Cleaning of Vacuum System. Previous to the first run, after each contamination run and as often as indicated by basic drain data, the entire system was dismantled and cleaned. The entire vacuum casing and traps were sand blasted (inside and outside) and washed in flowing c.p. acetone and c.p. ethyl alcohol (95 percent). Insulators were scrubbed with scouring powder and rinsed in distilled water and acetone. All glass parts of the system including ion gauges were cleaned with "Dreft" and hot water, washed in concentrated chromic acid made from 37 N c.p. sulfuric acid, and finally rinsed in distilled water, c.p. acetone and c.p. ethyl alcohol. Parts were assembled immediately with grease-free tools

*Early studies of electrode drain with Myvane 20 oil used an MC-500 oil diffusion pump.

DECLASSIFIED

and paper towels. None of the parts were touched with bare hands during assembly. All gaskets in the high-vacuum section of the unit were made from commercial 40-60 solder. Insulators were coupled to the system with lead foil covered gum rubber gaskets.

Typical base pressures of a kinetic system cleaned and pumped in the above fashion were of the order of 10^{-7} mm Hg as registered on a 1949 gauge. The lowest recorded pressure was 8×10^{-8} mm Hg.

Pressure Measurement. After some experimentation, the RCA 1949 ionization gauge was decided upon for pressure measurements. It was found that mercury and oil contaminated VG1A gauges could not be cleaned properly without the loss of the ion collector electrode. The Western Electric gauge was avoided because the filament of the gauge represents a strong source of electro-positive material (Ba-SrO).

Some difficulty was experienced in obtaining low leakage cables and good current metering tubes for the laboratories newest ion gauge power supply. After the 6SL7 input tube was replaced by a RCA 5691 and a seperate anode lead was run in the gauge cable, no further difficulties were encountered. The ion gauge metering supply used in these experiments was not sufficiently sensitive to meter pressure in the 10^{-8} mm range.

High Voltage Supply and Metering. Early work on electrode drain was carried out using a 100,000 volt, 3.5 amp power supply. Later phases of the work have been continued with a 100,000 volt, 10 ma. supply. A rather severe cascade RC-filter system was used to reduce the ripple to 0.3 percent at 110,000 volts.

Electrode voltages were first determined by measuring the power supply voltage and correcting for the drop in the electrode protecting resistor. Later in the program a 1,000 megohm resistor was constructed and calibrated to read the gap voltage directly. The power supply and gap voltage are known to within 2 percent.

A General Radio 715-A d-c amplifier was used in conjuction with an Esterline-Angus recorder to monitor electrode drains. The amplifier input was connected between the low voltage electrode (cathode) and ground. This construction and metering assures that the metered currents are independent of dark currents which drain from the high voltage electrode to the surrounding cavity. The relatively slow response (5 cps) of the recording drain meter gives a continuous integrated record of the electrode drain. Current drains could be metered with this arrangement from 10^{-8} to 10^{-2} amperes.

Electrodes. Both gap electrodes were hemispherically-capped cylinders of 1 inch radius. The gap between electrodes could be varied external to the high vacuum system through a sylphon bellows. Because of errors introduced by thermal expansion of the long (high voltage) anode support cylinder, it was found necessary to monitor the gap spacing continuously with a cathetometer. The electrode spacing is known to $\pm$ .05 mm.

DECLASSIFIED

Pumping Fluids and Trapping Agents

General. So that the data obtained for the comparison of pumping fluids would be meaningful, the geometry and electrode material of the gaps were standardized. Because of the ultimate usefulness of the data, electrolytic copper electrodes were chosen. After some experimentation, it was found that a gap of 2 ± .05 mm gave the maximum utilization of the available 100,000 volt power supply.

Since surface cleanliness was known to affect the electrode drain, several cleaning techniques were tried. The electrode cleaning process finally chosen was checked in contamination measurements and found to be satisfactory. If electrodes which had been oil contaminated and found to give high drains were polished with steel wool, cleaned with "Dreft", or Dutch Cleanser distilled water and c.p. acetone and reinstalled in the test cavity, the drains would compare favorably with the base value. Although more involved cleaning techniques were tried, they were not found to be superior.

Electrode Drain in Systems Pumped with Myvane 20 Oil. A proposed accelerator pumping fluid, Myvane 20 diffusion pump oil, was used in an MC-500 oil type, three stage diffusion pump. Several sets of data were collected for electrode drain versus voltage for the standard spacing of 2 mm. Different trapping agents were employed, sufficient data having been accumulated for each test condition. In the first series of tests, liquid nitrogen was used in the cavity trap and solid CO_2 immersed in trichlorethylene was used in the forevac trap. In the second series of data on oil the cavity trapping agent was changed to CO_2. The third series of tests was conducted without trapping agents. Only the water cooled baffle remained to impede the backflow of oil. Finally, even the water cooled baffle was allowed to become warm. Since the data for the last run were badly scattered (10^{4}:1) no consistent trend could be reported. The averaged drain versus reciprocal field relations for the several phases of the oil tests are shown in Figs. 2,3 and 4. Specific electrode drains for all cases were later shown to be high when compared to the data obtained for mercury pumps. It appears that there is no distinct advantage in using any trapping agent with Myvane 20 oil as far as the effect on electrode drain is concerned.

On the completion of these runs the electrodes were removed for cleaning and inspection. It was found that the cathode and anode took on characteristially different appearances (see Fig. 5 and 6). Underneath and around the heavily sparked area of the cathode can be seen the brown ring which has been found to appear on all electrodes used in oil or oil contaminated systems. The surface of the anode is seen to have a brightly burnished annulus surrounding the heavily sparked region. The appearance of the anode is the same regardless of the degree of contamination of the test cavity. No brown ring was ever found on anodes. As seen in Fig. 6 the anode surface has a multiplicity of crater-like impressions associated with the central heavily sparked region. Corresponding to these craters, the cathode contains a rough surface of built up globular deposits of copper. The craters of the anode and the globular deposity on the cathode have been found on all further anodes and on all materials tested.

While it is not possible to subject an entire machine to high temperature outgassing, it may be possible to heat restricted sections of an accelerator which will later be subjected to high voltages or intense electric fields. So that some idea of the possible advantage of local outgassing could be obtained, one set of electrodes, which had been cleaned by the standard process, was subjected to a 2

DECLASSIFIED 270 024

hour bake at 775° Cg. The drain versus gradient curves of Fig. 7 when compared with those of Fig. 2 shows an over-all reduction in drain by a factor of 25-30. Fig. 8 shows the cathode of this experiment. Note the large crystals which result from the heating process. No significance can be attached to the sparking area of the electrode as the surface of the metal was etched with nitric acid to bring out the crystalline structure for photography.

In order to determine the effectiveness of the bake-out procedure on electrodes which had been covered with an oil film, a pair of electrodes was outgassed 1 hour at 775° Cg after being contaminated with oil. Fig. 9 shows that the bake-out technique was not effective in reducing the drain for these electrodes. Perhaps a prolonged heating or a higher temperature would have been effective.

The effectiveness of continued sparking on the clean-up of electrodes in an oil pumped system was investigated. Because the energy consumed in the spark was not sufficiently limited, several milligrams of copper were transferred to the anode. The resulting distortion of the electrode surfaces was not negligible compared to the small spacing and so only a qualitative interpretation can be attached to the resultant experimental data. Electrode drains were reduced by approximately a factor of two while the sparking voltage was increased about 10 percent. Figs. 10 and 11 illustrate the destructive effects of energetic spark breakdown. The average energy per spark was approximately 3600 joules.

Electrode Drains in Systems Pumped with Mercury. Prior to changing to mercury as a pumping fluid the entire vacuum casing was degreased in hot trichlorethylene vapors, sandblasted inside and out, and washed in flowing c.p. acetone. Triple distilled mercury was used in the metal diffusion pump.

The first run with mercury as a pumping fluid showed that the drain for copper electrodes at the 2.0 mm spacing was so low that special shielding had to be installed to distinguish electrode drain from background. An average of several runs is shown in Fig. 12. From these data the drains are seen to be approximately three orders of magnitude smaller than found for oil pumping.

It is interesting to note that the electrodes did not fluoresce at the highest gradients unless the drain is correspondingly high. The surface of the anode for all oil pumped electrodes was found to contain hundreds of bright small blue-green spots approximately 1/10 mm in diameter. These spots were only found in the mercury pumped cavity when the electrodes had been contaminated by deliberate introduction of oil vapors. Although it is not possible to state whether these spots are due to the magnitude of the drain or the fluorescence of an organic film due to the layer of oil, it is probably that they are due to both.

Both liquid nitrogen and solid CO_2 were tested in the cavity trap. It was found more difficult to contaminate the electrodes when liquid nitrogen was used in the cavity trap.

Inspection of the electrodes on removal from the cavity showed that the cathode and anode appeared identical to those used in oil pumping with one important exception. No brown ring was found on the cathode.

As a further check on the effectiveness of an oil film in enhancing electrode drain, several experiments were performed in which oil was deliberately introduced into the mercury pumped cavity. New Nyvane 20 oil was degassed in separate glass vial and frozen with liquid nitrogen. This sample was coupled to

DECLASSIFIED

the unit and kept frozen until it had been established that the base drain of the system was low. When the oil was allowed to thaw and evaporate into the cavity the drain would rise to values comparable to those found in the oil pumped cavity. See Fig. 13. To check for reproducibility, the entire system was cleaned and the experiment repeated; the results were identical for several tries.

As a check on the cleaning process the electrodes were removed from the oil contaminated cavity and cleaned by the standard process. On reinsertion in the unit the drains were observed to be down to the base values. After 24 hours of pumping, the drain relation showed that oil remaining in this cavity had re-contaminated the electrode surfaces (see Fig. 14).

A test was run in the system with DC-703 silicone oil as a contaminant. Preliminary results indicate that silicone oils have little effect on the voltage-drain relation. On removal from the cavity the electrode surfaces were similar to those found for a clean mercury system, i.e., no brown ring was found. Since the base drain of the system was somewhat higher than used in other contamination tests, less significance can be attached to these findings. It would be necessary to clean the entire system and repeat the tests before a definite answer would be forthcoming. It does appear, however, that silicone oils are superior to Myvane 20 in this respect. Further work in this direction was held up by the radioactive tracer experiment.

It is not possible to say, on the basis of the above test data, whether the presence of an inorganic impurity in Myvane 20 oil or the cracked oil itself in the form of an insulating film is responsible for the high drains and reduced spark-over voltages encountered in oil pumped systems. It is, however, established that drains are decreased and spark-over voltages are increased when mercury rather than Myvane 20 oil is used as a pumping fluid.

Radioactive Tracer Studies*

Cu^{64} was used as a radioactive tracer to confirm the transfer of anode metal to the cathode in a non-sparking discharge in high vacuum. The number of atoms transferred during the discharge can be written as

$$N_t = \frac{\beta}{\alpha} \frac{QL}{F}$$

where: N_t = the number of atoms transferred to the cathode

α = the ratio of charged to uncharged atoms transferred

β = the fraction of the total charge carried by positives

Q = total coulombs of charge transported during the run

L = 6.023×10^{23} - Avagadro's number

F = 96.506 - Faraday's constant

This relation is solved for β/α and rewritten in terms of counting data in the

*For further details see H. G. Heard and E. J. Lauer, "Transfer of Anode Metal in a D-C Non-Sparking Discharge in High Vacuum," UCRL-1622

276 026
DECLASSIFIED

form $$\frac{\beta}{\alpha} = \frac{w_a}{Q}\,\frac{F}{M}\,\frac{D_c}{D_a}$$

where w_a = weight of anode sample

$D_a D_c$ = decay rates of the anode and cathode

M = atomic weight of the transferred material (63)

Experimental measurements yield the necessary data for computing β/α. One can compute β from the coulomb equivalent of the mass transfer of metal assuming $\alpha = 1$.

Results from the use of a 4.5 millicurie source of Cu^{64} indicate that:

1. A surprisingly large amount of anode metal is transferred across the gap in a non-sparking discharge.

2. The amount of transferred anode metal and its distribution on the surface of the cathode suggest that the anode metal is removed by an evaporation process. It was determined that this process takes place only when the electric field is applied.

3. The relatively large variation assumed by β indicates that much of the anode metal crosses the gap uncharged. Pertinent results are summarized in Table I.

Comparison of Drain and Breakdown for Uncutgassed Metals

Since previous data on drain-gradient relations and breakdown voltage were measured with oil pumped systems, data for uncutgassed metals in mercury pumped systems is needed. The program for measurement of these relations for copper, stainless steel, chromium plated copper, and cold rolled steel was started just prior to this report.

Because of the scatter of drain data, a photographic technique is being employed by which several hundred voltage versus drain relations can be accumulated in a few minutes. Each exposure comprises 100 runs and the photographs collectively represent four orders of magnitude of electrode drain. From these photographs it is possible to accumulate sufficient data to establish the range of the mean drain at a given voltage. From reduced plots of such data it will be possible to compare various metals.

In breakdown measurements the scatter of data causes a similar problem. Sufficient data are collected directly from a long persistence scope to establish the average spark-over voltage. The distribution of data appears to be normal.

General Observations

1. It has been established that spark-over voltage with d.c. electrodes is a function of the amount of energy delivered to the discharge. For an impulsive system which can deliver 50 joules per spark, the breakdown voltage is approximately 25 percent higher than when the available energy is only 5×10^{-3} joules per spark. All spark-over data must therefore be accompanied by the energy per spark for the

DECLASSIFIED

TABLE I

SUMMARY OF DATA ON TRANSFER OF ANODE METAL IN A NON-SPARKING HIGH VOLTAGE DISCHARGE

$\beta = \frac{q_t}{q}$

RUN	GAP SPACING (mm)	GAP VOLTAGE (KV)	AVERAGE ELECTRODE DRAIN (amps.)	SPARK	TOTAL CHARGE TRANSFER (COULOMBS)	TRANSFERRED METAL (gms)	β
1	14.2	100	5×10^{-7}	No	7.56×10^{-3}	8.7×10^{-9}	1:600
2*	12.6	100	3×10^{-7}	Yes	4.98×10^{-4}	less than 10^{-10}	
3	1.4	50	2×10^{-8}	Yes	1.60×10^{-5}	8.1×10^{-6}	1:10
4	3.5	50	5×10^{-8}	No	1.69×10^{-4}	6.8×10^{-8}	3:2

* Results of run 2 were included to show that the electronics spark alarm was sufficiently sensitive to trigger on a spark so small that no detectable radioactive material was transported across the gap.

UCRL-1490

data to be meaningful. Since a resistance in series with the gap reduces the available energy to the gap, all test data are being accumulated with an impulsive circuit.

2. Photographic data and photo-counting techniques point to the fact that the electrode drain is composed of at least two parts. Superposed on the average drain is a series of small pulses sharply separated in time and occuring randomly.

3. Breakdown voltages in high vacuum gaps have been found to fit a power-law function of the electrode spacing of the following form.

$$V = Kd^{\alpha}$$

For V in kilovolts and d in millimeters, K is approximately 50 and α is very nearly 1/2. As implied above, K is a function of the energy per spark and is presumed to vary with surface conditions, work function and electrode geometry, particularly for small gaps. D.C. as well as rf voltages for gap spacings from .005 mm to 750 mm have been found to fit this relation within a small factor. A comparison of data is given in Table II and Fig. 15.

Variation of Pressure and Drain with Gap Voltage

As noted in a previous report, (UCRL-1622) a reduction in electrode drain results from admission of an atmospheric leak to the cavity (even though the cavity pressure only increases by a factor 4 to 5 x 10^{-6} mm Hg.). This relation was later verified directly by photographing simultaneously (on a two beam oscilloscope) the variation of electrode drain and cavity pressure as a function of gap voltage.

After the cavity had been pumping for approximately 3 hours, a series of photographs was taken of each pre-spark drain pattern for 40 successive sparks. The drain and pressure as a function of gap voltage were observed to go through four phases.

Phase I First spark only. Pressure rises with voltage in an exponential fashion from 10^{-6} to 10^{-5} mm Hg. Drain begins to rise several times during the pressure rise but seems to be inhibited by the electrode outgassing. Spark occurs at about 10 percent of the drain scale.

Phase II Sparks 2,3,5 and 12. Drain not rise more than 1 percent before the spark. A burst of gas increases the cavity pressure by a factor of 20 and preceeds the spark by several seconds.

Phase III Sparks 6 - 11 and 13. Drain rises to 10 - 90 percent and drops abruptly when a burst of gas occurs. Spark occurs 5 to 30 seconds after the gas burst. Drain is down to 5 - 10 percent just preceeding spark.

Phase IV Sparks 14 and 15. Drain rises exponentially to 10 - 100 percent and spark occurs. Cavity pressure does not change prior to spark.

If the electrodes are allowed to remain unstressed for a short time (10 - 15 minutes) the pressure drain sequence reverts to phase III. For periods of greater delay without voltage stress, the phenomena returns to

DECLASSIFIED

TABLE II

SUMMARY: ONE-HALF POWER BREAKDOWN DATA

VOLTAGE	ELECTRODE SPACING RANGE (mm)	ELECTRODE MATERIAL	V= f(d)	ELECTRODE GEOMETRY	PUMPING FLUID	CONDITION OF ELECTRODES	REFERENCE
13mc.	.05-1.0	Tungsten Copper Aluminum	$V_{kv} = 38\ d_{mm}^{.44}$ $V_{kv} = 36\ d_{mm}^{.55}$ $V_{kv} = 33\ d^{.64}$	1" dia. sphere opposite plane	Oil	Mechanically Cleaned	9
13mc.	.1-1.5	Copper-Plated Steel	$V_{kv} = 36\ d_{mm}^{.54}$	Flat plates no dimensions given	Oil	Mechanically Cleaned	9
D-C	.18-80	Steel (No carbon content specified)	$V_{kv} = 105\ d_{mm}^{.43}$	1" dia. spehere opposite plate	Mercury	Mechanically Cleaned	10
D-C	.005-.015	Tantalum	$V_{kv} = 50\ d_{mm}^{.5}$	.020 mm. dia. sphere opposite plate	Mercury	Metal outgassed at fussion point 30 hrs	11
D-C	.5-3.5	Chromium Plated Copper	$V_{kv} = 53\ d_{mm}^{.52}$	2" dia. Hemispherically capped cylinders	Mercury	Mechanically Cleaned	This Report

phase II and after an hour or more to phase I. The remaining 25 sparks followed the patterns of phase III and IV. After consistent sparking at several sparks per minute, the cavity pressure remains constant. Figs. 16 - 18 illustrate Phases II, III and IV.

It is of interest to note that the actual spark-over is accompanied by bursts of gas which raise the cavity pressure by factors of 3 to 10 in the early sparking history of the electrodes. After continuous sparking relatively constant cavity pressure indicates that the amount of outgassing has been greatly reduced.

These observations indicate that:

1. Breakdown is not dependent on the average exponential variation of drain voltage. Sparks have been found to occur at drains which vary in magnitude by a factor of as much as 10^4 : 1.

2. Surface outgassing inhibits the average electrode drain.

3. Breakdown is not associated with the gross outgassing or removal of the surface film of gas on the anode.

4. The actual mechanism which results in the switch from high to low impedance occurs in a time interval of the order of 10^{-9} sec.

5. Considerable quantities of surface gas are removed in the early stages of sparking. Only a very small quantity of gas, perhaps in the form of small patches, remains on the anode after sparking.

Other Developments

Field Emission Microscope. A Muller projection tube has been constructed for study of gross surface contamination. Modifications in design which were indicated in preliminary tests are nearing completion.

Fast Transmission Line. A fast transmission line and switch is nearing completion for a direct test of the positive ion-electron secondary emission multiplication theory of high voltage breakdown.

DECLASSIFIED 276 021

REFERENCES

[1]R. H. Fowler and L. Nordheim, Proc. Roy. Soc., v. 119:A, p. 173 (1928)

[2]L. Nordheim, Proc. Roy. Soc., v. 121:A, p. 626 (1928)

[3]A. Sommerfeld and H. Bethe, Handbuch der Physik (1934) v. 24, Part 2, Sec. 3, Art. 19, p. 436.

[4]F. R. Abbott and J. E. Henderson, Phys. Rev. v. 56, p. 118 (1939)

[5]W. P. Dyke and J. K. Trolan, Office of Naval Research NS-ONR-72401, NR-074-171 (1951)

[6]W. D. Coolidge, Jour. Frank. Inst., v. 202, p. 639 (1926)

[7]C. C. Lauritsen and R. D. Bennett, Phys. Rev., v. 32, p. 850 (1928)

[8]Tuve, Breit and Hafstead, Phys. Rev., v. 35, p. 66 (1930)

[9]Schmidt, UCRL BP-29 (1946)

[10]Trump and Van de Graaff, Jour. Appl. Phys., v. 18, p. 377 (1947)

[11]Rother, Ann. d. Physik., v. 81, p. 317 (1926)

DECLASSIFIED 270 022

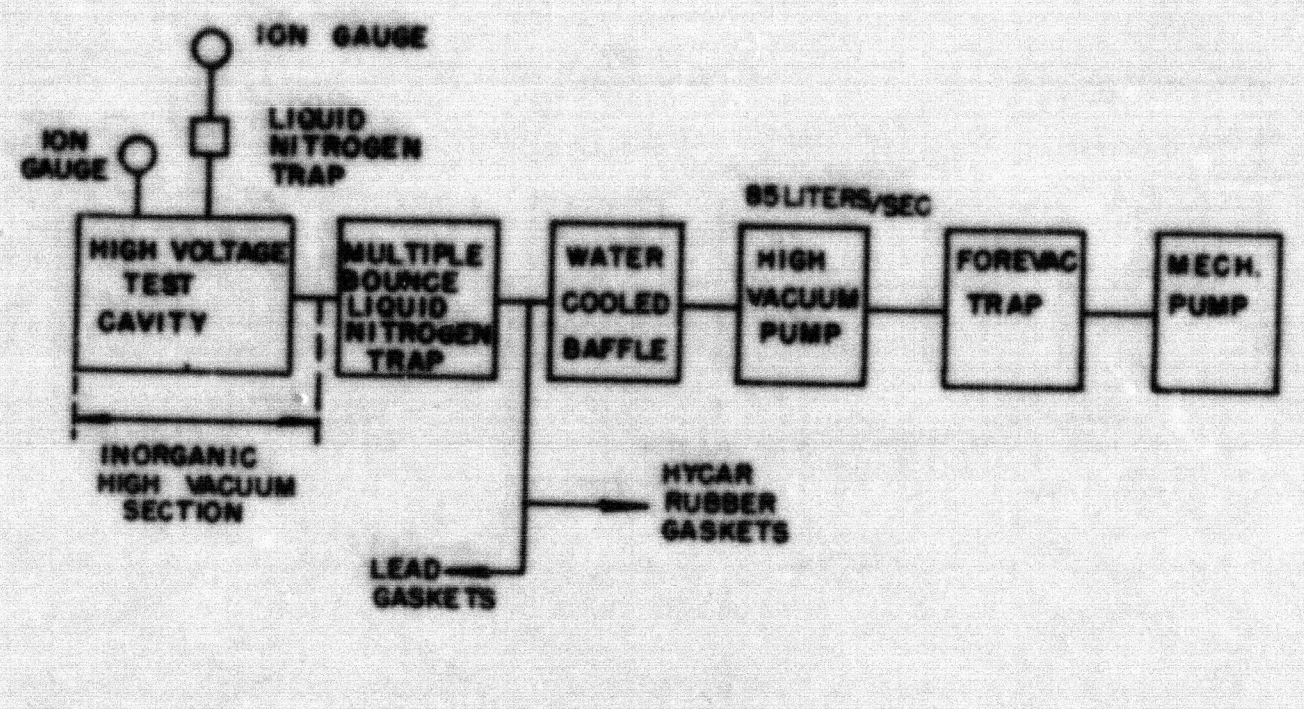

HIGH VACUUM TEST CAVITY

FIG. 1

MU3230

276 033

DECLASSIFIED

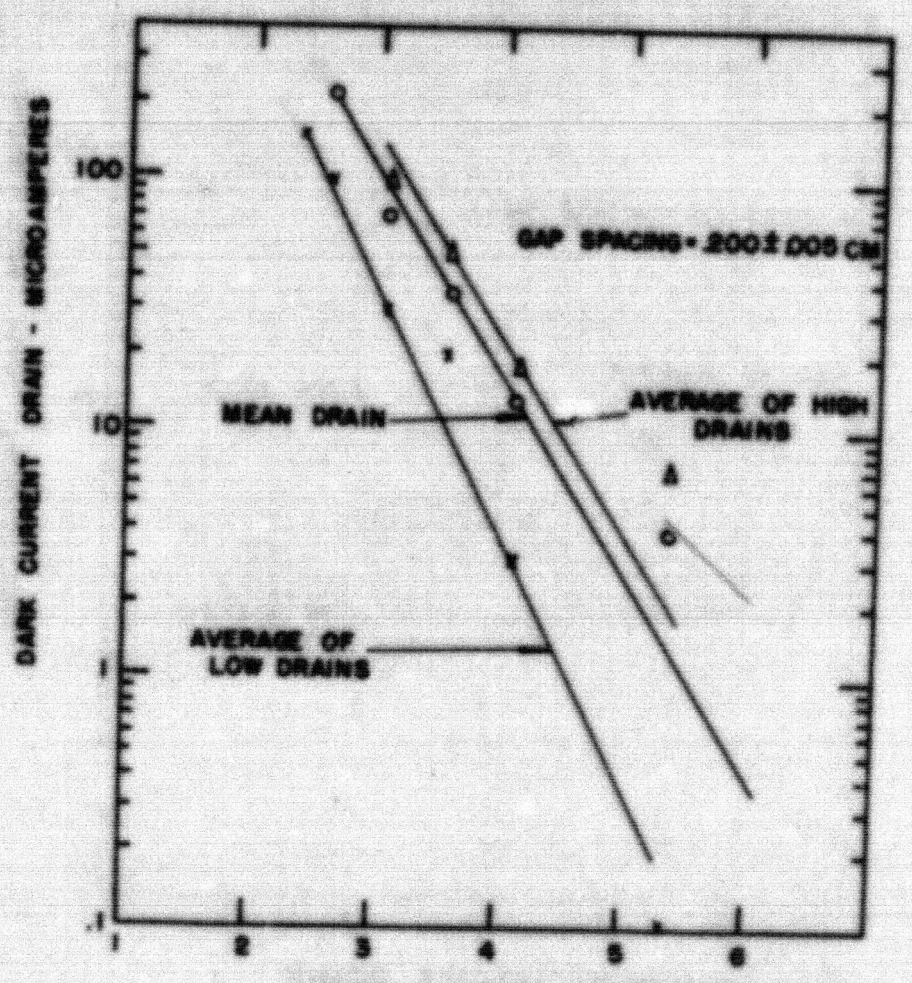

FIG. 2

MU3231

270 034

DECLASSIFIED

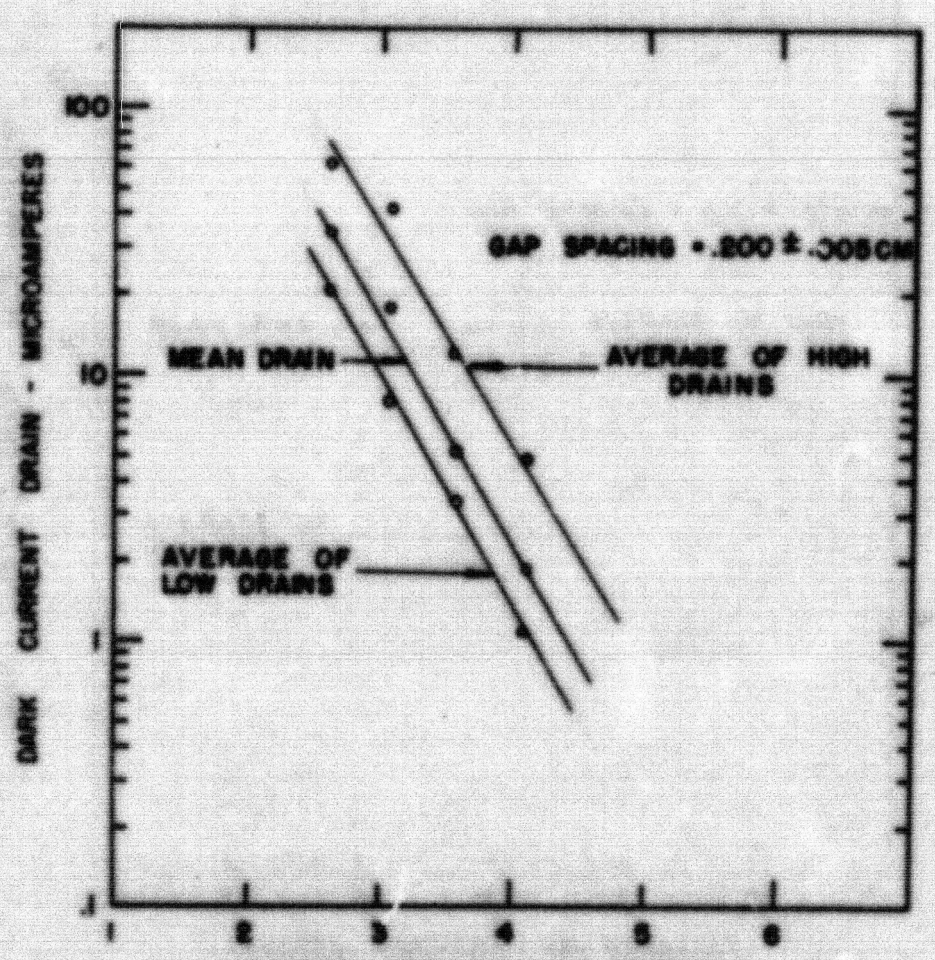

FIG. 3

MU3232

270 035

DECLASSIFIED

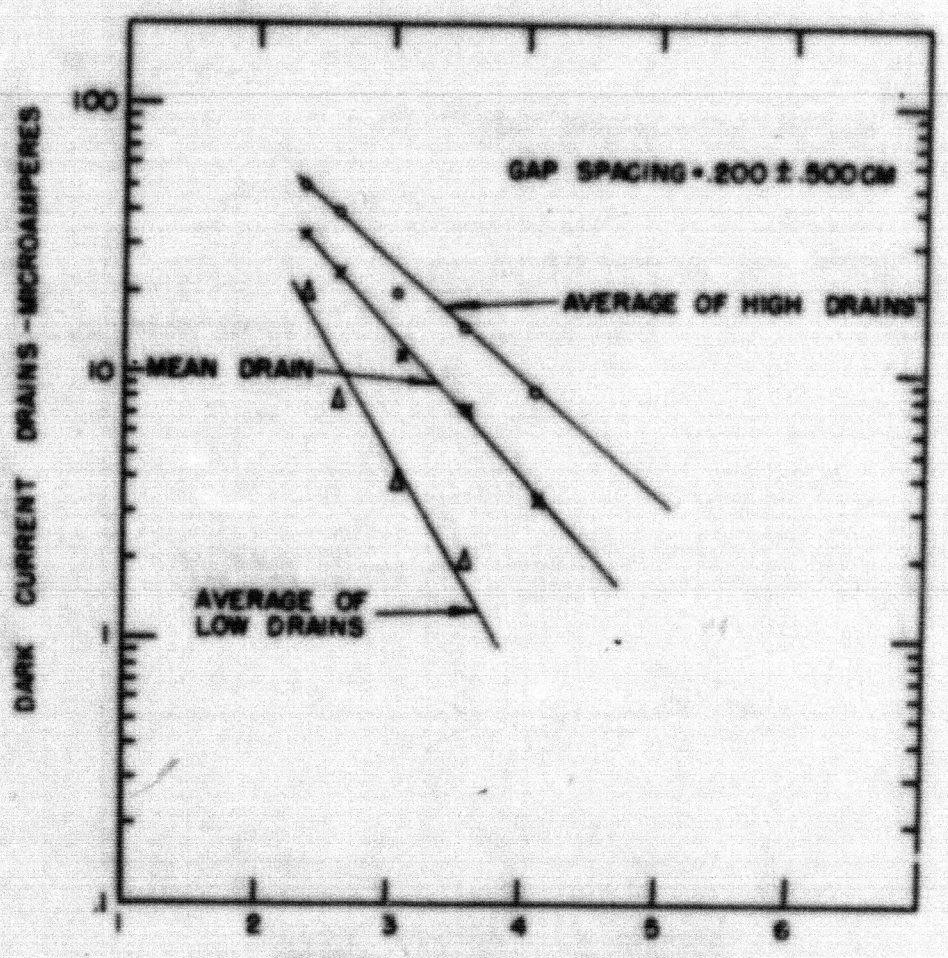

FIG. 4

MU 3233

DECLASSIFIED

276 036

Fig. 5 Copper cathode after approximately 100 low energy sparks in the system when pumped with Myvane 20 oil. Note brown oil ring just outside of heavy discharge area. Surface deposit is globular.

276 037

DECLASSIFIED

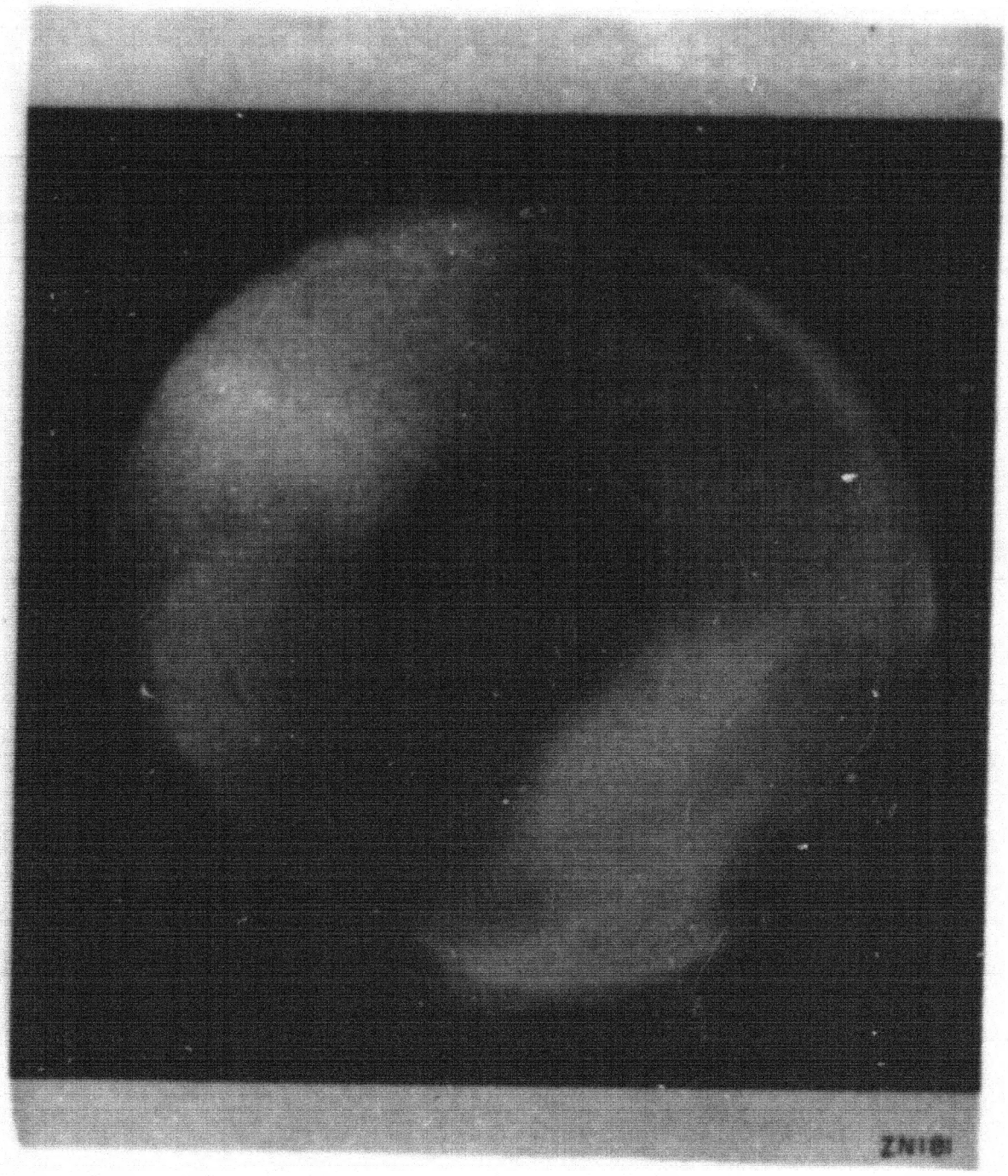

Fig. 6 Copper anode (mate to above) surface has many craters near center and bright ring around outside.

DECLASSIFIED 276 028

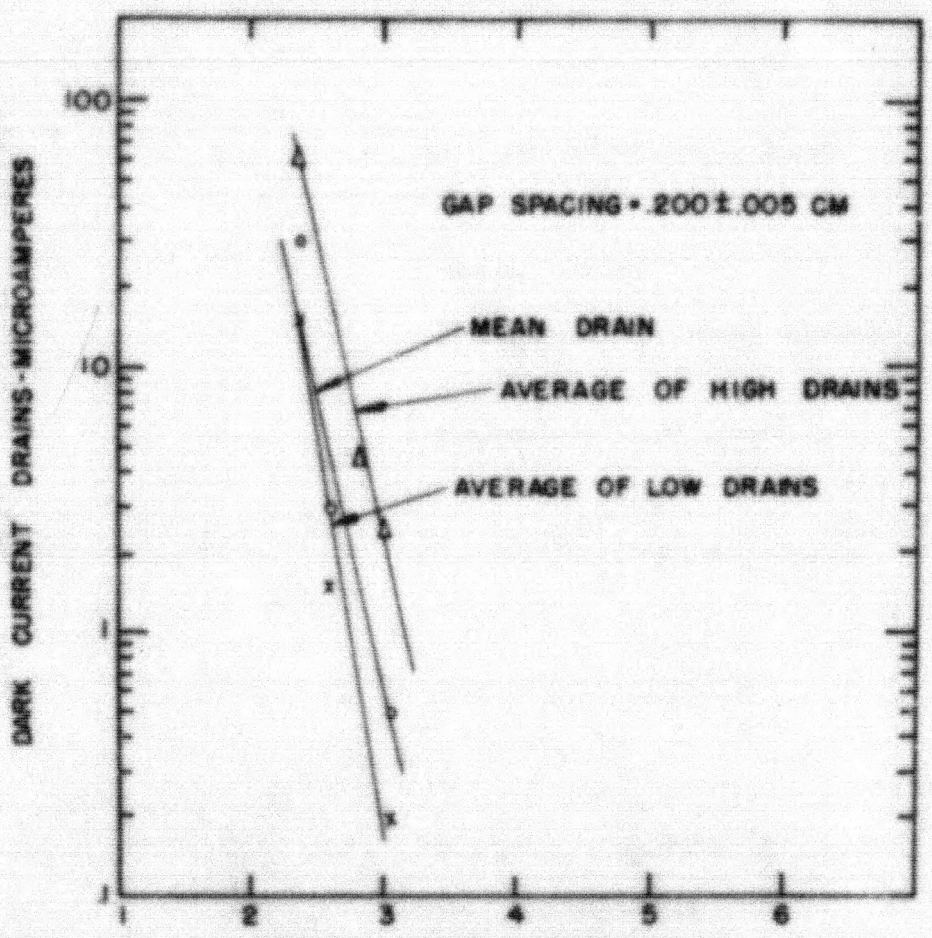

FIG. 7

MU 3234

Drain Versus Gradient for Two-Inch Diameter Hemispheres
Electrolytic copper electrodes polished with steel wool, cleaned with Duth Cleanser and washed with C.P. Acetone
Electrodes baked for 2 hours at 775° Cg. System pumped on Myvane 20 Oil with DPI MC-500 diffusion pump. Liquid Nitrogen trapping used.

Tank Pressure: 1.1×10^{-6} mm Hg (L.N. trapped gauge)
1.6×10^{-6} mm Hg (untrapped gauge)

DECLASSIFIED

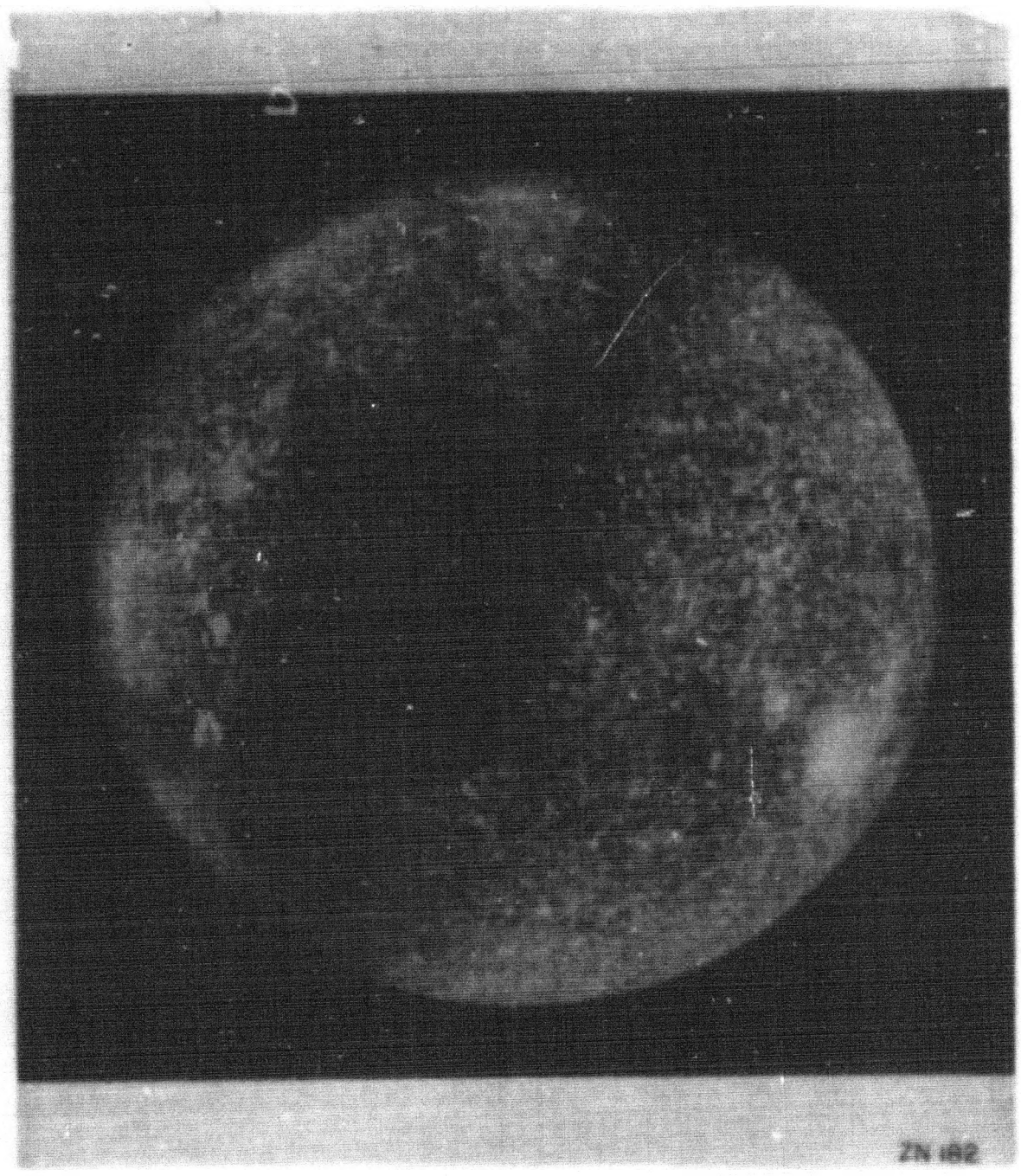

Fig. 8 Copper cathode after two hour bake at 775°C. Myvane 20 oil used as pumping fluid.

DECLASSIFIED

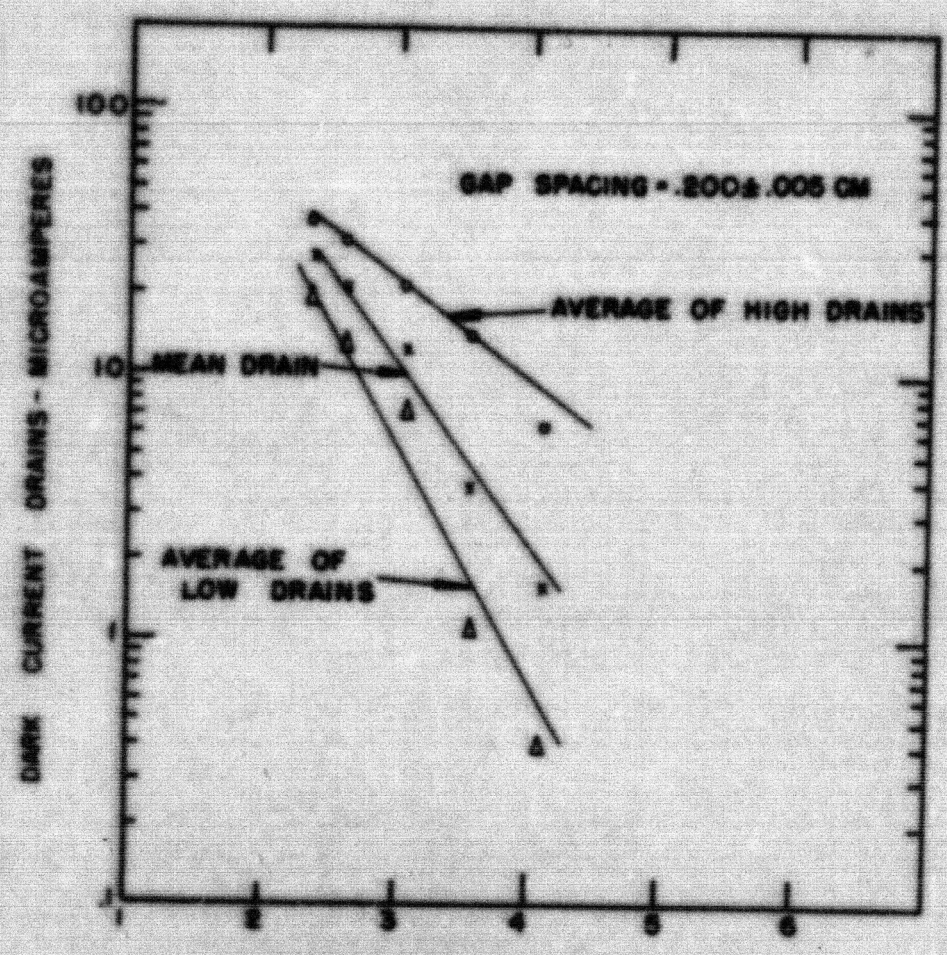

FIG. 9

MU 3235

Drain Versus Gradient for Two-Inch Diameter Hemispheres
Electrolytic copper electrodes polished with steel wool, cleaned with Dutch Cleanser and washed with C.P. Acetone. System pumped on Myvane 20 oil with DPI MC-500 diffusion pump. Electrodes baked 1 hour at 775° Cg; forevac to 200 microns for approximately 1 minute to allow oil to backstream. Oil contamination baked 1 hour at 775° Cg. Liquid Nitrogen trapping used.
Tank Pressure: 7.2×10^{-7} mm Hg (L.N. trapped gauge)
1.2×10^{-6} mm Hg (untrapped gauge)

276 041

DECLASSIFIED

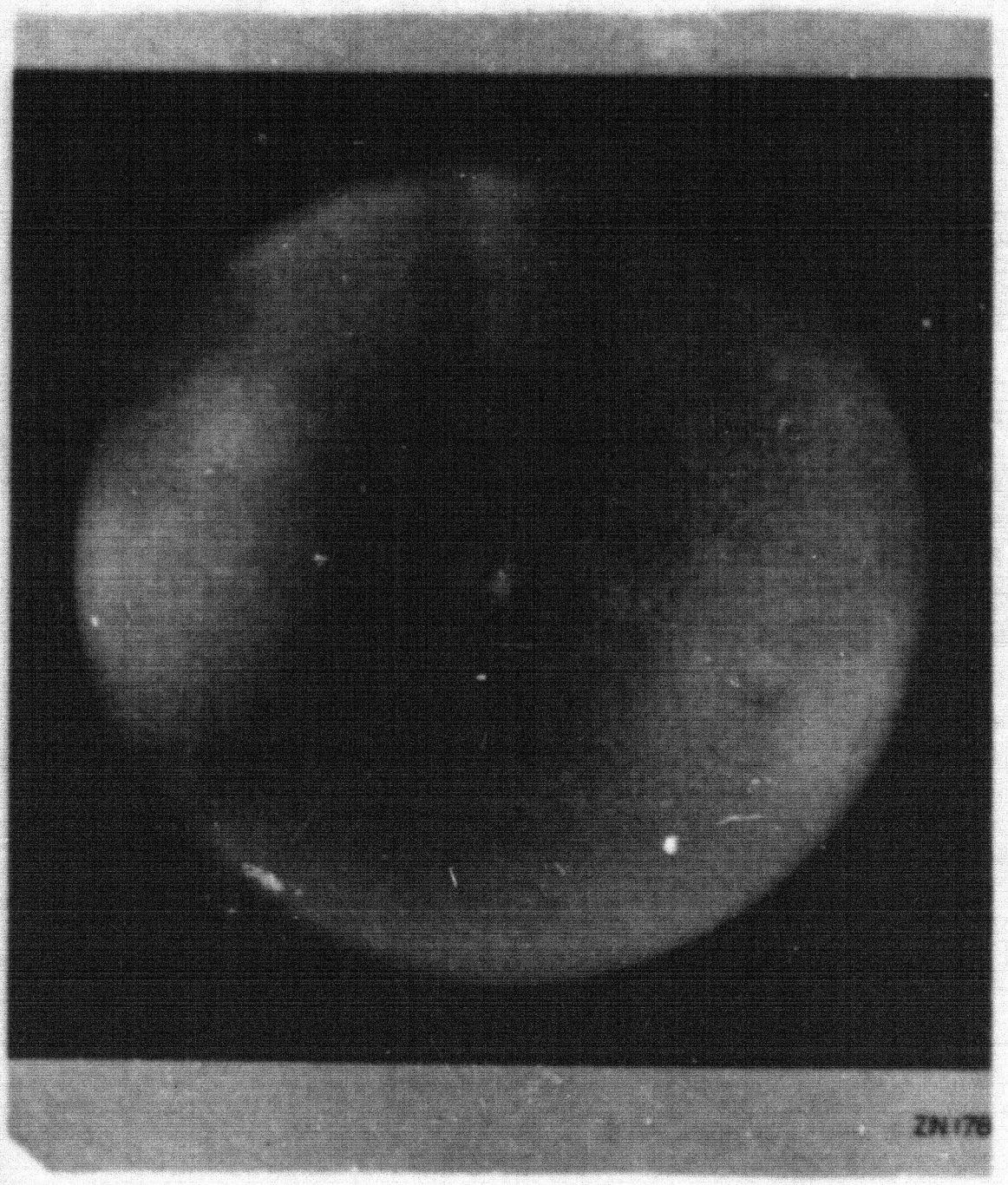

Fig. 10
Copper anode after heavy sparking (energy per spark 3800 joules) Note the large number of small cavities in the surface

DECLASSIFIED

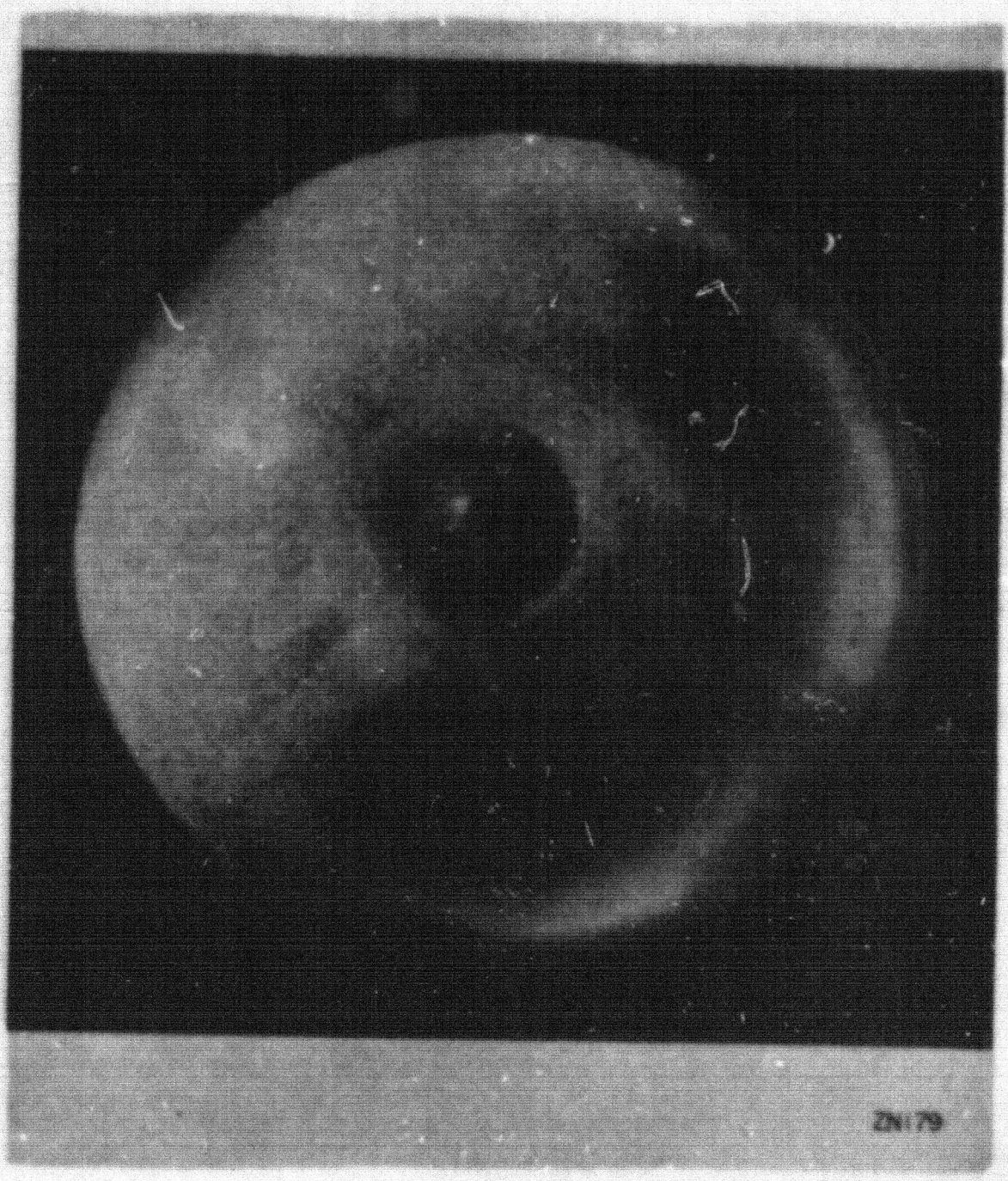

Fig. 11 Copper cathode after heavy sparking. Note globular structure of cathode deposit.

276 043

DECLASSIFIED

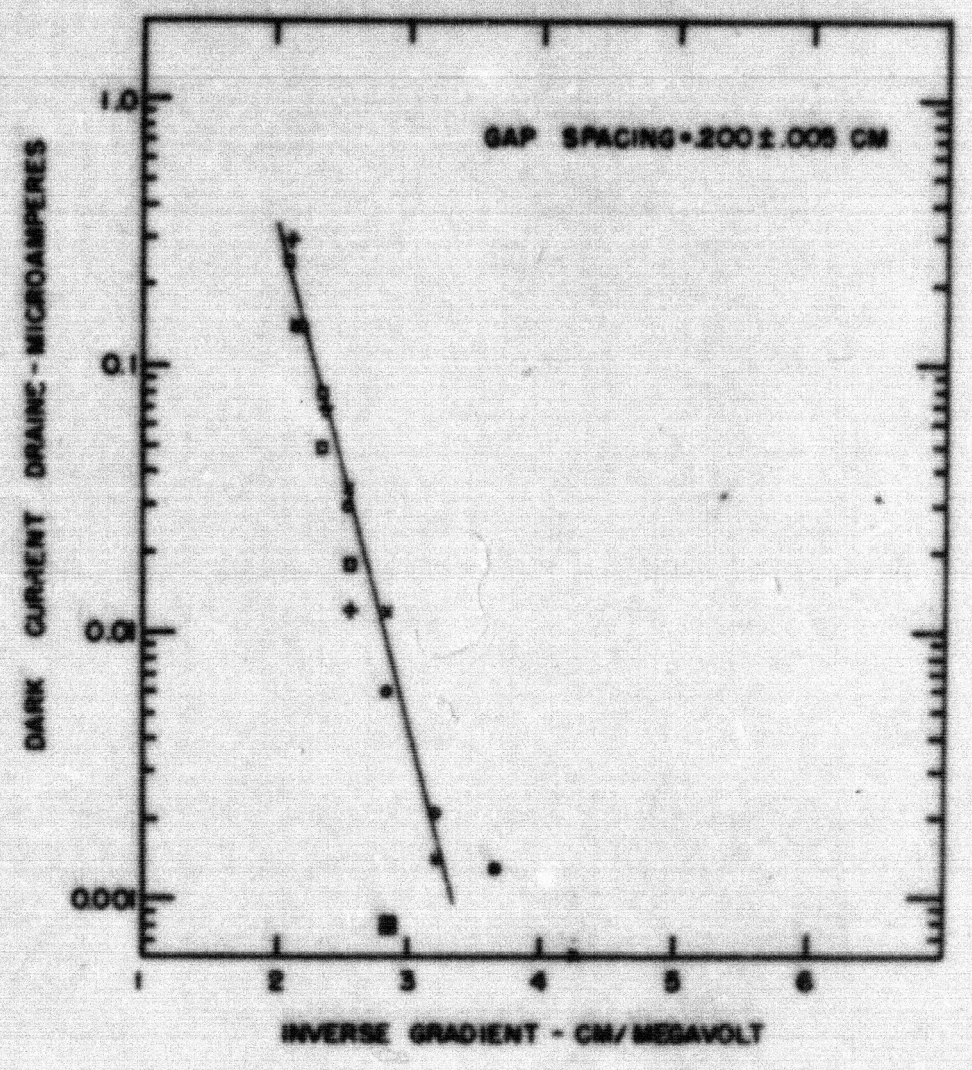

FIG. 12

MU 3236

ain Versus Gradient for Two-Inch Diameter Hemispheres

ectrolytic copper electrodes polished with steel wool, cleaned with Dutch Cleanser
d washed with C. P. Acetone. System pumped with mercury. Liquid Nitrogen trapping
ed.

k Pressure: 1.7×10^{-7} mm Hg (L.N. trapped gauge)

DECLASSIFIED

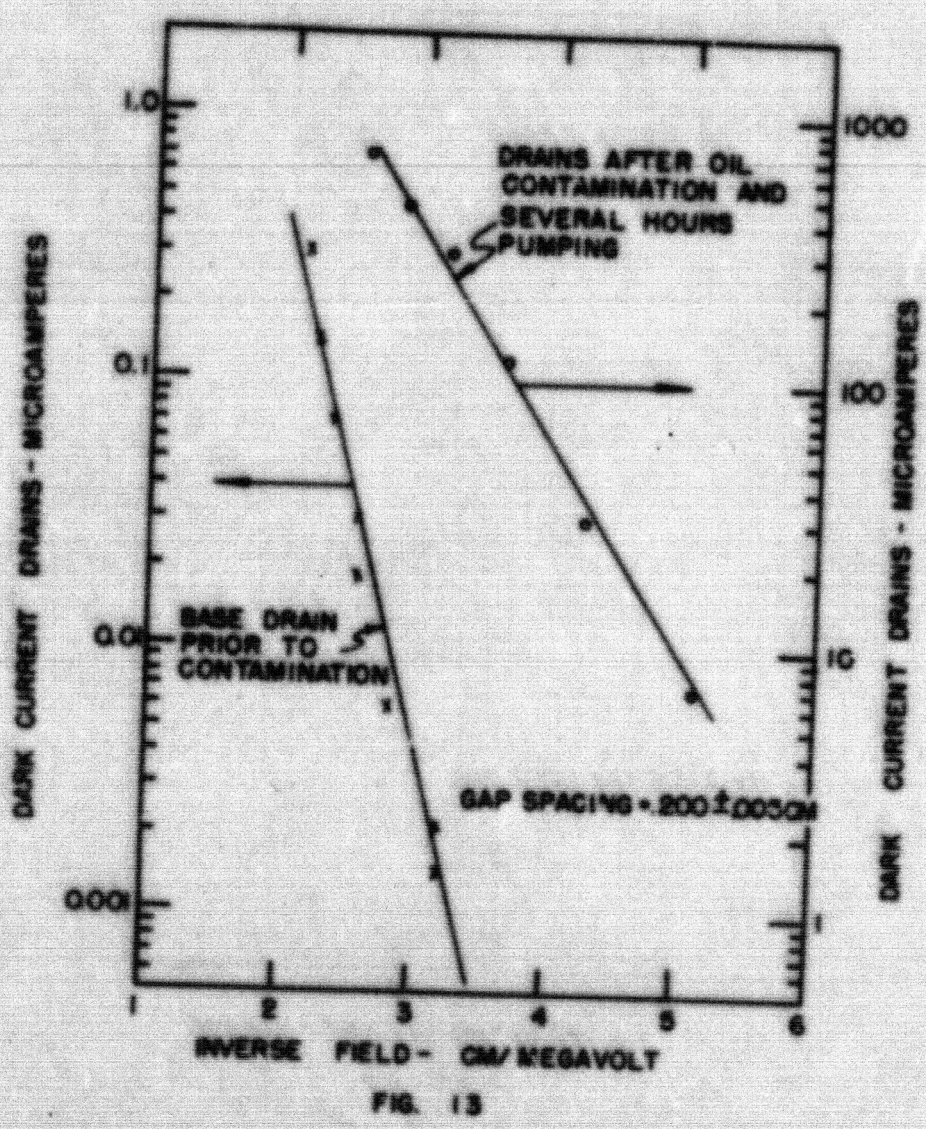

FIG. 13

MU 3237

Drain Versus Gradient for Two-inch Diameter Hemispheres
Electrolytic copper electrodes polished with steel wool, cleaned with Dutch Cleanser and washed in C.P. Acetone. System pumped with mercury. Myvane 20 oil contaminant released into cavity when base drains were taken.
Tank Pressure: 1.8×10^{-6} mm Hg (untrapped gauge)

270 045

DECLASSIFIED

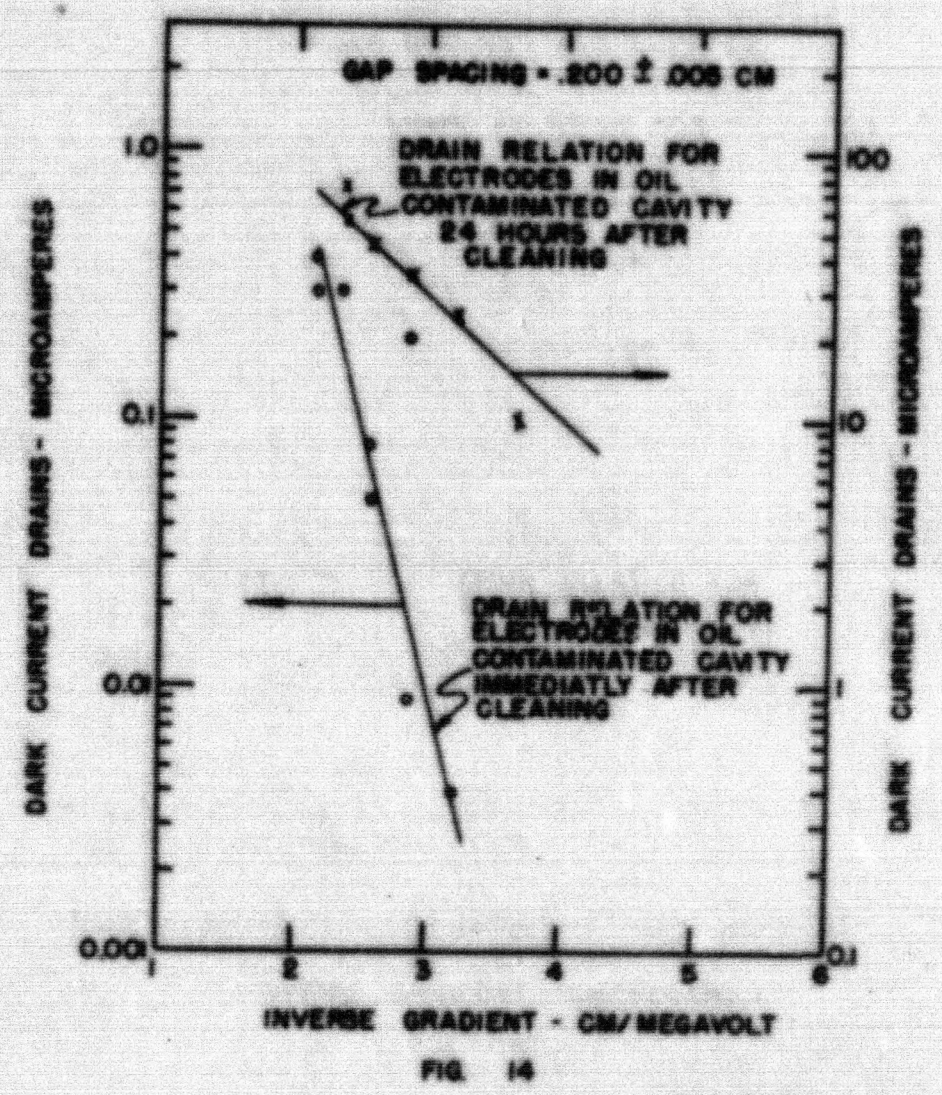

FIG. 14

MU 3238

in Versus Gradient for Two-Inch Diameter Hemispheres

trolytic copper electrodes removed from contaminated system, polished with steel l, cleaned with Dreft and distilled water, washed in C.P. acetone and returned to cavity. Electrode drain taken immediately and 24 hours later.

276 766

DECLASSIFIED

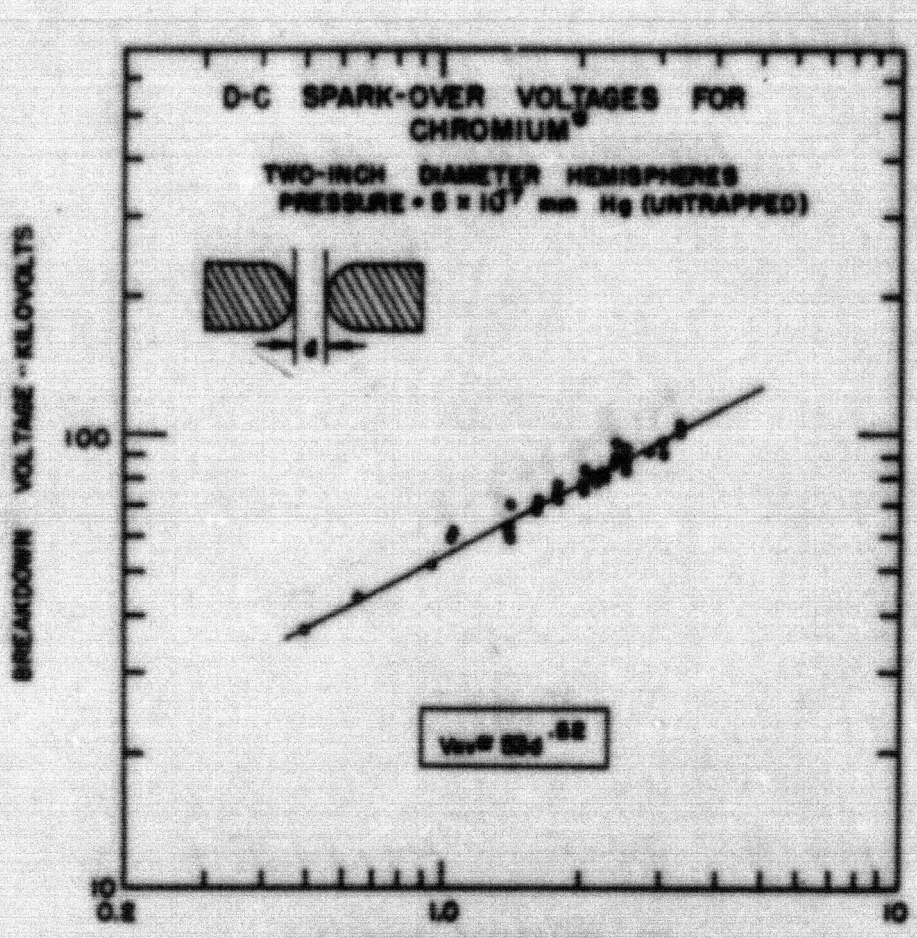

* HARD CHROMIUM PLATE .001 INCH THICK OVER COPPER

FIG. 15

MU 3239

270 047

DECLASSIFIED

Figs. 16 and 17. Drain and gas pressure versus voltage for 2-inch diameter hemispherically-capped cylinders of stainless steel. Spacing = .25 ± .05 mm. All voltage axes are horizontal. Scale is 4,000 volts per minor division. Current and pressure axes are vertical. Scale for current: 4×10^{-6} amperes per minor division. Scale for pressure: 4×10^{-7} mm Hg per minor division at 10^{-6} mm Hg. Mercury pumped system. In each frame top trace is gas pressure and bottom trace is drain.

276 645

DECLASSIFIED

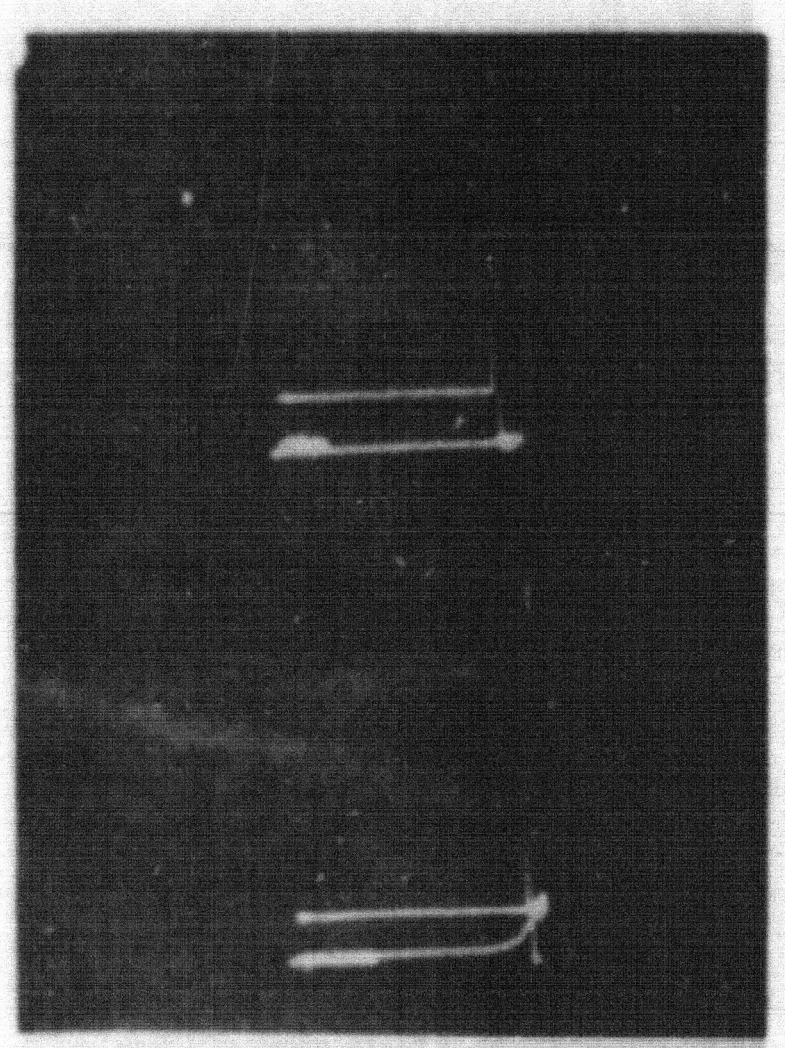

Fig. 16.1 Top Frame

Phase II: gas burst occurs several seconds prior to spark. Ion gauge tripped off scale by a Δ p of greater than ten from a base pressure of 1×10^{-6} mm Hg.

Fig. 16.2 Bottom Frame

Beginning of drain-spark relation in Phase III. Gas bursts trips ion gauge several seconds prior to spark.

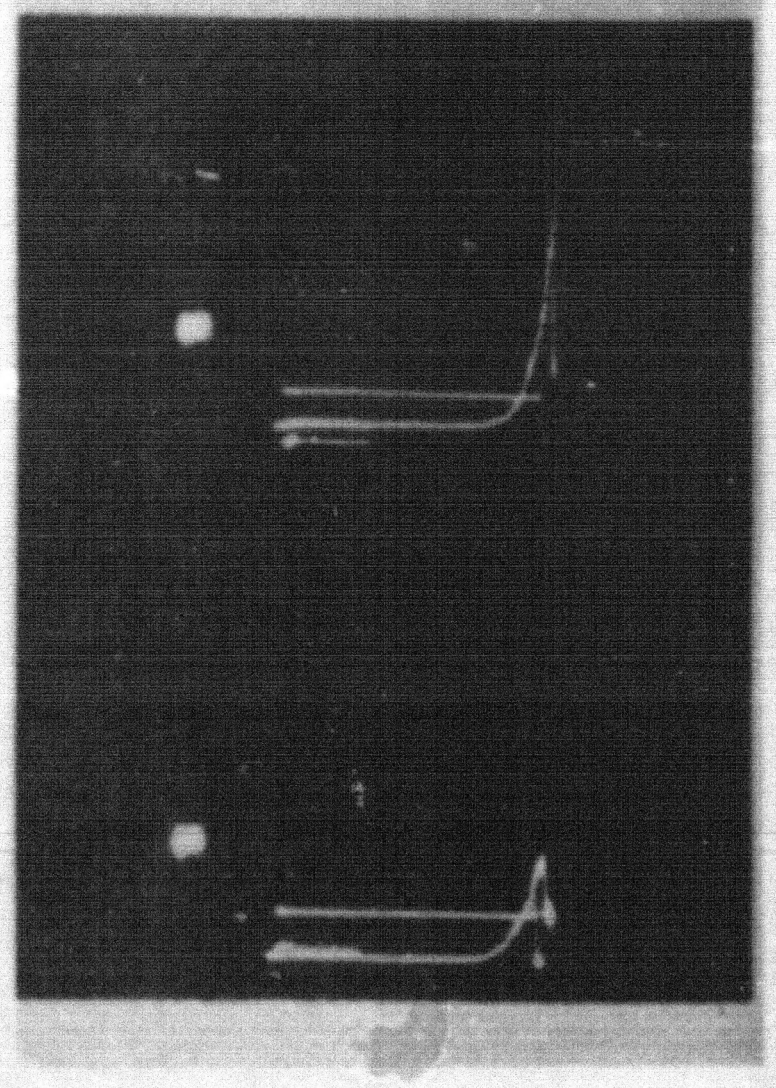

Fig. 17.1 and 17.2

Drain rises exponentially prior to change in cavity pressure. Gas burst causes an immediate reduction in electrode drain. Spark occurs several seconds after drain has been reduced by gas burst, i.e. Phase III

276 049

DECLASSIFIED

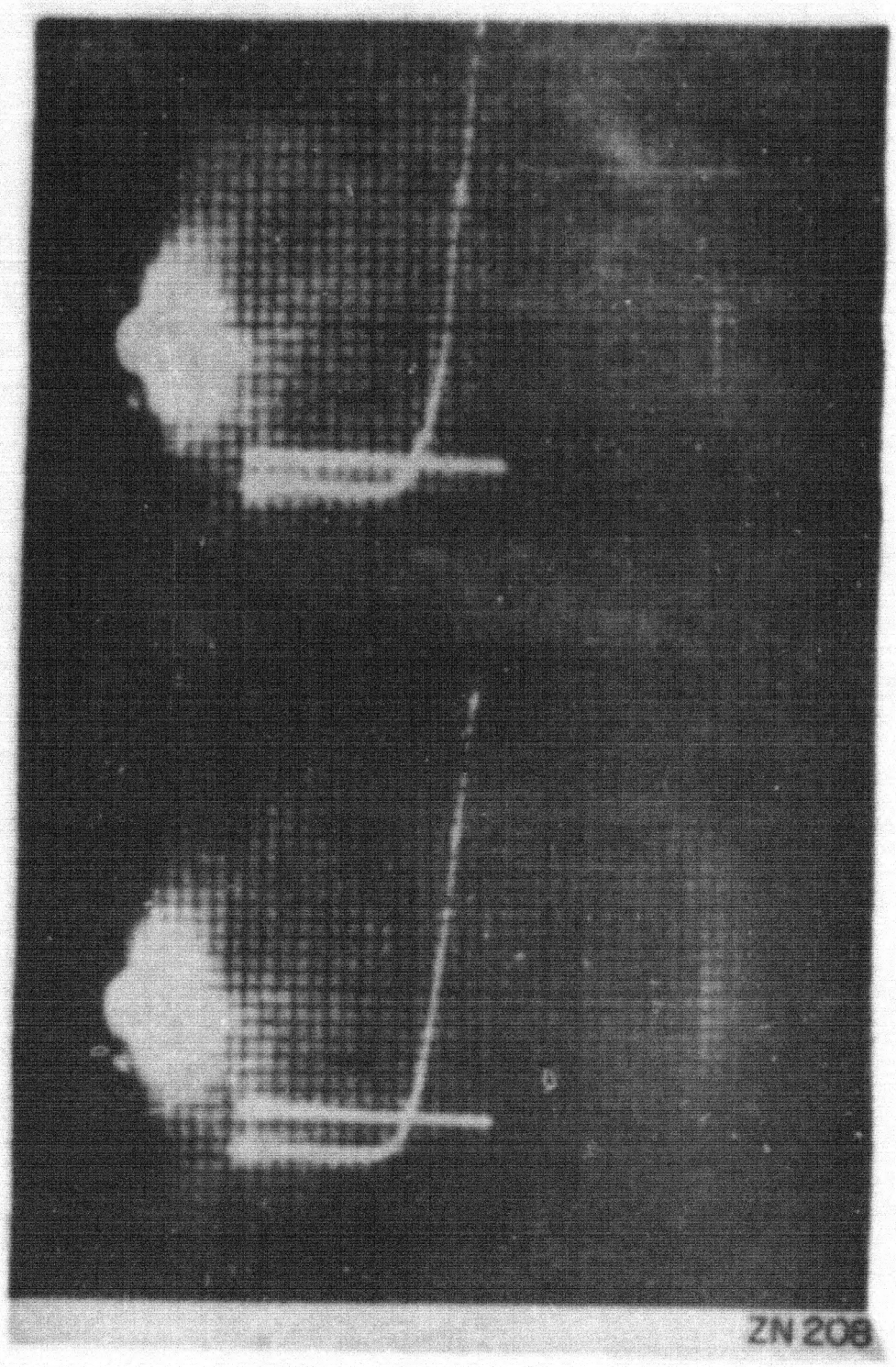

Fig. 18.1 and 18.2. Drain and gas pressure versus voltage for 2-inch hemispherically-capped cylinders of stainless steel. Spacing = .25 ± .05 mm. All scales and axes are the same as in Fig. 16 and 17. Note that in Phase IV (shown in these photorruphs) Δp is not greater than 4×10^{-7} at 1×10^{-6} mm Hg. Pressure remains sensibly constant while drain increases exponentially with voltage until breakdown or until the condensers across the gaps become fully charged. Drain has been known to remain within 200 microamperes for a period of minutes before breakdown occurs.

DECLASSIFIED

5. ION PUMP DEVELOPMENT

J. Foster and E. J. Lofgren
UCRL

Purpose of the Ion Pump

Existing evidence indicates that the presence of oil and possibly of mercury, will increase the sparking troubles in Mark I. For this reason, arrangements have been made to baffle the diffusion pumps. The baffles are to be cooled with liquid nitrogen, and it is hoped that this will prove to be sufficient, although it represents quite an operating cost. The purpose of the present ion pump investigation is to determine as soon as possible whether an ion pump can be developed which would be more satisfactory for this application than existing diffusion pumps.

General Description

The following is a rough description of the mechanism believed to be involved in the present system. A PIG type discharge is set up between a filament and cylindrical anode. Fig. 1 shows the essential elements of the system. The axial magnetic field and reflecting cathode force electrons from the filament to make many oscillations through the arc. Neutral gas molecules within the arc are ionized by electron impact, and are given some additional kinetic energy. The magnetic field confines these ions to helical paths, and hence they progress along the arc, making frequent collisions with other ions and electrons as they go.

If the magnetic field is strong, and the arc length is not too long compared to the anode diameter, the ions will have a very good chance of reaching the cathode or filament. Once an ion arrives at either the cold cathode or filament it may pick up an electron and now, as a neutral particle, it is unaffected by the fields and drifts away. If this molecule enters the arc again, it is ionized and returned to the cathode. There is also evidence indicating that some positive ions arriving at the cathode surfaces form non-gaseous compounds or mixtures and hence are "removed" directly..

In the regions of the arc where large numbers of molecules are being ionized continuously, there tends to develop a space charge of positive ions. This arises because electrons which leave the collisions have more mobility than the positive ions and hence leave the scene quickly. The more slowly moving positive ions feel a dispersive force due to their own space charge. This then results in a slight gradient within the arc column itself, tending to force positive ions toward the cathode.

This is the pumping action: gas within the anode region is quickly ionized and transported to the cathode; but very few ions in the arc ever get to the anode.

Experimental Models

During the last few weeks six designs have been sketched up and so far three of these have been built and investigated. The various models are designated by number, and a brief summary of the features found in each is

DECLASSIFIED

given below. Many of the components that were built for one unit were used on its successor. The dates after each unit denote the period of operation.

Ion Pump No. 1 (October 17, - November 6, 1951)

This model was the first to be completed and is shown in Fig. 2 .

(a) The lowest gas pressure measured at the center of the arc was at least 3.3×10^{-5} mm.

(b) It was found that by using a rather deep cathode grid, a pressure differential could be maintained between the center of the anode and the exit. This means that gas was actually pumped from a region of low pressure, 5×10^{-5} mm, to one of higher pressure (50×10^{-5}mm).

(c) A gas leak was admitted at the center of the anode, and the pressure read at an adjacent point. In this manner, pumping speeds of at least 800 l/s were measured. Larger arc diameter gave greater speeds.

Ion Pump No. 2 (November 13, - December 3, 1951)

The purpose of this model was to determine the effect of using two magnets some distance apart, so as to provide more access to the central region of the arc. (Fig. 3) In particular it was desired to measure the pumping speed resulting from a more exposed arc, and the pressure of this configuration.

(a) The base pressure was 2×10^{-5}mm. It is not known whether this is limited by the arc length or field shape or both.

(b) Pumping speeds up to 6000 l/s were measured.

(c) Various cold cathode diameters were used, and in each case the magnetic fields had to be adjusted so that the arc covered the whole cathode area, if the lowest pressure was to be obtained.

Ion Pump 2A (December 7, - December 14, 1951)

In this model, the magnet spacing was adjustable (Fig. 4).

(a) Larger magnet spacing resulted in higher center pressures, and the use of increased magnet current would restore the low-pressures.

Ion Pump No. 3

This design was never used as a complete unit. However, various components were built and used on the other models.

Ion Pump No. 4 (November 8, - December 12, 1951)

This model was built in an attempt to reach lower base pressures. The arc was ~10-1/2 feet. (Fig. 5.)

(a) The base pressure was 1.8×10^{-6}mm.

276 052

DECLASSIFIED

(b) The ratio of exit pressure to center pressure was greater than 600:1.

(c) Pumping speed measured at the center was 1800 l/s.

(d) Additional gas leaks were let in at the cold cathode end and at a point 20" from the center toward the exit. The results showed the center pressure to be virtually independent of the other leaks provided the total gas leak did not exceed 0.06 cc/sec. (S.f.P.)

(e) The cold cathode was made movable, thus changing the arc length. Shorter arc lengths gave higher pressures.

(f) The use of a filament at the exit end made it possible to start the unit at a pressure of 2×10^{-3} mm.

Ion Pump No. 5

This model was started as soon as the center pressure on No. 4 dropped below 5×10^{-6}. The object was to build an ion pump that would actually pump down a cavity. This unit is due to be tested on December 20, and if operation is satisfactory, it will be moved as a unit and connected to B-1. (Fig. 6)

Ion Pump No. 6

One of the principle mechanical problems is to design the manifold connecting a vacuum system to the arc so that it has a speed comparable to the speed of the exposed arc. Since the magnetic field must be maintained, an obvious answer is the use of a magnet winding in the vacuum, consisting of one layer of wire with considerable space between turns. The design shown in Fig. 7 is being built into an existing vacuum tank. The aperture speed of useable helix length is about 8000 l/s.

Operation and Controls

As has been indicated above, no model has been used to pump down anything but a very small volume. However, some comment on the operation of the models during experiments may be helpful. One notes from the various figures that these models still use a diffusion pump. There are several reasons for this, the primary one being that the ion pumps are experimental and with some geometries it is necessary to start the pump at low pressures. Also, no real effort has been made to design the exit region to handle exit pressures above two microns. However the speed required to remove gas from the exit may be at least five hundred times less than that of the ion pump, just because of the pressure differential. Hence, whether a diffusion pump or mechanical pump is used, it may need have only a relatively small pumping speed, and in either event from the point of view of contamination it would be isolated from the vacuum system by the arc.

The existing experimental models have controls for arc voltage and filament current. If a unit is disassembled for replacement of parts and then re-assembled, it will pump down to within 20 percent of its base pressure within about two hours if it is periodically adjusted. If it is adjusted for the lowest pressure, then the arc supply can be shut off and turned on a few minutes later and the unit will usually return close to its base pressure without tuning

0537

DECLASSIFIED

in a minute or two. No automatic controls have been designed, but arc conditions are quite steady and the control requirements are not stringent.

On the question of maintenance, little data has been obtained. Filaments are the most troublesome at present. Positive ion bombardment erodes the filament, usually in some local region. This is an unstable situation in that heating develops in those regions of the filament where the wire cross section has been reduced, and more arc current results. In extreme cases, heating due to the arc is so large that optimum arc conditions are obtained with little or no power from the filament supply. Larger diameter filament wire (.190") has helped to reduce this trouble, and the present filaments give 10-20 hours of experimental operation.

Magnetic Field

An attempt has been made to provide an adjustable axial magnetic field over the arc length, and in general this field has varied in magnitude from 500-3000 gauss. Experiments are being done to find out just how much field is needed, and what gradient is best. The most critical point in the arc tube seems to be where the gas input and pressure gauge is located. In most of the designs, this is because the magnetic field is very weak at this point. Fig. 8 shows the variation in center pressure on Model 2A, for various magnet separations and magnet currents. The next stage is to obtain a new set of curves for a larger anode diameter.

If there is a gradient in the magnetic field, then there exists a force on the ions and electrons in the direction of weaker field. Simple theory yields as a first approximation that the force F_z on particles with energy $V_\perp$ perpendicular to the axis, where the axial field strength is H_z, is given by:

$$F_z = \frac{-V_\perp e}{H_z} \frac{\partial H_z}{\partial z}$$

In some center sections that have been used in the models, this magnetic force is equivalent to an electric field as high as 0.3 volts/cm.

Model 4 usually runs with a lower field at the exit. However, since this reduces the arc cross section in the higher field regions of the tube effects are also present. Fig. 9 gives a plot of the magnetic field that existed when the best results were obtained.

Pumping Speed

The speed of the ion pump is measured just as one measures the speed of a diffusion pump. A leak L is let into the input region of the pump, and the corresponding pressure increase Δp in that region is recorded. The pumping speed S through that region is then given by S, where

$$S = \frac{L}{\Delta p}$$

Fig. 10 curve A, shows a typical curve that was obtained with Model 4

2276 054

DECLASSIFIED

Since most of the incoming gas molecules are ionized within a few inches of the point of entrance, the speed refers to only a short section of the arc. Figure 10 curve B also shows the change in center pressure when air is let in at a point 20" away, toward the exit. This indicates that very high speeds may be realized if one is able to expose large areas of the arc directly to the vacuum tank.

The Effect of Arc Lengths

From the base pressures that have been obtained on models to date, was found that longer models have given lower base pressures. However, since the pressure measuring techniques, exit geometries and available magnetic fields improved with each model, an accurate comparison is not possible. Present evidence indicates that the center pressure varies inversely as the arc length, in the range of arc length that has been studied.

On Model 4, the cold cathode was made movable and hence various arc lengths could be obtained. The optimum pressure at the center of the arc tube was recorded for each setting of the cathode. Note however that the ion gauge does not remain at the center of the arc. Fig. 11 shows the results. If one assumes that the arc center pressure does vary inversely as the arc length, then the pressure along a given arc is not constant but increases toward the ends. Fig. 12.

Arc Current and Voltage

The arc voltage and current are made somewhat independent by the filament control. Optimized values of arc voltage usually lie between 250 and 600 volts, but the actual value can be displaced anywhere within this range by control of the arc and filament supplies, without increasing the base pressure more than 20 percent.

Arc current on the other hand is often quite sensitive. The optimum arc current generally seems to reflect the "loading" on the arc. Figs. 13 and 14 show the change in optimized arc current with exit pressure and with various air leaks into the arc tube. The curves in Fig. 14 show a flattening off of the arc current at high leak rates. (0.06 cc/sec) The pumping speed curve (Fig. 15) also falls off in this region of leak. If air is let in at several points along the anode instead of just one point, then the curves flatten off when the sum of leaks is also about 0.06 cc/sec. This apparent "loading" of the arc is tentatively correlated with the following notion.

The total arc current is roughly due to electrons from the filament, ionization of molecules let in as a leak, and ionization at the exit of molecules that attempt to diffuse back up the arc tube. Normally the exit pressure is about 500 times the center pressure so that with the existing geometry, the rate at which molecules are ionized at the input leak is at least an order of magnitude lower than the rate at which molecules at the exit are ionized. Since the present arc supply is limited to about 15 amps, this means there is at most about 1 amp available to carry the air leak. The observation that the pumping speed drops for leaks above 0.06 cc/sec seems reasonable since 0.06 cc/sec corresponds to at least 0.5 amps of arc current. When lower exit pressures are used, the amount of leak that can be handled without "loading" is increased. (Fig. 16)

276 055

DECLASSIFIED

In the section on general operation, it was stated that electrons oscillate back and forth between the filament and reflecting cathode. This refluxing of the electrons represents a saving in electrical power. An experiment has been performed to demonstrate this point. The reflecting cathode was connected to anode potential so that little refluxing can occur. The data given below represent the best operating conditions under the two conditions. The effect of refluxing can be seen by the ratio of the required arc currents.

Reflecting cathode	Pressure at Reflecting cathode	Pressure at the center	Pressure at the exit	Arc volts	Arc amps.
grounded	2.8×10^{-5} mm	0.9×10^{-5} mm	12×10^{-5} mm	250	0.5
anode potential	6.6×10^{-5} mm	1.3×10^{-5} mm	16×10^{-5} mm	100	14

The exit pressures were deliberately reduced from 10^{-3} to about 10^{-4} mm in order to increase the range of available arc current.

Formation of Compounds

The following experiment was performed on Model No. 4. With the ion pump running, the gate valve to the diffusion pump was closed, so that there was no way for gas inside the system to escape. Then air was allowed to leak into the center of the anode tube (0.05 cc/sec). Over a period of one hour, the center pressure and exit pressure did not increase and arc conditions did not change appreciably. The experiment was performed again with an argon leak instead of air. In this case, the pressures rose and the situation went out of hand as soon as the gate valve was closed. With the gate valve open, the ion pump runs very well on argon. Helium gave the same results as argon.

At present the materials exposed to the arc are copper, molybdenum tungsten and stainless steel. There is evidence of considerable sputtering of the filament, reflecting cathode, and cathode shields. It is tentatively supposed that the above effects are due to the ability of some ions to form compounds. This effect has only just been noticed and further investigation is under way.

The group working on ion pump development during this period included W. Bassinger, P. Byerly, W. Chupp, B. Cork, W. Eukel, F. Fairbrother, J. Foster, R. Hester(CRDC), and E. J. Lofgren.

276 056

DECLASSIFIED

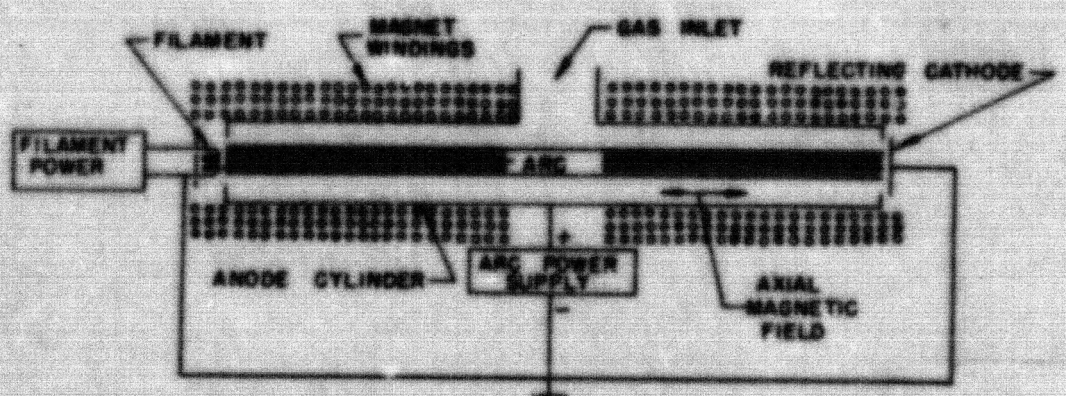

FIG. 1

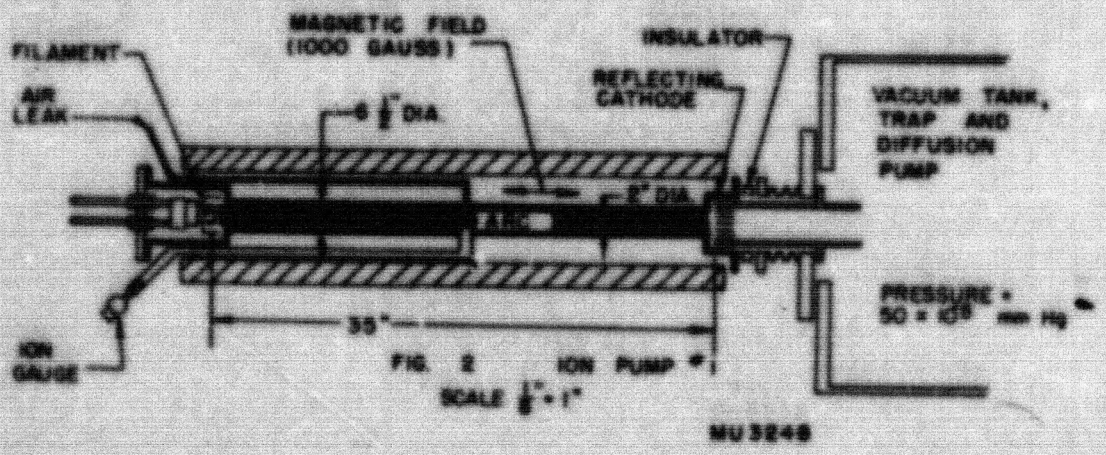

MU 3248

276 057

DECLASSIFIED

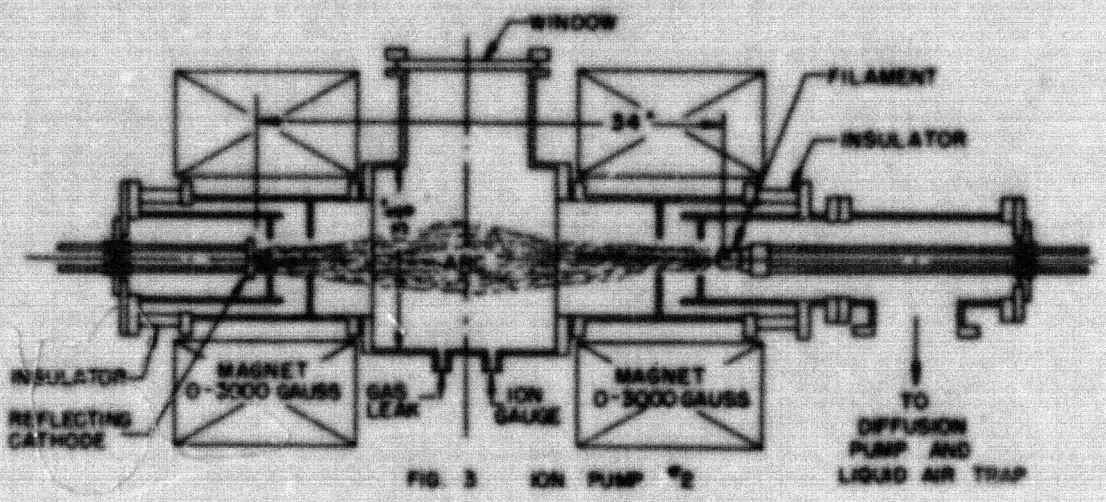

FIG. 3 ION PUMP $^{\#}2$

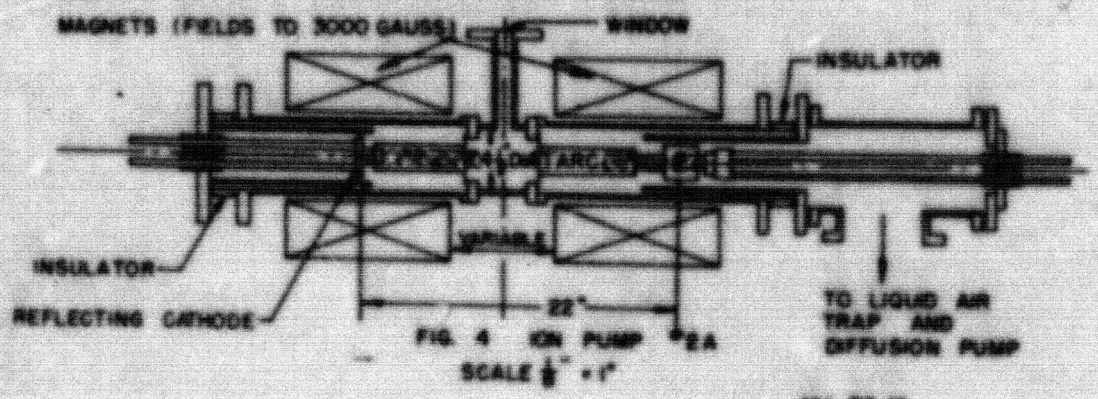

FIG. 4 ION PUMP $^{\#}2A$
SCALE $\frac{1}{2}$" = 1"

MU 32 49

DECLASSIFIED

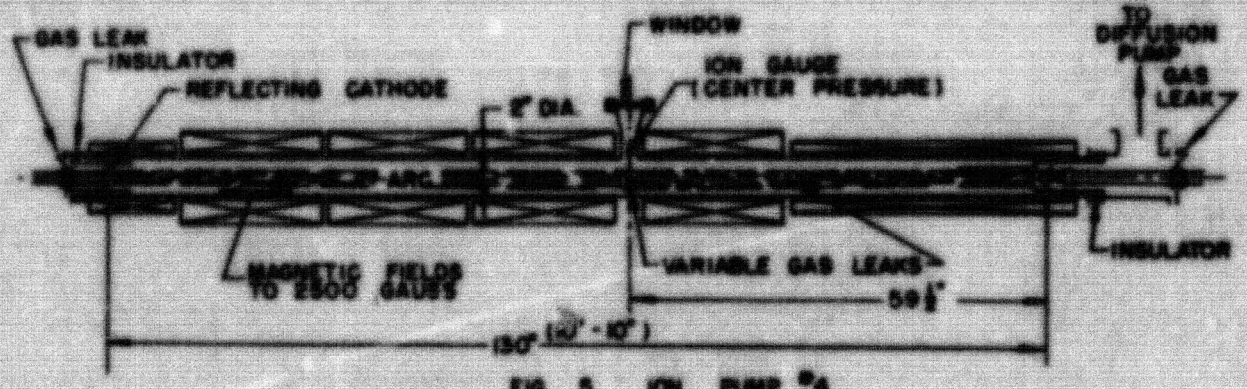

FIG. 5 ION PUMP #4

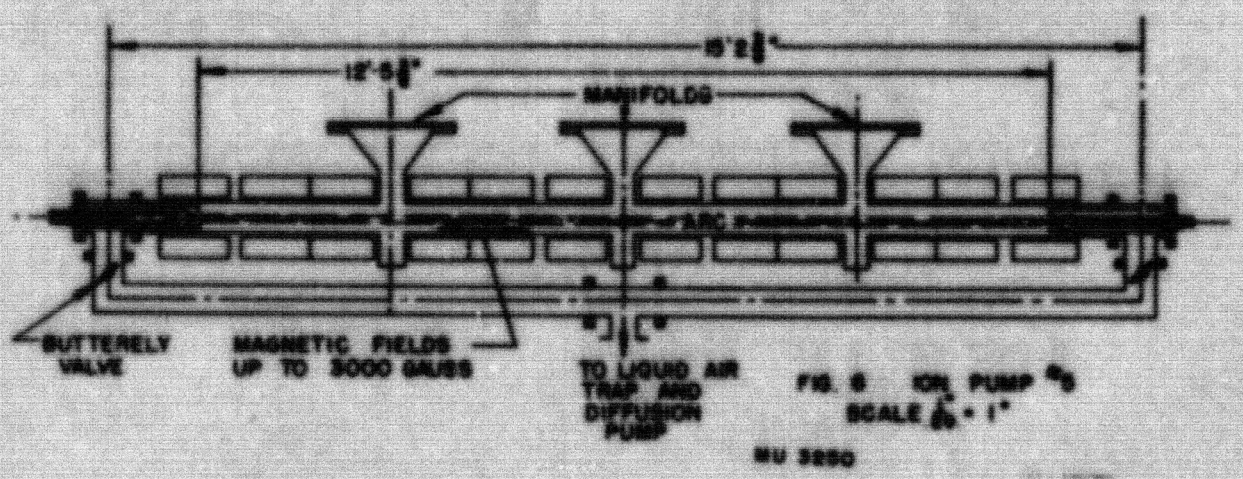

FIG. 6 ION PUMP #5
SCALE 1/8" = 1"

MU 3250

270 '59

DECLASSIFIED

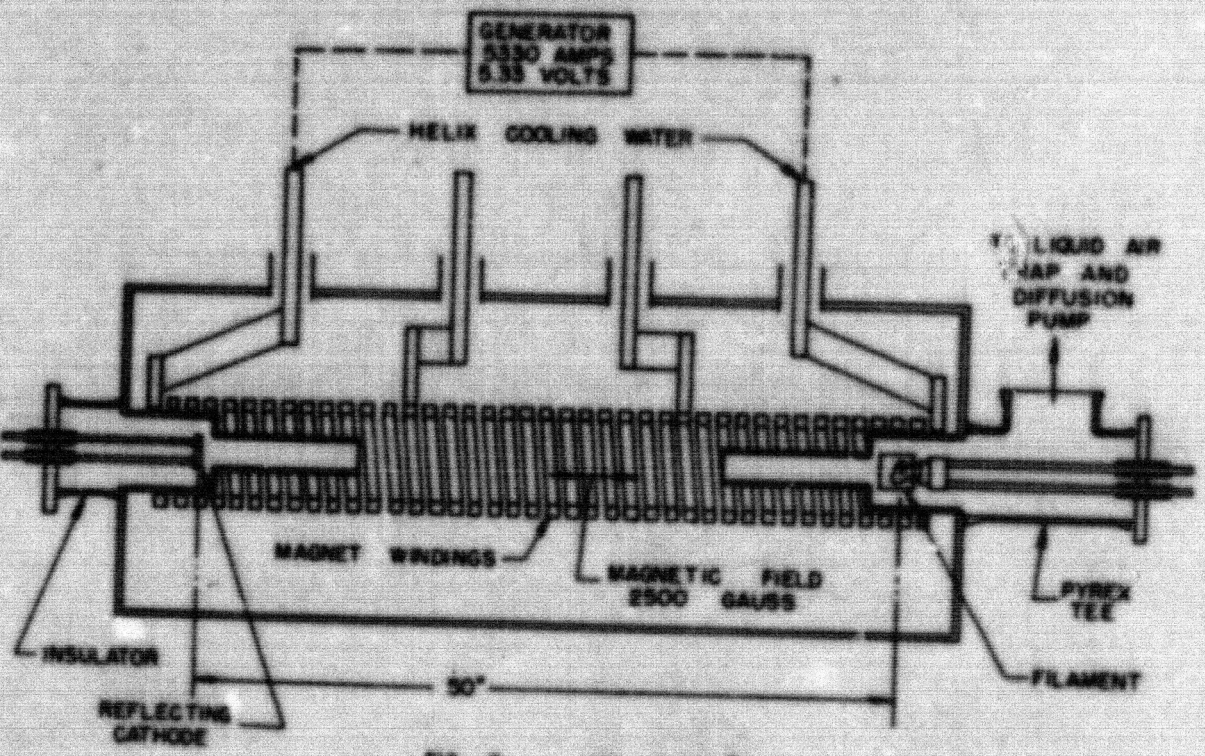

FIG 7 ION PUMP

SCALE $\frac{1}{8}$" = 1"

MU 3891

276 060

DECLASSIFIED

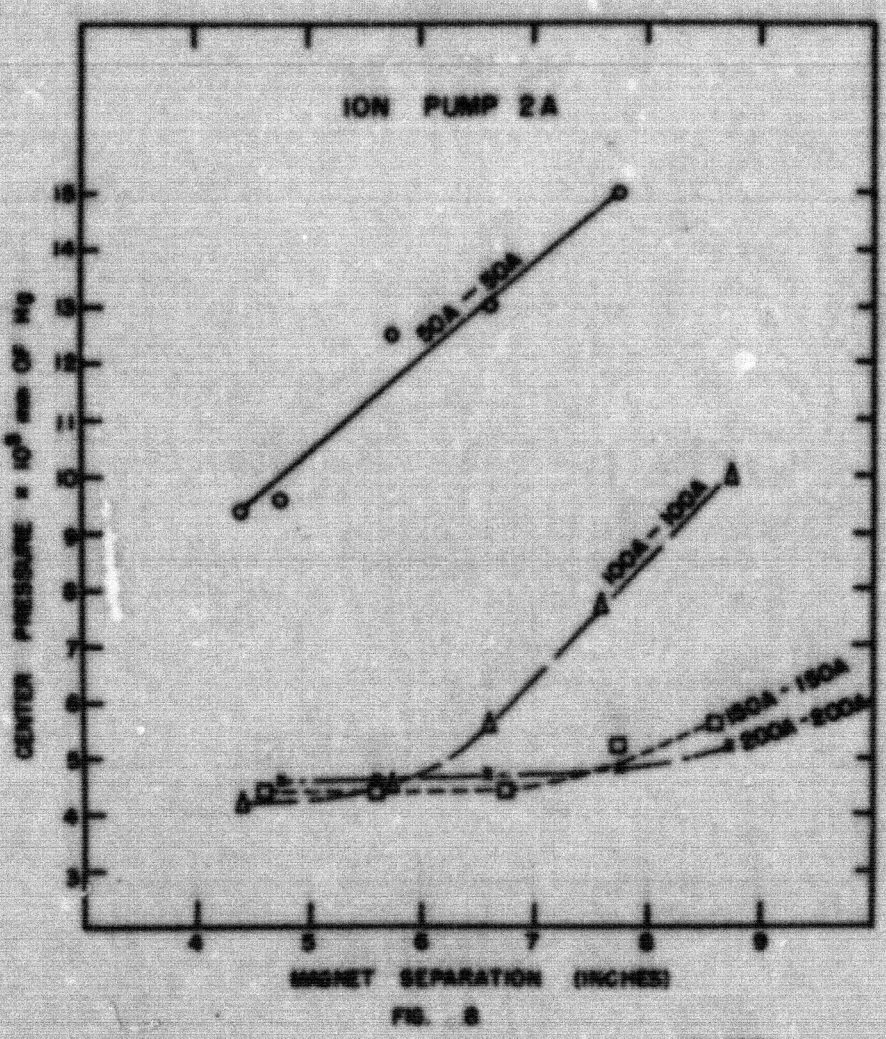

FIG. 8

MU 3252

27C-061

DECLASSIFIED

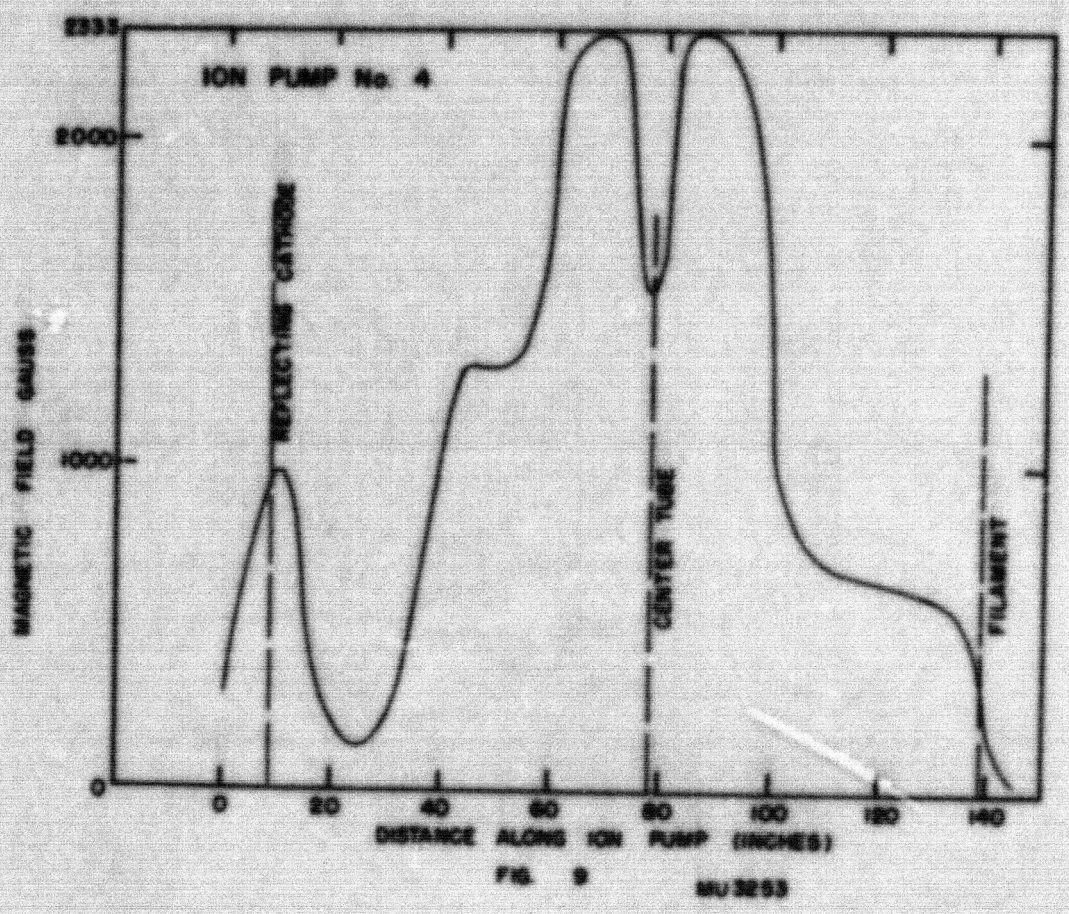

FIG. 9 MU-3253

DECLASSIFIED 276-62

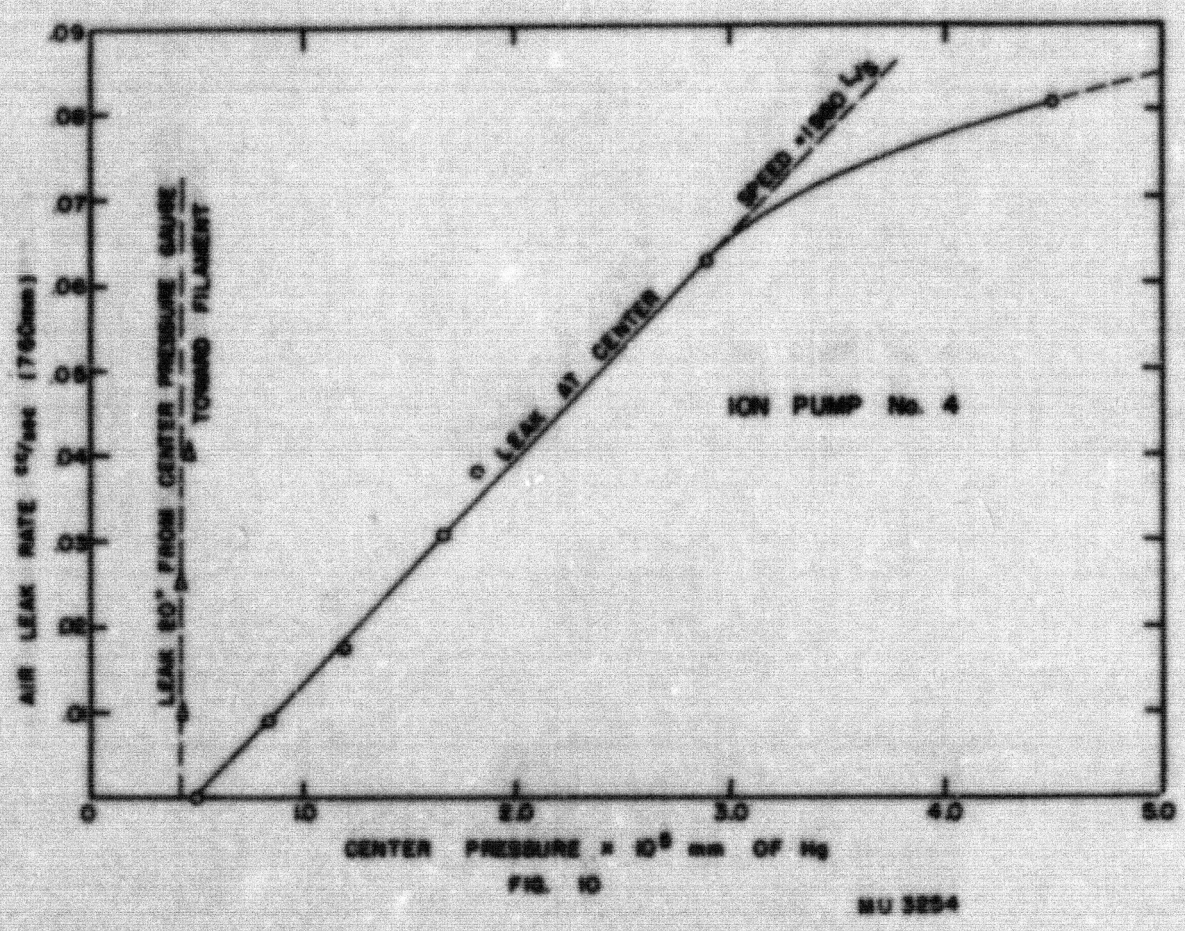

FIG. 10

MU 3854

276 -043

DECLASSIFIED

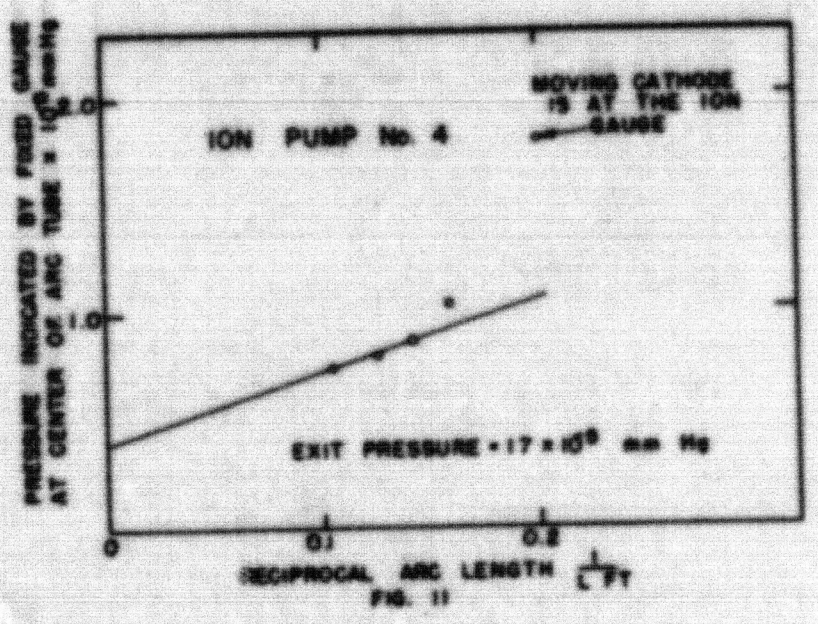

FIG. 11

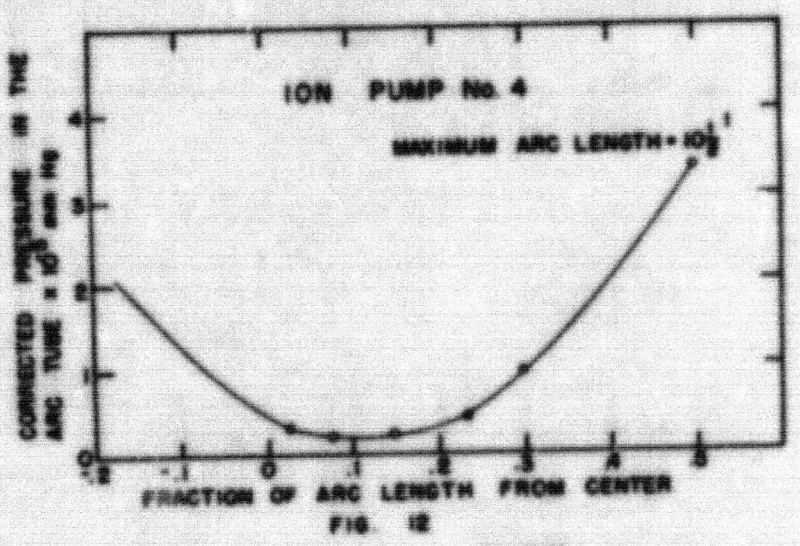

FIG. 12

MU3255

27C 064

DECLASSIFIED

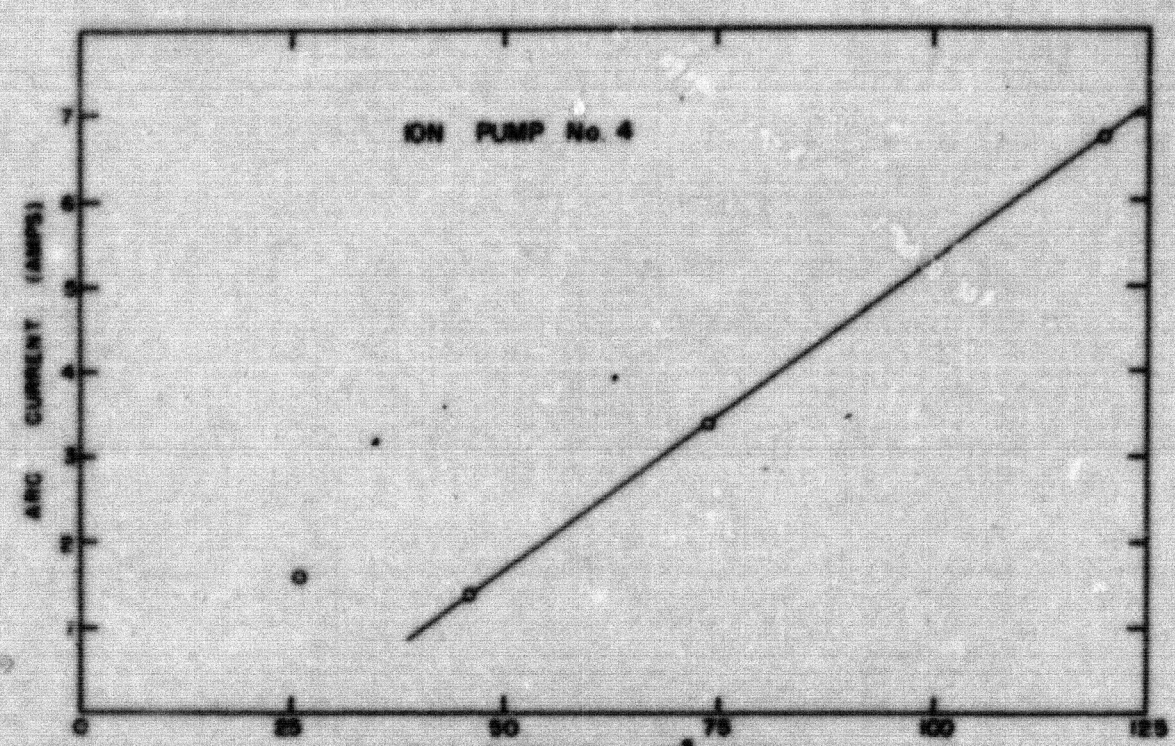

FIG. 13

MU 5256

DECLASSIFIED

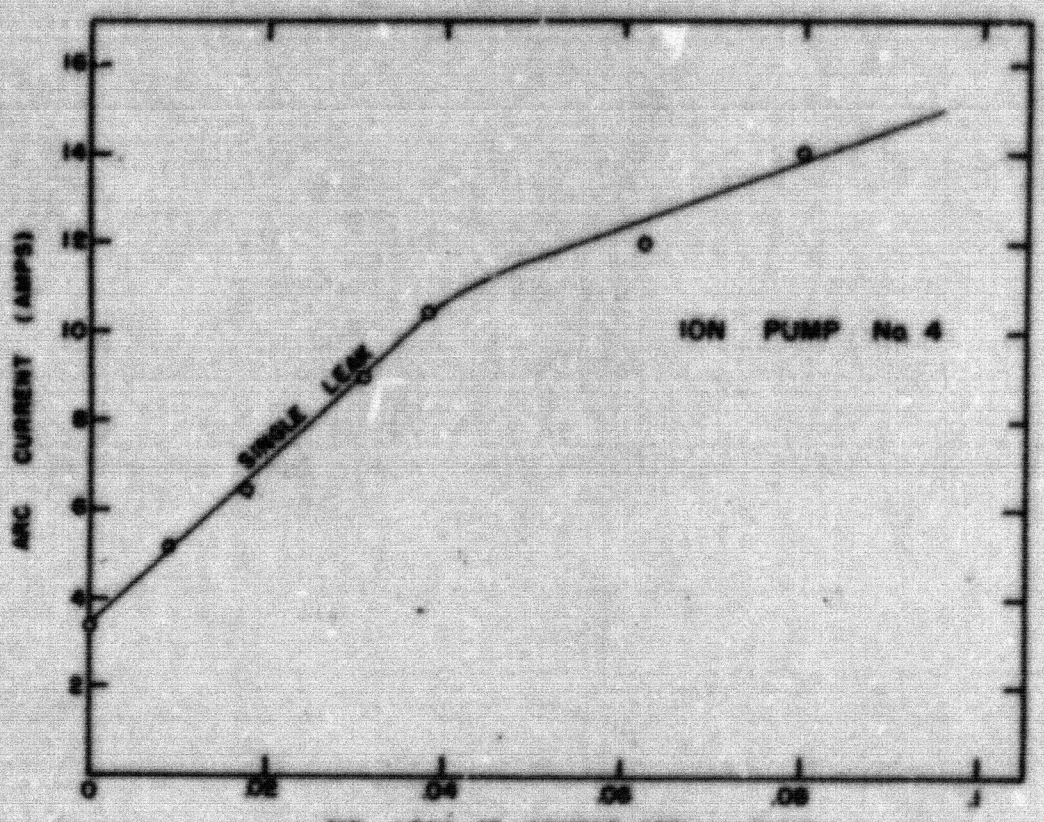

FIG. 16

MU 3257

DECLASSIFIED 276 066

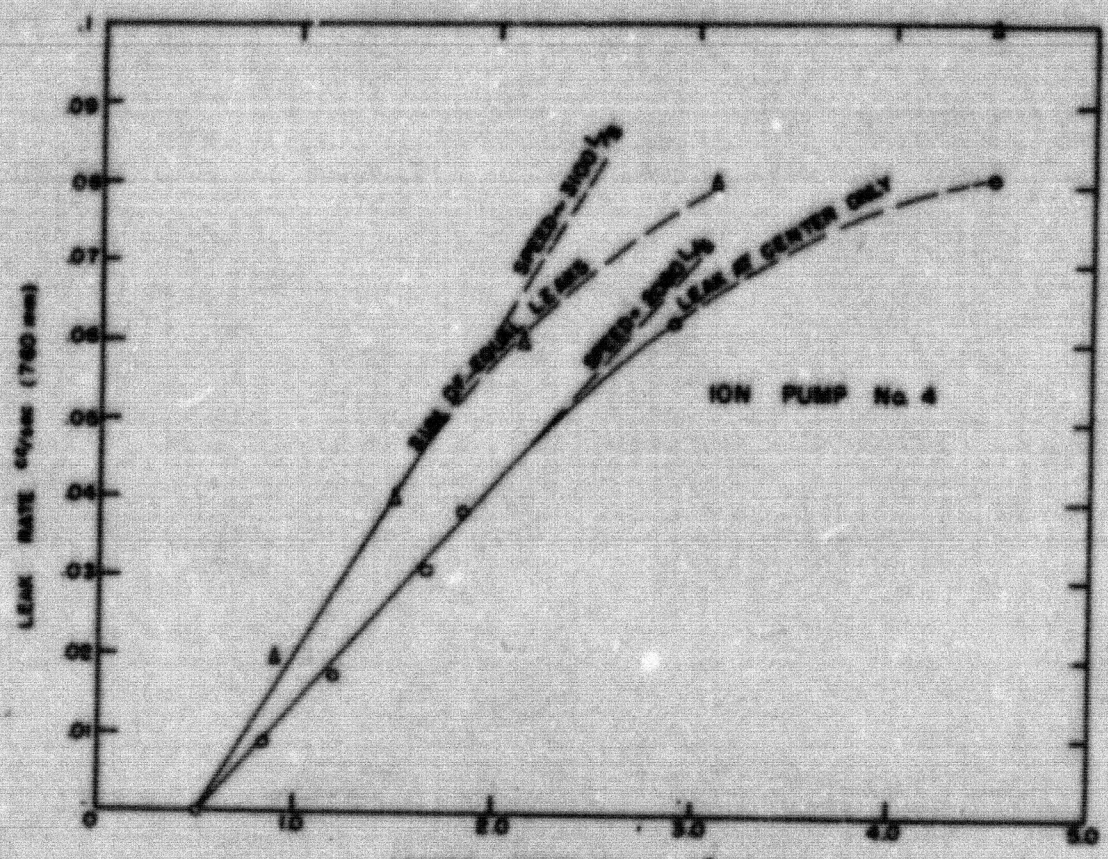

CENTER PRESSURE x 10^{-9} mm Hg

FIG. 15

MU 3258

276 067

DECLASSIFIED

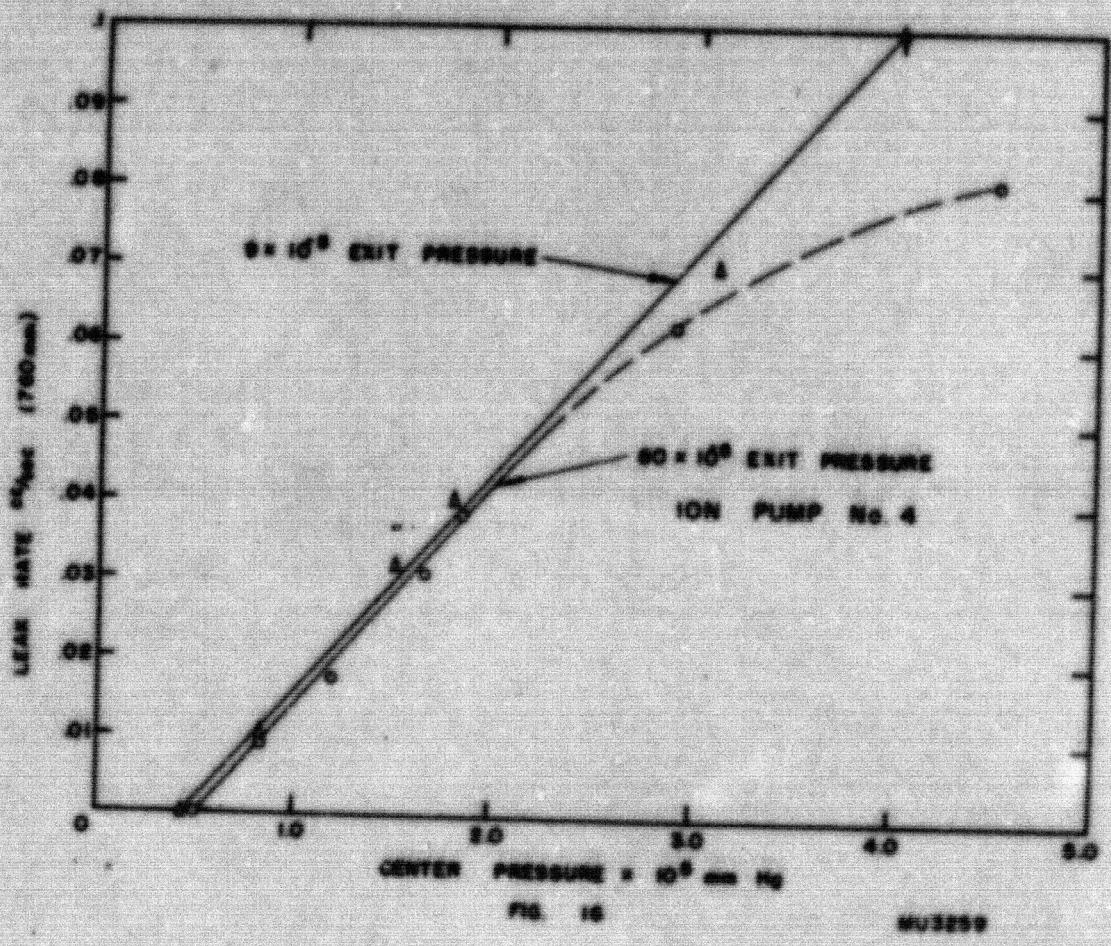

FIG. 16 MU3259

DECLASSIFIED

276 ccs

6. MARK I INJECTOR

W.A.S. Lamb, CRDC and E. J. Lofgren, UCRL

During this quarter the emphasis on the injector shifted from the testing and research of the full power model injector to the construction and preparation of the first plant model injector for testing. Research was carried on at a reduced rate on the following problems.

Injected Beam Profile

The intensity distribution of the injected beam, influences the shape of the beam from the accelerator and hence is of prime importance in the design of targets. The distribution of the injected beam was measured with a thermocouple probe, (See Fig. 1) and was found to be saddle shaped with about sixty percent of the maximum on the axis, and with the maxima occurring about 1-1/2 inches either side of the axis. The geometry which was used in these experiments was standard* geometry, with a grid in the grounded electrode. (See Fig.2)

Back Bombardment

Negative particles coming back to the injector from the accelerator are a possible source of damage to the components of the injector. As mentioned in the previous report two schemes are contemplated to minimize this damage; namely, 15 degree deflection of the beam, and "hole through arc" geometry. The first of these has the virtue of being able to dissipate the back bombardment if it is poorly focused. It has the additional virtue of removing the axial discontinuity from the beam profile at the target (See UCRL-792). The second scheme has the outstanding advantage of not requiring modification of the injector mounting on the accelerator. However, it is only useful if the back bombardment is rather well focused.

The 15 degree deflection is accomplished with a prismatic electrostatic lens system, and seems to operate in much the same manner as "normal" geometry. The "hole through arc" operates very satisfactorily with the details shown in Fig. 3. The beam current measured calorimetrically was 1100 ma., and this is believed to be somewhat low due to thermal losses.

Accelerating Electrode Grids

The accelerating electrode grids consist of spokes of pure graphite, rectangular in cross section (1/8" x 1/16"). See Fig. 1. The length of these spokes was varied in an effort to determine the optimum length from the point of view of operation at full duty cycle. In general, the more complete the grid the more beam it is possible to extract, but the limitation is the overheating of the grid, which causes spark down of the high voltage supply. It was concluded that an opening of around an inch was necessary to dissipate the power involved in full duty cycle operation.

---

*See UCRL-1137 for details of injector geometry.

270 469

DECLASSIFIED

Drifting Arc Length

The drifting arc length is an important parameter in determining the location and size of the focal spot. The length of the drifting arc electrode was varied in 1/2 inch steps from 2 inches to 5-3/8 inches and the properties of the beam observed in each case. It was concluded that for the present arrangement of the magnetic fields the present standard drifting arc electrode length of around 5 inches is optimum.

80 KW Collector

A collector consisting of a rectangular, water-cooled copper plate, inclined at approximately 45 degrees to the axis of the beam, was tested on the present injector with the possible requirements of the A-12 injector in mind. CW operation of this collector did not result in beams comparable with those obtained with the former deep shielded cup. The reason for the unsuccessful operation of this collector was the insufficient suppression of secondary electrons which drain back to the source and overheat the components and cause spark down of the high voltage supply. Another awkward feature of this collector was the measurement of the beam could only be accomplished calorimetrically. For research purposes it is desirable to have an electrical reading of the beam even if it is of doubtful precision in order to observe immediately the effects of altering the operating variables.

Half Voltage Operation

Since the accelerator will be started on protons, with the field at half gradient, experiments were performed to determine if any changes of the geometry would be required to deliver a reasonably large beam at half voltage or the same velocity at which a deuteron would be injected at 80 kv. Preliminary experiments just before shutdown gave 300 ma. with standard geometry. More work on this type of operation is contemplated during the testing of the plant model injector.

Plant Model Injector

By the end of November the parts for the plant model injector were nearly completed, and the unit about 85 percent assembled. The governing delay was the delivery of mercury diffusion pumps from Distillation Products, Inc. The delivery of these pumps is scheduled for about December 15.

The plant model injector is essentially the same as the injector previously mentioned in these reports, except for changes on arrangement of the HV ducting to facilitate quick replacement at the accelerator, and the change to mercury diffusion pumps.

The work on injector development is being carried out by J. DePue (CRDC), W. H. Gust (CRDC), W.A.S. Lamb (CRDC), E.J. Lofgren, R. Richter, and H. Smith.

DECLASSIFIED '76 '70

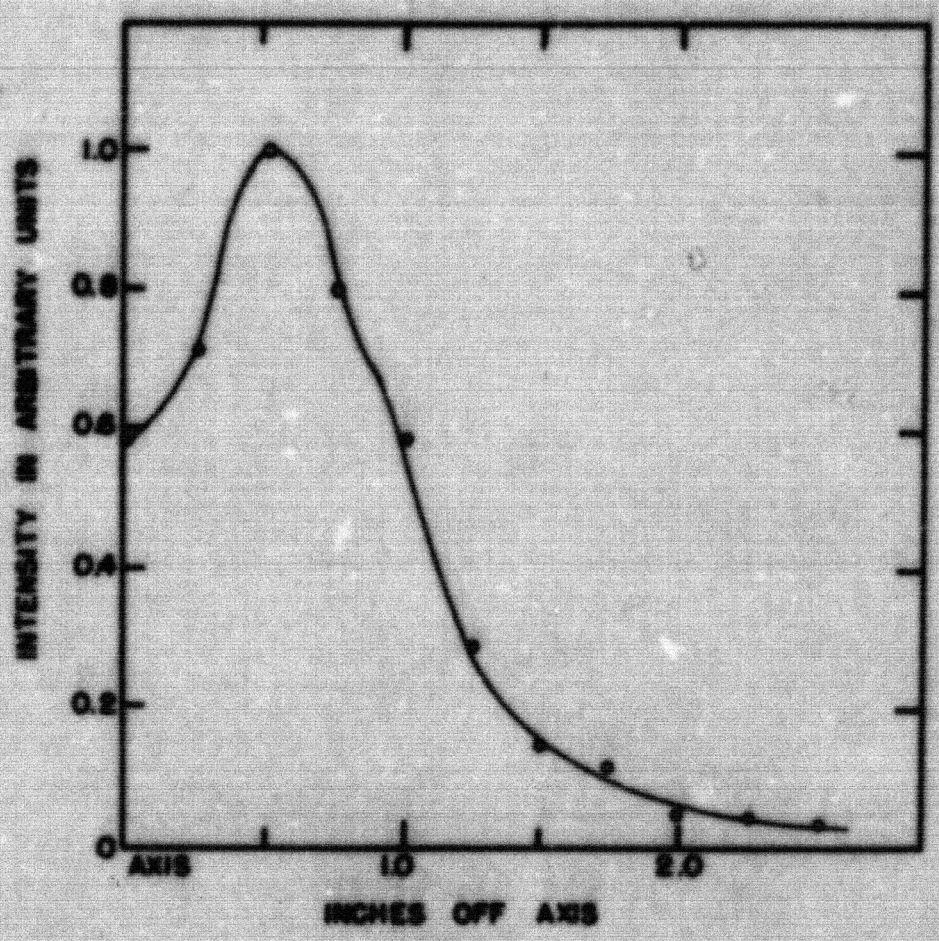

FIG. 1

MU 3227

Intensity distribution of beam at 20 inches from the source magnet, measured along a radius with a thermocouple probe. Beam 750 ma., duty cycle 1 percent.

270 .071

DECLASSIFIED

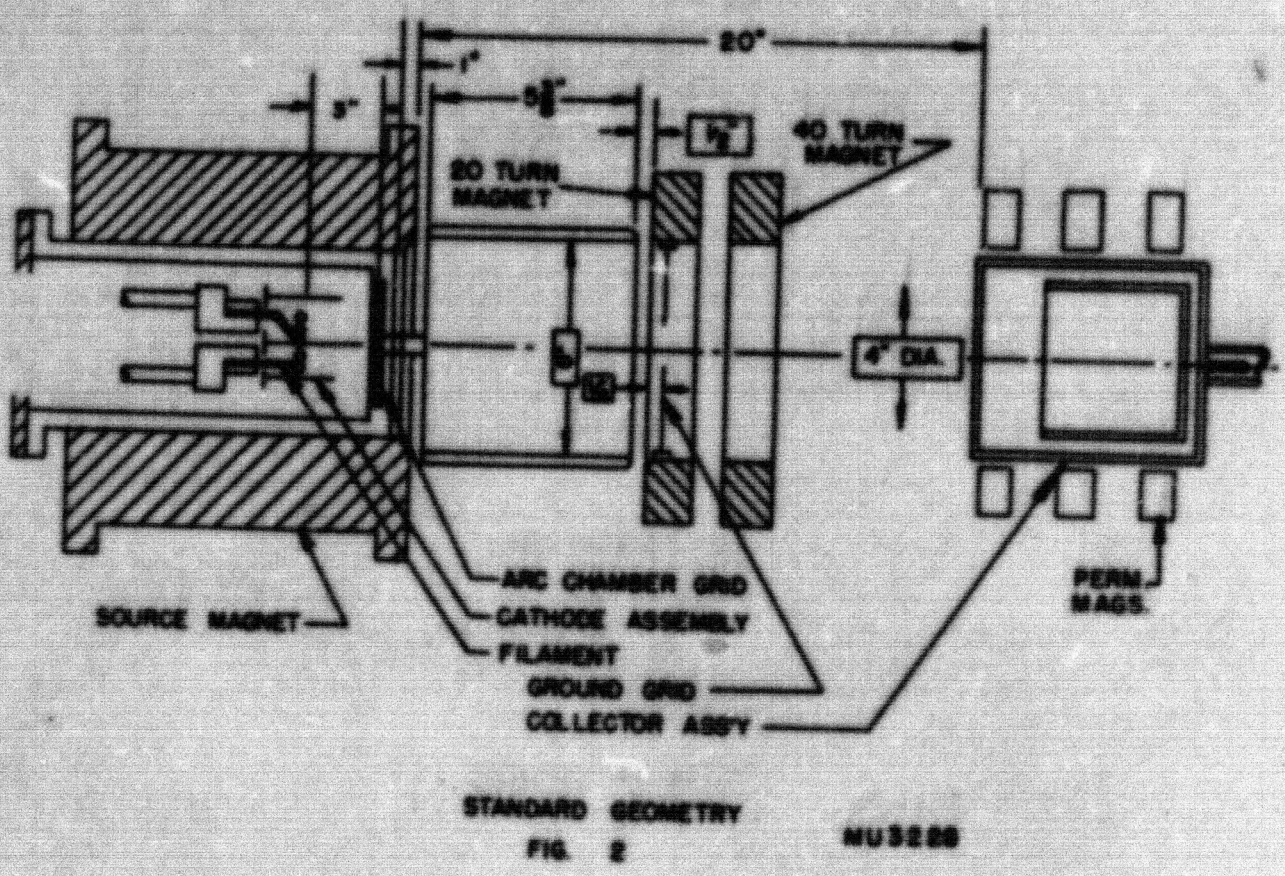

STANDARD GEOMETRY
FIG. 2 NU3288

270 072
DECLASSIFIED

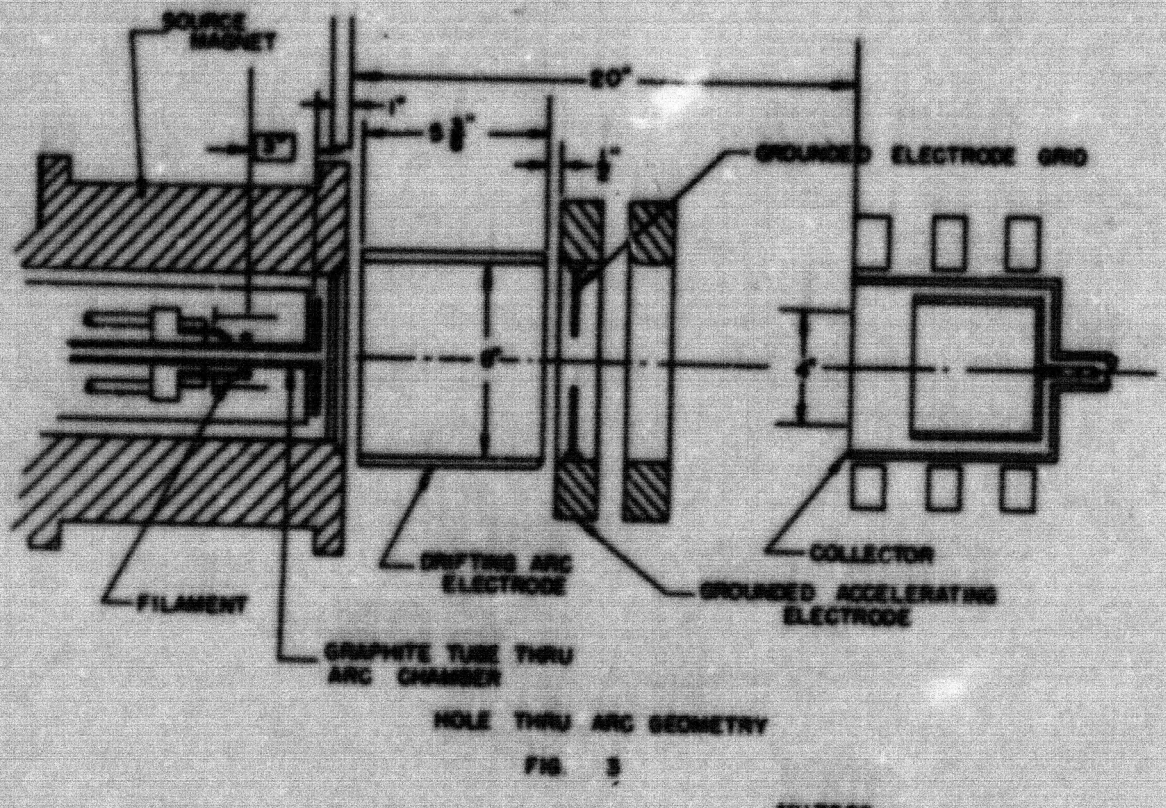

HOLE THRU ARC GEOMETRY

FIG. 3

MU 3289

276 .073

DECLASSIFIED

7. INJECTOR ELECTRICAL EQUIPMENT

H. M. Owren
UCRL

Building #51 Facilities

There have been no major changes in the electrical equipment during this period. Trouble was again experienced with the 2400 volt, 220 kva induction regulator used on the high voltage accelerator. This regulator was repaired by the manufacturer and should be a satisfactory unit.

Some additional low voltage-high current magnet power supplies were installed during the period.

The early troubles with the telemetering system have been accounted for and it is expected that the future wide band telemetering units will be satisfactory. In addition, two simpler types of narrow band telemetering have been developed. Both of these units look to be quite satisfactory.

Mark I Equipment

The electrical equipment being supplied by UCRL for the Mark I injector has been designed and ordered. Most of the major components were constructed and delivery scheduled before 1952.

The 100 kv insulating transformers have not been shipped as scheduled. Part of the order has been delivered, and it is not expected that the delayed delivery of the additional units will hold up Mark I operation. The results of the tests to date indicate that these transformers will be satisfactory.

Assistance has been given to the CRDC engineering staff in the circuitry and controls for Mark I operation.

270 .074
DECLASSIFIED

8. HIGH FREQUENCY PROGRAM

W. R. Baker
UCRL

The B-1 resonant load has been in operation now for more than two months with the new mercury diffusion pumps and special chemical cleaning of all surfaces exposed to high fields. No significant improvement was obtained in the x-ray level and sparking rate, however, until a thin film of dust was discovered and removed from the high voltage electrode surface. This immediately lowered the x-ray level more than a hundredfold and reduced the sparking rate by a similar factor. Where a rate of four sparks per minute was once considered to be good operation, the system now runs with about one spark per hour. Dust alone was not the entire answer, since the problem was not solved without chemical cleaning and mercury pumps.

To determine the effect of higher voltage on sparking, two oscillators were paralleled into the load and about three million volts obtained. After initial flurries the rate was approximately the same for the higher voltage as for the normal two million. This experiment was done before the dust removal, however, and may not be representative of the present system.

Five of the nineteen Mark I oscillators have been tested and several minor troubles corrected. Breakdown across the air side of the upper transmission line insulators proved to be due to a faulty variation from the original model line that put sharp edged copper gaskets on the insulator surface at high field points. Also, a very serious grid shorting trouble has come up with respect to several of the 5831 tubes. It has been traced to a mechanical resonance in the grid structure that is excited by the normal pulsing of the oscillator. After a few pulses the amplitude builds up to such a degree that an actual physical connection is made between the grid and beam forming cylinder. Experiments with electrical damping have been tried but are only partially effective. A practical solution that is now being investigated by the tube manufacturer is an increase in the grid tension. Several of our present stock of tubes - mostly those with low serial numbers - will have to be sent back for alterations since they show this effect strongly at plate voltages as low as 13 kv.

Not much progress in solving the 980 MC parasitic can be reported, although many things have been tried. The present scheme uses a simple lossy element in series with the tube grid flange which is composed of two groups of approximately 50 thin iron shims insulated by temperature resistant paint. Both ordinary steel shim stock and transformer iron have been tried and the latter found slightly better. The normal oxide insulation on the transformer iron proved ineffective so "Sileo" paint was tried. This worked, but again several variables had to be explored. This paint comes in black and white forms that contain lamp black and titanium dioxide, respectively. The black pigment allowed lower temperature operation and less warping of the shims, so the problem then became one of adjusting the thickness of the paint and the number of shims. This thickness turned out to be unexpectedly important and unfortunately for the heat problem, a rather thick coating seems to be required.

By a combination of water and air cooling this shim suppressor can be

DECLASSIFIED 276 .075

considered a fair solution to the problem but certainly leaves much to be desired. Some work is being done with a new approach that should prove much superior. This will be a resonant lossy trap at the same location as the present shims. Such a trap should be lossy to the 980 parasitic only and not to the fundamental frequency. This approach to the problem seems reasonable in view of the close frequency uniformity of the parasitic in all of the 5831 tubes.

Some low level rf excitation in air of the Mark I tank was effected using one of the A 2332 pre-exciter oscillators adjusted for C.W. operation on the higher frequency resonance of the cavity without drift tubes. Operation was very difficult because of spurious frequencies arising from the loop being too large and the line not correct for the higher frequency and also because of a cross mode in the tank only 50 Kc removed from the correct mode. To further aggrevate matters, the Mark I power supply was full of bugs and the d.c. crowbar proved too slow to prevent the oscillator tube from gassing up on sparks. This forced an upper limit on the plate voltage of around 15 kv and a maximum output of only 250 kw. Fortunately, this proved sufficient to satisfy the rf joint test requirements.

During the present period considerable thought has been given to the Mark II oscillator although no experimental work has been done. It now appears that a very simple system is possible for pre-exciting the tank that would eliminate not only separate unit pre-exciters but separate sub-exciter supplies and pulse lines as well. The system would operate by phase controlling the main power supply or supplies to an intermediate output sufficient to permit a reasonable plate current to flow. After sufficient current has appeared this would then be quickly modulated at the tank frequency by a gated high gain rf amplifier similar to the one in use on the present pre-exciter. The resultant current to the normal loops will then be sufficient to develop the necessary rate of rise of rf tank voltage to break through the ion lock barrier. When the tank rf had reached its equilibrium value, the power supply phase control would then be shifted to a value just sufficient to permit necessary automatic voltage regulation. No-load voltage changing transformer taps can be used to adjust for best maximum operating voltage. An electronically controlled phasing system will permit very fast recovery from tank sparks. The high gain amplifier is necessary only for the pre-excitation cycle and can be shunted out by direct drive from tank to oscillator at a sufficiently high level. To further simplify the system it is very unlikely that a program bias supply will be needed.

270 076

DECLASSIFIED

9. MARK I ELECTRONICS STUDIES

Walter H. Nelson
UCRL

During the last quarter the 1/2 kw pulsed oscillator built for Q-measurement was used on the Livermore cavity, the resulting measurements checking calculations. Additional functions had been added to the equipment, included remote push-button control of the carrier, and built-in 60 cps square wave generation for periodic pulsing, which tests on the portable 12 mc/sec cavity had indicated were desirable.

The dynamic characteristics of an oscillator driving a high-Q cavity were investigated by means of a low-power scale model attached to the 12 mc/sec portable cavity. It was found that the plate current behavior looking in from the oscillator d.c. terminals simulates that of a capacitor, whether the variations in plate current are induced by variations in plate voltage or in plate loading. The highest efficiency operation yielded the highest effective capacitance.

Since this effect has a bearing on the dynamic stability of the rf field intensity control system to be used at Livermore, the closed-loop control system was scale modeled on the portable 12 mc/sec cavity, using this low-power oscillator. The effective capacitance looking into the oscillator terminals, combined with the inductive reactance of the rectifier smoothing reactor, introduces a network into the control loop which cuts off higher frequencies at an excessive rate, corresponding to 12 db per octave, or 180 deg. ultimate phase shift. The steady-state frequency characteristic of the scale model shows the expected peaks in open-loop response of about 30 percent before cutting off and the expected 4/1 peak in closed-loop response before cutting off. For sudden variations in plate current produced either by changing plate voltage, or changing plate loading, the circuit exhibits an oscillatory overshoot. A combination of phase-lead network affecting the relative phase relation of frequencies in the critical range with a phase lag network reducing the gain in the critical region of the frequency spectrum controls this overshoot tendency completely in the scale model set-up, which is simpler than the Livermore set-up in that there is no significant time delay in plate voltage control. The time delay in the rectifier phase-advance and retard networks will be measured in the near future at Livermore, with test equipment specially built for the purpose. This equipment has been used by others for studying the transient behavior of the oscillator d.c. distribution system at Livermore. It provides pulses which are continuously variable from a few microseconds to more than 50 milliseconds in both length and delay, so that the overall response of any regulator may be readily observed.

The sub-exciter rectifier power supply #6 at Livermore was studied, its regulation curves recorded and troubles analyzed. Spurious signals in the protection circuits were traced and remedies suggested. It was found that the d.c. performance of the supply was limited principally by the auto-transformer used for voltage adjustment, and the spurious control signals arose from stray capacitive coupling.

276 077

UNCLASSIFIED

10. DRIFT TUBE MAGNET TESTS

Duane C. Sewell
UCRL

The test on the full-scale magnets for drift tubes 1 through 3 have been completed. The results of these test are given in Table I along with the results previously reported on magnets 4 through 6. The first line of this table gives the currents required to produce the proper focusing effects. The effect of adjacent magnets was taken into account in arriving at these currents. The second and third lines of the table give the voltage and power necessary to produce this required current. It is to be noted that neither of these quantities includes the losses that will be present in the leads through the drift tube stems.

It may be noted that the required powers in Table I are considerably less than those given in the previous quarterly reports, especially for the last five magnets. This is the result of an error found in working up the test data. At the time this was found the magnet copper was not yet delivered and the quantity was reduced about 20 percent. However, it was not considered practical at that time to change the motor-generator specifications so that as a result their capacity is higher than necessary. Since the error in calculation from the test data had been incorporated in the design discussed in the third and fourth quarterly reports, UCRL-1297 and UCRL-1436, the required voltages and powers in the tables in those reports are incorrect.

The values for the water flow in line 4 of the table were determined from measurements made at given pressure drops across the magnet terminals. These values were reduced to the pressure drops that will be available at Livermore by assuming that the flow rate varies directly as the square of the pressure drop.

Additional measurements were made to determine the repulsive force at operating position on magnet 1 and 2; 2 and 3. These forces were determined by using calibrated strain gages. Full scale measurements gave 184 pounds force between magnet 1 and 2. Comparable measurements on the model magnets gave 193 pounds. The force between full scale magnets 2 and 3 is 1950 pounds. Comparable model measurements gave 1700 pounds. This indicates an error on the model measurements between magnets 2 and 3 of 15 percent. Since the maximum allowable force is about 6000 pounds there is an ample margin of safety.

270 073

DECLASSIFIED

Table I

Drift Tube Magnet Specifications

(from results of tests on full scale magnets)

Magnet Number	1	2	3	4	5	6	7	8
Required Current-Amps (for theoretical* $\int H^2 dl$ along axis, including the effect of adjacent magnets)	598	572	890	950	1050	1000	1075	1100
Required Voltage - Volts (across magnet terminals for 32°C inlet water temperature)	69	148	167	167	149	142	154	157
Required Power - KW	42	82	152	159	156	142	165	173
Magnet Cooling Water								
Pressure Drop PSI (across magnet terminals)	114	114	64	64	64	64	64	64
Flow Rate - GPM	14	24	34	37	39	39	39	39
Water Temp. Rise - °C. at required power	11	13	17	16	15	14	16	17
Coil Resistance (ohms) (across magnet terminals at 20°C)	.1086	.2405	.1737	.1616	.1324	.1320	.1328	.1322
Number of turns	405	741	645	615	665	665	665	665

*As determined from beam dynamics calculations

270 079

DECLASSIFIED

11. M.T.A. MECHANICAL DESIGN

W. M. Brobeck
UCRL

Distribution of Activities

During this period approximately 46 members of the mechanical engineering and drafting section were employed on the MTA project. The distribution of their effort was approximately as follows: 20 persons on the Mark I accelerator; 10 on the Mark II accelerator; 7 on the Mark II target; 9 on the Mark III program.

Mark I Accelerator Program (Livermore Linac)

Follow-up. Most of the Mark I effort during this period could be considered as "engineering follow-up" - (1) making changes found necessary during construction, acceptance testing, or installation; (2) field inspections and consulatations; (3) preparation of servide manuals, master drawing lists, and spare parts lists. The following paragraphs describe the status and some of the necessary changes to components designed by UCRL.

Injector. The design and construction have been completed except for installation of the mercury diffusion pumps and assembly of the mechanical parts (alignment gages, high voltage ducting, adapter tank) necessary for installing the injector at Livermore. The diffusion pump barrels will be cooled to 5° or 10°C with Freon from the same system that supplies the baffles, and if this is satisfactory it will eliminate the need for refrigerated water.

Drift Tubes. Design and construction for the following have been completed: (1) changes in the vacuum pumping provisions to prevent dust particles from entering the Mark I tank through the bore tubes; (2) relief valves to prevent large pressure differences between the drift tubes and the Mark I tank; (3) strain gages for the lifting bolts; (4) equipment for measuring the inter-magnetic forces on the full-size magnets. Overall fabrication and assembly of the drift tubes, including the stems, was approximately 90 percent complete as of November 30, 1951.

Oscillator Transmission Lines. Most of the lines have been installed at Livermore, but recently the following changes, which are not in progress, were found necessary: (1) several lines will be moved to new positions as a result of information that oscillator efficiency could be improved when accelerating protons if the smallest loops are installed in the regions of maximum field; (2) new insulator gaskets and a new spark gap electrode are to be installed to prevent sparking and damage to the insulator and to reduce the exposure of thin copper sheets to the electric field; (3) provisions are to be added for manually rotating the lines to adjust the loop for tuning the cavity.

Pre-exciter Transmission Lines. It is not now planned to rf glow discharge the Mark I cavity with the pre-exciters so that a pump installation will not be required. However, openings are made in one line to permit future installation of pumps if this plan is revived. The lines and their rotating

DECLASSIFIED 276 080

mechanisms have been assembled and are being vacuum and mechanically tested. The problem is to develop a suitable rotating vacuum seal for the 20 inch diameter lines that does not require oil or grease lubrication.

Miscellaneous. The rf voltage pick-up loops have been fabricated, but tests are now in progress to determine whether the chevron vacuum seal design is satisfactory. The temporary booster pump liquid nitrogen baffle fabricated by UCRL has been installed at Livermore. It will be replaced with an identical baffle except for electroless nickel plated surface before the mercury diffusion pumps are operated.

Equipment for monitoring the Mark I beam which has been designed includes: (1) thermocouples to qualitatively determine the beam diameter and centering; (2) a faraday cup for checking the unaccelerated beam current and position at the target end; (3) two radio-autographing devices for determining the accelerated beam profiles and energies.

Mark II Program (Full Scale Linac)

Mark II Accelerator. UCRL contract with the detail design of the accelerator has been limited primarily to liaison with CRDC through weekly or semi-monthly engineering meetings at which UCRL physicists concerned have been brought in as required. Preliminary studies have been made by UCRL on the periscopes, oscillators, drift tube magnets at target end for minimum costs, and optimum roughing pump displacement. Most of the UCRL effort associated with the Mark II accelerator program has been directed toward the experimental equipment (discussed in the next section) necessary for determining design bases.

Mark II Target. Preliminary design work was completed on a water cooled, water moderated target for a 0.1 ampere, 350 Mev beam, and a summary report has been drafted but not yet released. A joint UCRL-CRDC group was formed at Livermore on October 1, 1951 to work on the preliminary design of a U-233 producer with a 0.5 ampere, 350 Mev deuteron beam, but this design work has been terminated and an interim summary report will be completed during the next quarter. Some work has been started on plutonium targets. The rough draft of the summary report for the NaK cooling systems studied has been completed.

A function generator is being designed for studying hot spots (e.g. overexposures on a film) caused by various Lissajous patterns of a light beam. From these studies it is hoped to optimize the Mark II Lissajous beam sweeping frequencies and amplitudes and the location and cooling of the target elements. As presently planned, the equipment will consist of a light source for a 3-inch dia. beam, a filter for reproducing an intensity distribution similar to that predicted for the Mark II beam, and a film or photoelectric cell mounted on a double carriage with motions duplicating various Lissajous figures.

Experimental Equipment for Mark I and Mark II Accelerator Programs

Ion Pumping. Several ion pump models have been designed to determine the feasibility of this type of vacuum pumping for the Mark II vessel. These ion pumps are backed up with Kinney roughing pumps. In ion pump No. 5 the magnet is external to the pump barrel and is interrupted at

DECLASSIFIED

the three pump inlets. After preliminary tests, ion pump No. 5 will be connected to the B-1 cavity. In ion pump No. 6 the magnet is located within the vacuum chamber, thus eliminating the problem of interference between the magnet windings and the pump inlet. Construction of ion pumps 5 and 6 is in progress.

D.C. Vacuum Test Cavity. Miscellaneous parts have been designed and constructed for the d.c. vacuum test cavity to investigate sparking problems with d.c. voltages up to 100 kv and for the field emission microscope to investigate the effect and the elimination of contaminations on surfaces subject to sparking.

B-1 Cavity. The conversion of the 20-inch diffusion pumps and associated equipment from oil to mercury has been completed. Equipment was designed and constructed for studying the amount of pumping required to prevent rf glow discharge within the pre-exciter lines but these studies now have been deferred in view of the current opinion that it will not be necessary to use the pre-exciters for glow discharging the Mark I cavity.

B-4 Cavity. The mechanical design and construction of this 200 MC cavity (for studying electron emission with high rf fields under carefully controlled conditions - utmost cleanliness, mercury diffusion pumps, metal gaskets) has been completed, and rf power has been turned on the cavity.

L-2 Cavity (Livermore). In addition to advising CRDC on design details, UCRL will furnish the following equipment to CRDC: voltage pick-up probe, pre-exciter loop, voltage pick-up loop, and cavity discharge probe. Overall cavity design is approximately 50 percent completed.

Mark III Program (Cloverleaf Cyclotron)

Electron Model. Miscellaneous parts for the present electron model have been designed to further basic studies of the cloverleaf cyclotron program. An extension tank has been completed to permit extraction of the beam to a considerable distance from the machine in order to study deflection problems. Design of a new electron model containing the latest ideas for shaping the magnetic field is nearing completion. This model is somewhat larger and is intended to operate an equivalent deuteron energy of 300 Mev.

20-Inch Cyclotron. Operation of the 20-inch cyclotron has pointed out the difficulty of controlling relative phase between the three resonators with the servo operated tuning condensers originally planned. Considerable design work is in progress for improving the phase control mechanism and the apparent difficulty of this problem has lead to the study of a single phase machine operated on the third harmonic of the ion frequency. The 20-inch cyclotron has also been devoted to the study of ion source and starting problems and design work on the various sources has been a portion of the engineering problem during this quarter.

XC Machine. Sparking tests in the XC machine have continued indicating that chromium plated copper has outstanding properties as regards suppressing destructive sparking. More data have been obtained to determine the limit of voltages and fields which are permissible. Design work on an ion source to determine the effect of a copious supply of ions on sparking

DECLASSIFIED 276 082

has been completed. Design work is also underway on a 2/3 scale model, to be installed in the XC magnet, of the central portion of the J-16 machine based on the single phase third harmonic principle. This problem will permit the determination of starting conditions including space charge problems which cannot be studied conveniently on the 20-inch cyclotron.

J-16. Design work on the magnetic models has been pushed intensively during this quarter and the magnet group is approaching the final design for the J-16 machine. A one-third scale rf model of the J-16 third harmonic accelerating system has been completed and is undergoing tests to determine and improve its shunt impedance. Some design work has been done on the structural problem of the J-16 magnet and exciting coil in an attempt to be ready for intensive detail design at any time approval is given for proceeding with the J-16 program.

276 .083

DECLASSIFIED

13. A-12 TARGET AND LATTICE DEVELOPMENT

Introduction

C. M. Van Atta
UCRL

A very significant change in the organization of personnel working on the MTA target development was the establishment on October 1, 1951, of a joint target design group consisting of mechanical engineers and draftsmen from both CRDC and UCRL. This group is under the direction of Dr. E. D. Kane of UCRL and initially consisted of seven men from CRDC and four additional men from UCRL. At the end of November the group had grown to 16 men by additions from CRDC.

The joint design group is provided with basic information by the CRDC nuclear chemistry group and the UCRL experimental and theoretical physics groups and is assisted by the CRDC analytical and materials groups.

During the two months since its establishment the joint design group has largely completed a preliminary design study of water moderated thorium lattice and water cooled uranium target for U^{233} production. This design study will be summarized within a few weeks and the next design study, that of a very similar unit for Pu production, will be started with the understanding from the AEC that Pu is to be the production goal of the MTA unless otherwise specified.

Computations of target performance considering the water-cooled uranium plate structure as a lattice have continued with some success in predicting a reasonable free neutron output identified as fast and thermal leakage neutrons and internal flux distributions in approximate agreement with that expected from nuclear chemistry results on the distribution of capture events (Np^{239}) in a solid block uranium target.

Lattice computations have been carried out in some detail for a water moderated thorium lattice for U^{233} production. During the next period the somewhat more complex problems of Pu production will be studied. The choice of moderator as a function of U^{235} content of the fuel will be explored and a more detailed calculation for a water moderated lattice using fuel will be attempted.

The physics and radiochemistry experimental programs have continued at about the same level as previously. In the physics program the main effort has been directed toward the development of a proportional counter system for determining the energy and angle distribution of neutrons from the target. In the radiochemistry program further refinements have improved the fission and capture distribution measurements. Also a variety of new results on (d,2n) and (n,2n) cross sections of interest in determining the quality of the product formed in the primary and secondary targets have been obtained.

270 ONL
DECLASSIFIED

Target Design

E. D. Kane, P. J. Hernandez and R. J. Burleigh
UCRL
J. E. Mahlmeister, B. W. Ela, R. C. Gerber,
K. Bernstein, D. H. Cronquist, H. C. Hollister,
J. C. Ekvall, J. L. Smith and F. J. Sterbentz
CRDC

U^{233} Target

On October 1, 1951, a joint design (UCRL-CRDC) group was activated at the Livermore Research Laboratory. The initial group was under the direction of a UCRL engineer, and included four full time men and one part time engineer from UCRL with seven men from CRDC. The design objective selected was:

Deuteron beam energy (Mev)	350
Deuteron beam current (amp.)	0.5
Main product	U^{233}
Moderator	H_2O

Design work continued on this objective until December 1, and is now being summarized. The joint group totaled 16 engineers and draftsmen at the end of this quarter.

Miscellaneous Studies

Analysis and design work continued on a number of items bearing on the design of target components. These studies included:

(a) Methods of holding and separating primary target plate elements.

(b) Selection of design standards on heat transfer rates, fouling factors, friction factors, and calculation methods for heat transfer and pressure drop in water-cooled primary target.

(c) Analysis of heat transfer and pressure drop for thorium lattice arrangements in water during normal operation, shutdown, and an for certain accidents.

(d) Design basis for vacuum tank structures.

(e) Design basis for tubing used in primary target (in S.S. 316, S.S. 347, Zr, Ti, Al).

(f) Preliminary design specifications for

1. Primary cooling water activity (CRD-T1-67)
2. Secondary cooling water activity (CRD-T1-68)
3. Lattice cooling water activity (CRD-T1-69)
4. Lattice activity (shutdown) (CRD-T1-72)

Items 3 and 4 refer specifically to the 0.5 amp U^{233} target.

DECLASSIFIED 276 085

(g) Mechanical design and arrangement studies of primary and secondary target manifolds, tubes, lattice structures, shielding, etc. were incorporated in approximately 50 sketches assigned drawing numbers during this period.

Preliminary specifications were written for one item of experimental equipment proposed for construction at Livermore, namely a flow circuit capable of testing a primary target tube and plate subassembly and manifold. The resistance cycle tests at ORNL were reviewed and suggestions made for revisions in the operating conditions. The ORNL test results were summarized and analyzed, and design work started on new equipment capable of simulating target service conditions more closely.

Target Development

R. L. McKisson, N. R. LeRoy and M. F. Katzer
CRDC

Beam Sweeping Studies

An investigation of Lissajou sweeping patterns on rectangular targets has been initiated. Attention has been directed to the use of rectangular targets in an attempt to reduce the heat loads per tube. The assumption in using the rectangular targets is that the tubes will run parallel to the short direction and, for a given target area, would be shorter (but more numerous) than for a square target. The width-height ratio of the rectangular targets studied varied from 1.75 to 2.75. To date eight fundamental Lissajou patterns have been investigated (frequency ratios 5/2, 8/3, 10/3, 11/3, 7/2, 13/3, 9/2, and 5/4) and to four of these the third harmonics have been added and optimized (8/3, 10/3, 11/3, 5/4). The optimization process consists of adjusting the amplitudes of the third harmonics to minimize the current intensity of the peak point in the pattern. The following table summarizes the significant results; all data has been computed on the basis of a target 144 ft^2 in area.

Table I

Results of Rectangular Lissajou Sweeping Study
0.5 ma Beam Current

Fundamental Patterns	Width/height ratio	U_{max} (μ amp per in^2)	$U_{max}/(U_T)_{ave}$	Q_{max} (μ amp per in width)
5/2	1.75	141	5.84	5760
8/3	1.83	123	5.12	6060
10/3	2.17	130	5.40	5580
7/2	2.25	147	6.14	
11/3	2.34	137	5.68	5640
13/3	2.66	155	6.42	
9/2	2.75	164	6.80	
5/4	1.75	124	5.15	5820
5/4	1.00	107	4.44	7092
1/1 Circular	1.00	142	5.89	6780

Optimized Patterns	Width/height ratio	$\bar{U}_{max}$ (μ amp per in^2)	$\bar{U}_{max}/(UT)_{ave}$	Q_{max} (μ amp per in width)
8/3	1.83	87	3.62	4368
10/3	2.17	89	3.69	4140
11/3	2.34	88	3.67	4092
5/4	1.75	93	3.85	4248
5/4	1.00	89	3.69	

$\bar{U}_{max}$: Time average current intensity on target point for most heavily loaded point.

$\bar{U}_{max}/(\bar{U}_T)_{ave}$: Ratio; time average current intensity on most heavily loaded target point to the average current intensity over the entire target.

Q_{max}: Time average current intensity (per inch of target width) over length of tube on most heavily loaded tube.

The results of this preliminary study indicate that the rectangular targets offer the advantage over square targets of reducing the tube loads while maintaining low peak-point current intensities. This study is being continued and will ultimately cover the following variables: beam contour, beam size to target size ratio, and phase-shifts in fundamental and third harmonic frequencies.

A spiral beam sweeping investigation is in progress. The study will

DECLASSIFIED

investigate the effect of varying the pitch of the sweeping pattern, and of varying the beam-target size ratio. No results of significance are now available.

A 'television-type' beam sweeping investigation is also in progress. This study is in an exploratory phase and no results are available.

Energy Dissipation in Coolant and Construction Materials

In order to facilitate heat load calculations for the primary target, Mev/inch curves for coolants and tube-wall materials have been prepared. These curves give the Mev/inch energy dissipation ratio assuming that the materials are present only in thin sections in an otherwise pure uranium target. This means that the number and type of energetic particles present at any target penetration can be determined solely by consideration of nuclear processes in uranium. The materials studied and the maximum Mev/inch value for each are: Aluminum, 120 Mev/inch; titanium, 180 Mev/inch; zirconium, 216 Mev/inch; steel, 288 Mev/inch; H_2O, 60 Mev/inch; and NaK, 35 Mev/inch.

Materials Research

(a) Materials Testing

P. J. Charley
CRDC

Resistance Cycler

Previous experimentation has shown that alpha rolled uranium is subject to elongation in the direction of rolling when subjected to thermal cycling under the following conditions:

1. The cycling rate was relatively slow (several cycles per hour).
2. The specimens were heated and cooled to temperatures which were uniform throughout the metal.

A series of tests was performed in order to determine if such growth would occur when the center of a 1/4" diameter rod was subjected to more rapid cyclic variations in temperature which normally would cause a large amount of elongation, while the surface was kept relatively cool. Five samples were cycled up to 7,000 times at 30 cycles/min with center temperature between 100°C-500°C while surface temperatures varied between 60°C-120°C. Using a gage accurate to 0.1 percent no elongation was detected. Therefore it may be concluded that target elements operated under such conditions will be dimensionally stable to thermal effects. In all cases noted above severe corrosion took place along with considerable cracking and splitting. It was felt that these effects were due to a combination of corrosion and high values of thermal stress. It should be noted that these tests were performed on that type of uranium which normally exhibits the worst behavior. It is to be expected that more stable forms (or alloys) will show less severe effects.

It may also be concluded from these tests that the corrosion of uranium by distilled water is not severe below about 100°C. However, the

DECLASSIFIED

presence of steam will cause rapid and vigorous attack.

A series of experiments to establish the limits of mean stress and stress reversal in uranium is now underway. Failures have been obtained at a mean stress of 60,000 psi with a 600 psi calculated swing. In this 1/4" rod, this corresponds to a power input of 150 KW/in^3 with 1/3 duty at 40 cycles per second. In these cases failures occur as minute cracks parallel to the rolling direction. It is possible that these cracks are caused by inclusions (e.g., carbides) rolled into the metal and which may not be present in specimens prepared under more controlled conditions. CRNL is conducting metallographic examinations to clarify this point.

It is planned to extend this program to thorium, zirconium and structural materials at a later date.

The resistance cycler will also be used to test the quality and effectiveness of claddants.

(b) Fabrication Studies

R. B. Small
CRDC

Zirconium Cladding of Uranium

Three methods have been used to obtain uranium clad with zirconium:

1. Extrusion of a uranium billet canned in a cylinder of zirconium;
2. Rolling a tubular sandwich consisting of a uranium rod in a zirconium tube to a flat.
3. Rolling the conventional picture frame of zirconium enclosing a rectangular billet of uranium.

The three methods have certain characteristics peculiar to each. The extrusion to a clad rod occasionally results in a core having an extremely irregular cross section. The reason for this is not known at present. Bonds having a shear strength of 48,000 psi have been obtained, although a diffusion layer, such as that produced with rolling, is not evident.

Rolling the tubular sandwich results in metallurgical bonding on the flat surfaces. By a combination of rolling at 620°C(alpha) and 900°C (gamma), bonding also is obtained on the edges. This high temperature rolling, however, tends to produce a slight hour-glass shape to the cross section.

Rolling the picture frame produces plate having the minimum of cladding with the greatest uniformity. Bonding at the edges, however, has been non-existent. Cladding having a thickness of 4 mils has been produced.

All assemblies for cladding are evacuated and sealed under a vacuum of 0.1 microns after electrolytic polishing of mating surfaces.

Zirconium Cladding of Thorium

The same three basic methods as used for uranium have been used with

DECLASSIFIED 276 089

careful surface preparation and evacuation. Extrusion to clad rods has to date yielded variable results. Extrusion at 1700°F with a 9 to 1 reduction resulted in partial bonding with a definite diffusion layer revealed metallographically in both zirconium and thorium. Another billet extruded under presumably more favorable conditions, 1775°F and 12 to 1 reduction, resulted in no bonding. The difficulty of core irregularity is experienced as found with uranium.

Rolling of tubular sandwiches has lead to the conclusion that rolling at a temperature of 1950°F with a reduction of 10 to 1 results in metallurgical bonding. Edge bonding is lacking and there does not appear to be available a rolling sequence as used with uranium to remedy this.

Rolling of picture frame assemblies with 10 to 1 reductions at 1950°F results in excellent bonding on the flat surface, but no bonding at the edges. Diffusion layers are seen metallographically. Due to the high temperature required, however, the zirconium surface must be protected by jacketing in a mild steel can during rolling. A liquid phase is formed between zirconium and iron which squirts out during rolling. Not only is the assembly damaged but a serious personnel hazard results. Tantalum foil has been used as a barrier with more success than other materials, but is still not satisfactory.

Emphasis has now been placed upon producing thorium plate clad on both sides with zirconium without regard to the edges. Attempts will be made to weld or braze the edges. In order to overcome the barrier problem, high reductions, diffusion annealing and thin foils will be used to obtain bonding when rolling at 1700°F or less.

Dimensional Stability

The induction cycling work has been terminated with the following results:

1. Alpha rolled uranium will grow with 50°F temperature swings around 250°C when the cycling occurs at 4 per second.

2. The growth per cycle is approximately that resulting from cycling at a rate of 30 per hour from 100° to 275°C.

The low gradient NaK cycler is being used to plot the growth characteristics of alpha rolled material in the region of 275°C where the growth per cycle appears to be very small. Also, tests cycling from 100-350°C showed that alpha rolled material continued to grow but at a decreasing rate until, at 7500 cycles, severe longitudinal cracking appeared.

(c) Corrosion

M. H. Boyer
CRDC

Liquid Metal Corrosion

Inasmuch as interest in liquid metals as coolants appears to have subsided to a considerable extent during this quarter, work on corrosion by liquid metals has been reduced to the indexing of information as it appeared.

UNCLASSIFIED 276 090

Corrosion by Water and Aqueous Solutions

Work on this phase of the corrosion problem consisted of a continuation of studies on metals listed in the quarterly report for June to September.

(a) Stainless Steel

Stainless steel owes its corrosion resistant properties to the phenomena or passivity, a condition brought about by oxidising environments. This property is apparently derived from the chromium, a component of all stainless steels, the concentration of which is the most significant factor in evaluating the corrosion resistance expected of a partisular alloy. The next most important alloying element, nickel, increases corrosion resistance with increasing concentration, if present about 6-7 percent, at which point it converts the alloy to a homogeneous austenetic structure. Below this amount it may be detrimental due to the formation of a non-homogeneous structure. Carbon is generally detrimental and should be kept to as low a value as is consistant with over-all requirements.

The stainless steels are generally not resistant to attack by strong acids except under simultaneously existing highly oxidising conditions, i.e., concentrated nitric does not attack stainless steel.

A very important fallibility of the stainless steels is their tendency to corrode by pitting attack in the presence of halides. Chloride ion is more effective than bromide or iodide in bringing this about, though fluoride may be still more effective than chloride in destroying passivity.

Corrosion of the 18-8 stainless steels by pure water up to 300°C less than 0.1 mil per year. Experiments in superheated steam to temperatures of 940°C indicate corrosion rates increasing to about 1.0 mil per year at a temperature somewhat below 910°C, with a breakdown of passivity and rapid corrosion above 910°C.

(b) Aluminum

Aluminum has high resistance to attack by water only within the pH range of 55 to 70. Within this range and up to temperatures of 100°C, the average corrosive penetration over the surface will be 0.1 to about 1.0 mil per year for most alloys. Above 100°C, additional data is needed on corrosion rates over long time exposures. Indications are that average penetrations of from 1 to 6 mils per year at 150°C up to 30 mil per year at temperatures near 315°C may be expected while above 315°C there is danger of rapid disintegration. Above 100°C, corrosive attack on clean aluminum surfaces is much higher during the first day or two, i.e., 50 to 100 mils per year, than the average rate over extended periods.

A serious problem in aluminum corrosion is pitting. The frequency of pitting is ordinarily low in pure water in the above specified optimum pH range; however, those pits which form penetrate the metal at a considerably higher rate than is indicated by the average penetration.

It does not appear possible to specify conditions under which

DECLASSIFIED 276 091

pitting does not occur. However, appropriate concentration of dichromate in the water materially reduces pit formation. Protection is also afforded by the use of alclad materials with which penetration of the base metal is prevented by sacrificent corrosion of the coating in case the coating metal is perforated.

Corrosion of aluminum may be accelerated by small concentrations of halides (usually Cl^-) and silica, which tend to accentuate pitting attack. Consequently the corrosion of aluminum in demineralized water may be more serious than in pure water under otherwise the same conditions. Observations on the effect of H_2O_2, of interest because of its presence in irradiated aqueous systems, are somewhat inconsistant, but in concentration ($\sim 10^{-3}$ M) an increase in general and pitting attack may occur.

(c) Zirconium

A report (CRD-T2C-63) summarizing the corrosion properties of zirconium and its alloys has been prepared.

Film Formation

A study of the problem of film formation on heat transfer surfaces in contact with water has continued. For distilled or demineralized water, film deposition appears to be mainly due to hydrous oxides of the trivalent elements iron, aluminum and chromium, iron being probably the most commonly encountered of these. No limit for iron concentration has been found below which it can be certain that iron film will not deposit. An an iron content at 0.05 parts per million, or below, and small amounts of sodium silicate seem to exhibit film formation. The aluminum concentration of demineralized water is in the vicinity of 0.01 to 0.03 parts per million and this appears to be too low to cause deposition of aluminum film under conditions so far studied. Concentrations of 0.02 parts per million of chromic ion are not regarded as capable of increasing the rate of film formation by water to which silica inhibitor has been added.

Silica in water can lead to film deposition when present in high enough concentration. At lower concentration it appears capable of inhibiting the formation of iron and chromium films.

(d) Radiation Damage

W. E. Browning, S. Siegel, R. V. Steele,
R. A. Heckman and S. E. Bramer
CRDC

Experimental Equipment

The design specifications for "hot" cells were made a part of the Process Development Laboratory specifications and is now ready for construction.

Detailed methods and equipment are being worked out for removing irradiated specimens from probes, transferring them to test machines, and

DECLASSIFIED 276 092

carrying out tests of mechanical and other properties. These operations will be done remotely in the "hot" cells.

Preliminary design of a basic probe shaft for use in the Mark I accelerator has been prepared for design engineering. Specialized probe heads for carrying out specific irradiation experiments are being designed. Those receiving first priority are designed to perform experiments involving irradiation of :

1. Specimens under controlled temperature conditions for testing physical and mechanical properties after irradiation;
2. Specimens during measurement of thermal conductivity;
3. Specimens during creep measurement.

Hydrogen Accumulation in Irradiated Specimens

The aluminum specimen previously irradiated on the 60" cyclotron to determine the effect of hydrogen accumulation from the beam was tested further. Since the deuteron beam was used it was possible to distinguish between hydrogen from the beam and impurity hydrogen. The amount of hydrogen retained in the metal was determined by vacuum fusion and mass spectrometric determination of the released gases, with the result that 97 percent of the theoretical amount of beam hydrogen was recovered. This differed from 100 percent by less than experimental error. The recovered deuterium was essentially all released at or below 600°C, which is below the melting point of the aluminum.

Samples of this target specimen have been submitted for metallographic and x-ray line broadening examination. A device for carrying out an accelerated fatigue test on a portion of the specimen has been designed.

Gasket Materials

A calculation was made of the expected stability of rubber-like gaskets in the A-12 primary target water cooling systems as far as gamma radiation from induced activity in the water is concerned, using reported data from other AEC projects. It was found that there exist rubber-like materials which would remain serviceable for ten years of operation, assuming a specific gamma activity of 1.5×10^9 (0.5 Mev) gammas per cm^3 of cooling water per sec. Associated beta radiation will contribute negligibly. An oxidation resistant rubber should be used to avoid attack by decomposition products in the water.

Target and Lattice Calculations

Harold Brown*
UCRL

This period was very largely occupied with surveying the problems of target production and lattice efficiency and multiplication, so that the reports in this section are in the nature of status reports.

The purpose of the work carried on was to decide just what the

DECLASSIFIED 276 93

alternatives were in the way of target material, lattice fuel and lattice moderator and to begin to obtain the characteristics (such as size, degree of simplicity, etc.), fuel and moderator requirements, and production of each combination of these variables.

In the lattice, the possible fuels considered were thorium and depleted uranium of various U^{235} concentrations. The moderators are water, graphite and heavy water. Different moderators require different volumes. For example, a water moderated lattice would be only a foot or two thick and could be close into the target, whereas a graphite lattice would be at least four feet thick and much larger inside than the outside dimension of the target. Furthermore, the structural features will vary considerably. One can, however, for each configuration, obtain a ratio of product in the lattice to neutrons incident on the lattice. This ratio may, and in general does, exceed 1 for the case of depleted uranium fuel.

On examining the target itself in an effort to find just how many neutrons do emerge from it, it has been determined in calculations by CRDC and UCRL that the introduction of water cooling may have sufficient moderating effect to alter significantly the number of neutrons emerging from the target. A number of uncertainties remain in these calculations. The accuracy to be obtained in a three group calculation for a case in which only 20 percent of the neutrons reach the thermal group is questionable. The age to resonance in uranium-water mixtures containing 25 or 30 percent water has not been well determined experimentally. The effect of using the diffusion equation (especially since so much of the neutron source lies within two mean free paths of the face) is difficult to estimate. The distribution of the source function, however, appears to be fairly well in hand (UCRL-1587) after a number of false starts. The differential yield curve previosuly given was integrated to produce the source function shown in Fig. 1.

Such questions as the optimum thickness of the secondary target, and the possibility of using instead a portion of the lattice more heavily loaded with uranium or thorium will depend on the results of calculations on the escape of neutrons from the primary and secondary targets.

A further conclusion which has been reached from some sample lattice computations performed during this period is that not only the total but even the relative productions to be expected with different moderators in the case of Pu production cannot be closely estimated from the productions in an infinite lattice, because the structural absorption has markedly different effects for the different moderators. It has furthermore been obvious for some time that the perdentage of 25 present in the fuel also strongly affects the amount of additional production to be gotten in the lattice by using graphite or heavy water moderation. Thus the moderator to be chosen for Pu production cannot be established without first knowing the 25 concentration of the fuel.

It does seem clear that water moderation is indicated for thorium fuel, since when the absorption of neutrons by the beam hole, target, and structure are included in the calculation, the ratio of (useful capture/neutrons in) is as near one for water moderation as for graphite or heavy water and water, besides being cheaper, appears also to be more convenient.

The nature of the plutonium-producing lattice will thus depend strongly on the percentage of U^{235} in the fuel, and until such data is avail-

DECLASSIFIED 276 094

able, calculations will have to be made on all moderators.

Nuclear and Engineering Physics

D. H. Imhoff, W. H. Harker, C. C. Old and J. R. Donaldson
CRDC

Flux Distributions in Water-Moderated Lattices

Calculation methods for light water moderated lattices have been developed and applied to thorium absorbing semi-infinite lattices. The light water-moderated lattices under consideration have the significant feature of sharply reducing both fast and thermal neutron flux levels in the cavity as compared to equivalent graphite moderated lattices.

The obvious consequence of such reduced flux levels is to greatly reduce the loss of neutrons to the target and associated equipment and the loss from the inside lattice face to the beam hole.

Similar calculations for D_2O and Be moderated absorbing lattices have resulted in the following comparative fast flux levels in the cavity for lattices of similar inside area. In each case the fuel loading is such that the fast flux levels are a function of moderator material alone.

Table II

Moderator	Fast Flux Level Normalized to 1.0 for Light Water
H_2O	1.0
D_2O	2.1
Graphite	3.0
Beryllium	3.1

Since thermal fluxes are almost entirely dependent upon the fuel loading, a similar comparison for thermal fluxes is not presented.

276 - 095

Water Cooled Primary and Secondary Target Studies

A series of studies on water cooled uranium targets have been completed with the objective of attempting to evaluate external neutron yields as well as additional Pu^{239} production within the target as a result of thermal fission. Since water-uranium mixtures of the type considered in present target design have the property of slowing neutrons down as effectively as pure water alone, many fast neutrons produced within the target are slowed down into the thermal and resonance energy regions before they escape from the target. These neutrons can be captured to form Pu^{239} or may cause thermal fission, thus releasing a new generation of fast neutrons. By the use of two group diffusion theory and an exponential source of fast neutrons, the performance of various targets has been estimated. For a typical water cooled design it appears that only about 70 percent as many neutrons will escape from a water cooled target as compared to a NaK cooled design. The additional heat load resulting from thermal fission appears to be about 60-70 percent greater than the comparable NaK cooled design.

Uranium-Heavy Water Lattice

Preliminary calculations have been made for a heavy water moderated lattice containing depleted uranium / fuel rods. For 1.0" rods on a 4.9" square spacing it appears that k_∞ in a hot and poisoned condition will be approximately 0.90. For a lattice geometry with inside dimensions of 25' x 25' x 60' and a 13.5' x 13.5' water cooled, zirconium clad depleted / uranium primary and secondary target, the following production estimates were calculated for a 0.5 ampere, 350 Mev machine.

DECLASSIFIED 276 096

Neutron Losses to Beam Hole 0.4 mols/day

Neutron Adsorption in Targets in Construction Materials within the Cavity 1.5 mols/day

Neutron Losses Externally to Reflector 0.2 mols/day

Residual Heat Loads in Thorium Fueled Graphite Moderated Lattices

The expected heat loads in graphite moderated, thorium fueled lattice after beam shutdown have been calculated as a function of time from shutdown to one year after shutdown, for various operating periods. The calculations were based on a 0.5 ampere case in which the lattice production amounted to 3.5 mols/day. For example, after one half year operation, at which time the average U^{235} content is approximately 0.1 percent, the lattice heat load after shutdown as a function of time is given in the following table.

Table III

Time	Q	Q watts/lb fuel
1 minute	7.24 MW	29.7
10 minute	7.11 MW	29.1
1 hour	7.05 MW	28.9
5 hours	5.85 MW	24.0
10 hours	5.27 MW	21.6
100 hours	4.22 MW	17.3
1 month	2.20 MW	9.0

Experimental MTA Lattice Neutron Program

As various MTA target studies have progressed, the need for an experimental neutron diffusion program to supplement design information and provide a firm basis for an operable and optimized design has become more and more apparent.

The initial phase of the proposed program is to use artificial neutron sources such as polonium-beryllium to study the behavior of neutrons in cavities and adjacent absorbing lattices as a function of geometry to crystallize the basic equations governing neutron behaviors in and around cavities.

276 97

DECLASSIFIED

Calculation of Target Neutron Leakage

Frank L. Adelman
UCRL

A significant portion of the computing effort during the last period has been spent in an attempt to estimate the number of neutrons escaping from a primary-secondary target configuration. By treating the system as a two-group, one-dimensional, two-medium lattice with a source function of fast neutrons, one could estimate the number of neutrons escaping from the model. Unfortunately, both media are multiplying, so that the exact solution of the equations for this geometry is impracticable. Therefore, an iterative procedure was chosen treating the multiplication as a perturbation. Two different source functions were assumed, but the case of the best source function (UCRL-1587) (see Fig. 1) is being carried out by CRDC and will be covered in the next progress report. Also, in the calculations reported here, a slowing down area $\tau = 33$ cm^2 was chosen for both primary and secondary. More nearly correct values, taken from CF-1875, are used in the CRDC computation.

In general, it was found that the neutrons which escape constitute 3/4 of the neutrons which are created in a primary target (containing 2" U) with no secondary; 1/5 of these due to the multiplication properties of the medium. The only effect of the source function seems to be to change the percentage of the neutrons which escape in the direction of the beam. With a secondary target (containing 6" U), the total neutron output decreases somewhat, while the internal production of Pu^{239} increases. Most of the neutrons escape toward the beam hole. It appears that, for the production of Pu^{239}, a thick U secondary is indicated, whereas, for U^{233}, a secondary target of Th (possibly preceded by an inch or two of U) is to be preferred. The optimum balance, of course, must await the more detailed calculations of CRDC.

Calculation of Internal Neutron Flux Distribution for Solid Uranium Target

F. L. Adelman and J. V. Lepore
UCRL

Since the only practical method for treating problems involved in MTA target design is the use of diffusion theory, there is considerable interest in finding how satisfactory an answer it yields in the case of the pure uranium target. We have assumed that the measurements of Hicks and Stevenson on the concentration of Np^{239} in the target interior represent the fast neutron density and that this density is due mainly to group of neutrons with an energy spectrum roughly like the fission spectrum. The source of this group is taken to be direct deuteron and stripped neutron spallation-fission processes. Fast fission due to neutrons within the group is treated

270 098

by altering the diffusion length.

It is hoped, in this way, to find suitable constants for the source function which is taken as a sum of exponentials. A reasonable source function has been proposed by C. M. Van Atta (UCRL-1587) (see Fig. 1).

Because of the largeness of the effective diffusion length it is not permissible to treat the problem as one dimensional. We have therefore solved the problem for the case of a square target, choosing the flux to be zero on its extrapolated boundaries. The source is supposed to be uniform over a small cross section around the target axis. This is reported in UCRL-1620.

The agreement with experimental data is surprising and relatively insensitive to the choice of source function.

The calculated neutron density on the axis (Fig. 3) shows the rapid rise and fall within the primary but the height of the peak is hard to duplicate. If one matches areas under the experimental and calculated curves the peak height is too small by a factor of 1.8. It is interesting to note that an earlier attempt by H. Brown* to fit this data on the basis of a one dimensional analysis showed only a very slight fall within the primary. One may therefore ascribe this feature of the calculations as due to correct treatment of the target geometry.

Better agreement can be expected in the case of the flux density off the beam axis. This work is being continued in order to compare the calculated values of leakage from the target with the measurements of Hildebrand.

*Brown's calculation represents, however, a fair approximation to the average of the flux over the cross section of the target.

270 099

DECLASSIFIED

Nuclear Chemistry

K. Street
CRDC

Fission and Capture in Mark II Targets

H. G. Hicks, R. A. Gilbert and W. Hutchin
CRDC
P. C. Stevenson
UCRL

Investigation of the fission and capture events taking place when various configurations of uranium and thorium are bombarded with deuterons has been continued. The experimental arrangements and techniques used are similar to those described in the previous quarterly report.

Ionization chamber measurements of the deuteron beam have been found to be unreliable. To eliminate dependence on the ionization chamber, the nuclear reaction $Al^{27}(d,\alpha p)Na^{24}$ has been calibrated against a faraday cup in such a way that 0.005 inch aluminum foil can be used to measure the external deuteron beam. The aluminum measurements have shown the ionization chamber measurements of the deuteron beam to be low by about 30 percent.

The counting geometry of the geiger counters used for comparing samples was measured with Bureau of Standards radium DEF beta standards to be 3.23 percent. Previously the geometry was taken to be 5 percent. This change does not affect the fission data since the Zr^{97} fission yields were measured on the same counters and a corresponding increase in the measured fission yield of Zr^{97} occurs. Taking the counting efficiency of Np^{239} as 13.5 disintegrations per count[1] under the conditions used (this number is being checked), the data given in Table IV appears to be the most reliable yet obtained for the fissions and captures in a block of uranium.

Table IV

Fission and Capture in a Block of Uranium Using 190 Mev Deuterons

Target Dimensions	Fission		Capture	
	Primary Target	Secondary Target	Primary Target	Secondary Target
12" x 12" x 8-5/8"	0.11	0.39	0.04	0.45

A preliminary bombardment of a thorium block has been completed but the results are not yet available.

[1] H. M. Neumann, UCRL-840.

UNCLASSIFIED

Isotopic Composition of Product in Primary and Secondary Targets

W. W. T. Crane, R. E. Batzel and G. M. Iddings
CRDC

In order to monitor the internal deuteron beam of the 184-inch cyclotron so that excitation functions of deuteron induced reactions on uranium, thorium, coolants and construction materials could be measured, the excitation function for the $Al^{27}(d,\alpha p)Na^{24}$ reaction has been determined. This work was done by the stacked foil technique as given in the last quarterly report. The results previously given were based on an absolute cross section of 0.048 barns at 190 Mev as determined by H. Hubbard[1]. The absolute cross section for the $Al^{27}(d,\alpha p)Na^{24}$ reaction at 190 Mev has been remeasured and found to be 0.025 barns. The counting of the samples was done by comparison with several National Bureau of Standards calibrated sources and the absolute disintegration rate was checked by coincidence methods. The corrected curve is shown in Fig. 4.

In order to estimate the amount of U^{232} present in U^{233} formed in a thorium primary target, the cross section for the $Th^{232}(d,2n)Pa^{232}$ reaction has been determined as a function of deuteron energy. Since the values given in previous reports were based on the old figures of the $Al^{27}(d,\alpha p)Na^{24}$ reaction, a corrected excitation function has been calculated and is shown in Fig. 5. Extrapolation of the data to 350 Mev indicates an average cross section of 0.0036 barns in the energy region from 0 to 350 Mev.

A similar excitation function for the reaction $Th^{232}(d,4n)Pa^{230}$ has been determined. Since 10 percent of the Pa^{230} decays to U^{230}, this cross section is important in determining the cooling time of product formed in a thorium primary. The excitation function for this reaction is shown in Fig. 6. Extrapolation indicates that the average cross section for U^{230} production is 0.001 barns in the energy region from 0 to 350 Mev.

In the secondary target where the fast neutron flux will be high, the cross section for $Th^{232}(n,2n)Th^{231}$ reaction becomes important. Since undesirable amounts of U^{232} can be produced by the sequence of reactions

$$Th^{232}(n,2n)Th^{231} \xrightarrow{\beta^-} Pa^{231}(n,\gamma)Pa^{232} \xrightarrow{\beta^-} U^{232}$$

Rough values of the n,2n reaction cross section have been determined and are given in Table V.

Table V

Mean Neutron Energy	Cross Section (barns)
6 Mev (1-8 Mev spectrum)	0.05
10 Mev (1-18 Mev spectrum)	0.75
45 Mev	0.05
90 Mev	0.05

1 Hubbard, Phys. Rev. 75 1470 (1949).

276 101
UNCLASSIFIED

Fission Yields as a Function of Neutron Energy

R. E. Batzel, W. W. T. Crane and G. D. O'Kelley
CRDC

Absolute fission yields of a number of nuclides formed by fission of U^{238} have been determined as a function of neutron energy. These measurements were made by counting the fissions in an ionization chamber and then chemically isolating the elements investigated from a larger sample of U^{238} irradiated in the same neutron flux. These data are essential to the determination of the fission events occurring in the secondary target. Absolute cross sections for formation of some of these nuclides have also been determined at neutron energies from 45 to 90 Mev. These cross sections were determined relative to $C^{12}(n,2n)C^{11}$ reaction. The results are given in Table VI.

Table VI

Energy of Neutrons	Fission Yields (%) Zr^{97}	Ag^{113}	Ag^{115}	Ba^{139}	Cross Sections (millibarns) Zr^{97}	Ba^{139}
1 - 3 Mev	5.0	0.3	0.3	5.5		
45 Mev	5.2	2.2	1.3	4.3		
70 Mev						84.0
80 Mev						60.0
90 Mev	4.3	2.6	1.4	4.0	51.0	40.0

Charged Particle Fission of Thorium and Uranium

M. Lindner and R. N. Osborne
CRDC

Bombardments have been started to determine the extent of formation of various fission and spallation products in thorium and uranium primary targets. Preliminary to a more exhaustive study that should allow extrapolation of the results for both thorium and uranium to bombardment with 350 Mev deuterons, several bombardments of thorium with 350 Mev protons have been made for comparison with the existing data on uranium.[1] The 5 mil thorium targets were monitored with 1/2 mil aluminum foil, using a cross section of 10 millibarns for the $Al^{27}(p,3pn)Na^{24}$ reaction. The fission products examined included the elements Ni, Se, Sr, Pd, Ag, Cd, Te, Ba, and Os. Under the conditions of the experiment no Se or Os activities were found. The cross section for formation of the fission products studied are given in Table VII, together with the results obtained by Folger in bombardments of uranium, also with 350 Mev protons.

[1] R. Folger, Ph.D. Thesis, University of California, 1950.

DECLASSIFIED

Table VII

Element	Mass	Th	U(Polger)
Ni	66	1.5 mb	0.9 mb
Sr	89	13.5 mb	35.0 mb
	91	9.1 mb	35.0 mb
Pd	109	21.0 mb	-
	112	29.0 mb	-
Ag	111	35.0 mb	48.5 mb
Cd	115	13.0 mb	12.0 mb
	115 m	31.0 mb	34.0 mb
Te	131	1.0 mb	6.0 mb
	132	1.2 mb	-

Deuteron Produced Activities in Coolants

R. E. Batzel and G. Coleman
CRDC

In order to determine the shielding requirements for the cooling systems of the targets, and the long term hazard of coolant escape, the level of activities induced in the coolants must be known. In the case of NaK cooled targets one of the important activities produced is the 2.6 year Na^{22}. Preliminary measurements show the cross section for the $Na^{23}(d,dn)Na^{22}$ reaction is ~80 mb at 190 Mev and ~ 120 mb at 100 Mev.

In the case of a water coolant one of the important activities is the 53 day Be^{7}. The cross section for the $O^{16}(d;2\alpha,2p,n)Be^{7}$ reaction has been measured as 9 mb at 190 Mev.

Diffusion and Corrosion Introduced Activities

L. M. Lits and S. A. Ring
CRDC

Estimation of the activity diffusing into NaK, based on theoretical considerations, indicates this source of activity will be several orders of magnitude lower than that from recoils and directly produced activities in a NaK cooled bare thorium target. However, the introduction of activity into the coolant by corrosion of the target elements and structural material may be very important for both NaK and water cooling.

A shielded manipulator box to be used in studying diffusion and corrosion is almost completed and experimental results should be available soon.

2?6 103
DECLASSIFIED

Instrumentation

G. D. O'Kelley
CRDC

During the past quarter it became increasingly evident that a gamma ray spectrometer of high counting efficiency was needed. Such an instrument would permit assaying the Pa^{233} content of Pa^{231}-Pa^{233} mixtures, and would be valuable for measurement on the (n,2n) products of uranium and thorium where beta-particle counting is not practical because of the low specific activity of the samples which must be used. With these ends in view, a gamma-ray scintillation spectrometer was constructed, using as the detector a 1 inch diameter, 1 inch long NaI · TlI crystal.

Although no attempt was made to obtain optimum resolution, the results on the present apparatus have been quite acceptable for general use. The "peak to valley" ratio for annihilation radiation (0.511 Mev) and the Cs^{137} gamma-ray (0.661 Mev) is about 6, and the pulse height vs. energy relation is linear within the resolution of the apparatus from zero to about 2.8 Mev. The instrument is now in routine operation.

276 194

DECLASSIFIED

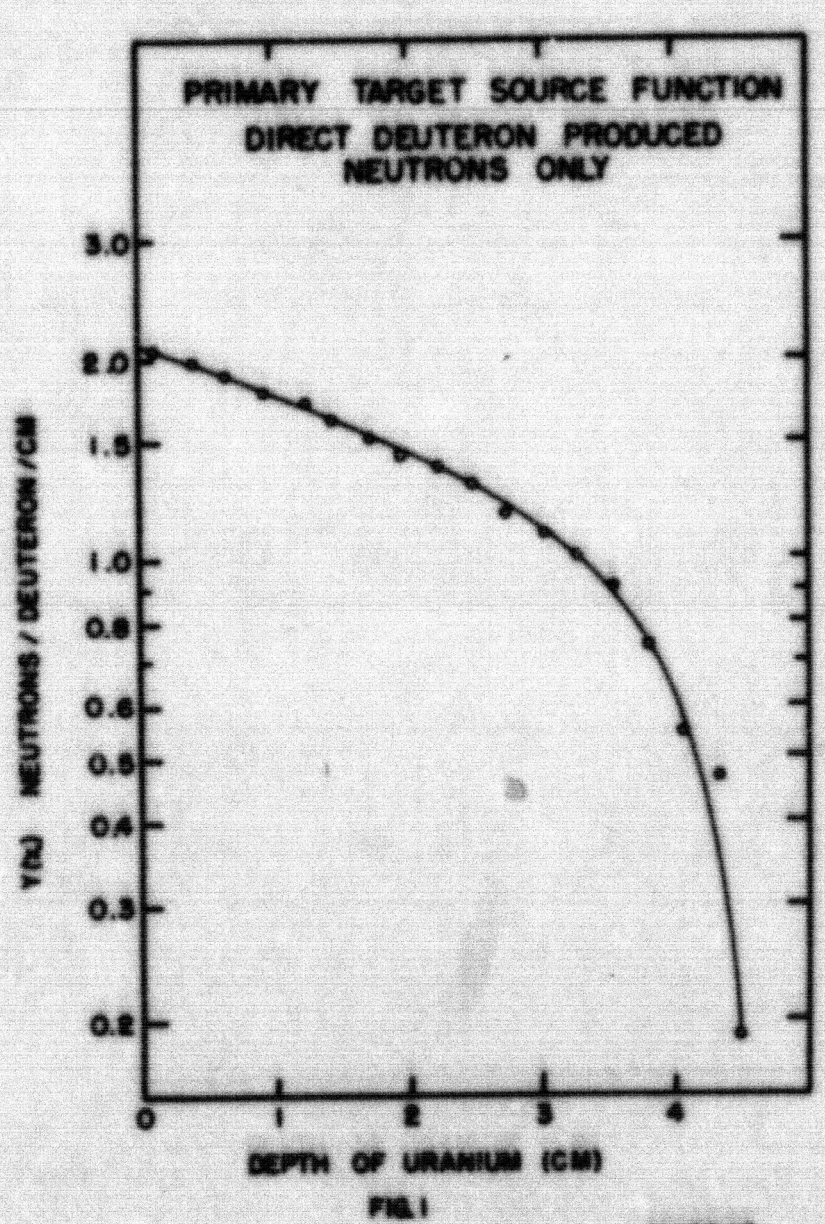

FIG. I

MU3242

270 105

DECLASSIFIED

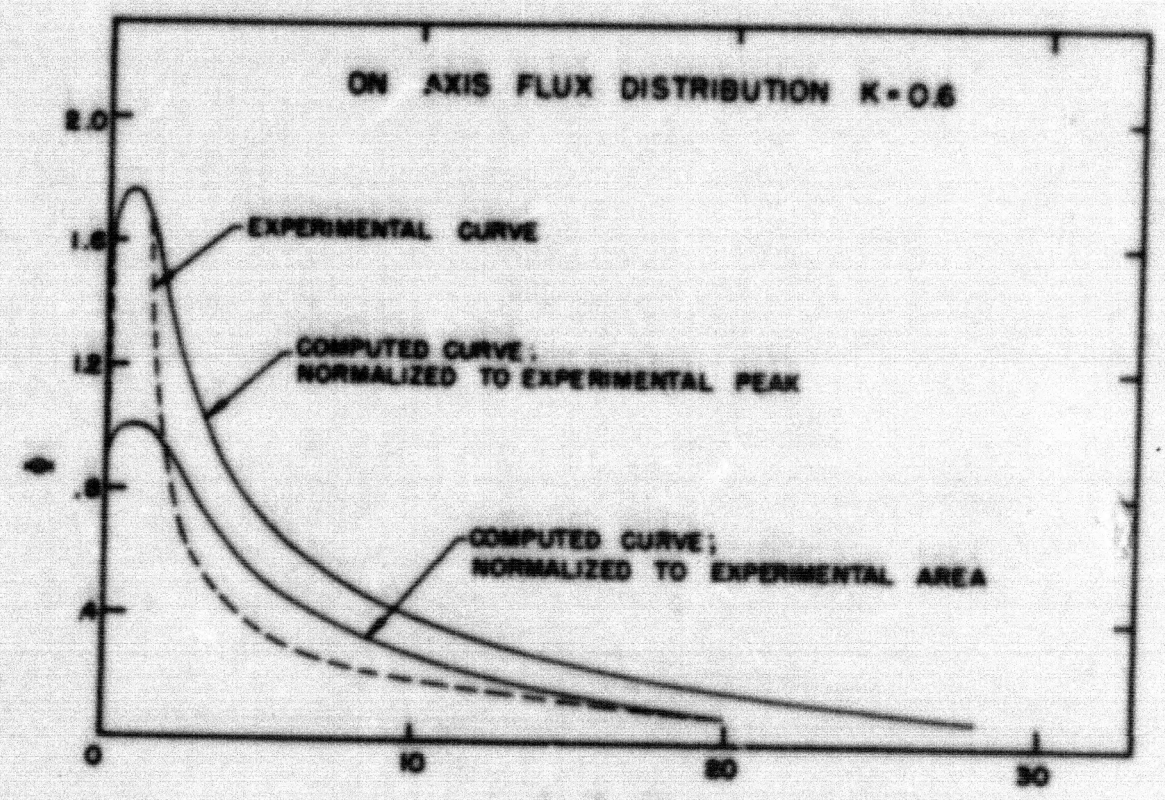

FIG. 3

MU 3244

276 106

DECLASSIFIED

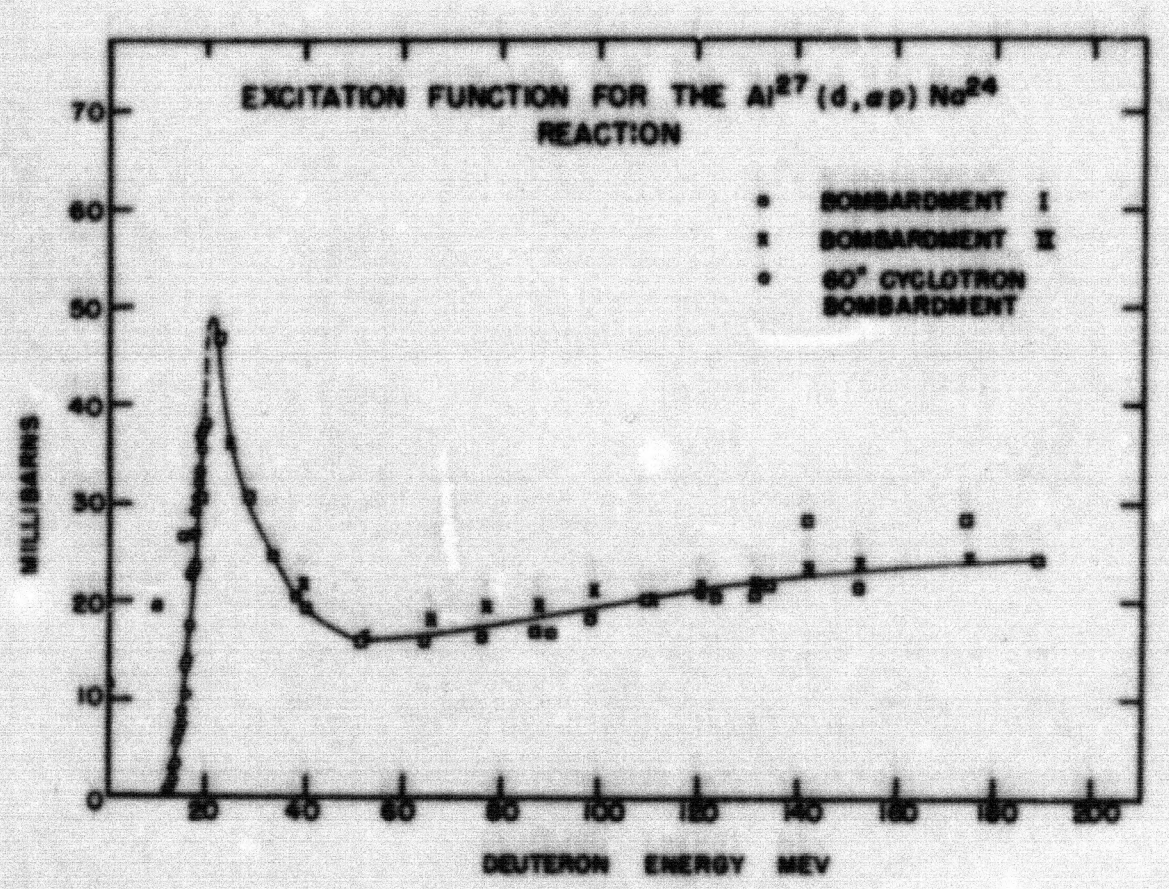

FIG. 4 MU 3245

DECLASSIFIED

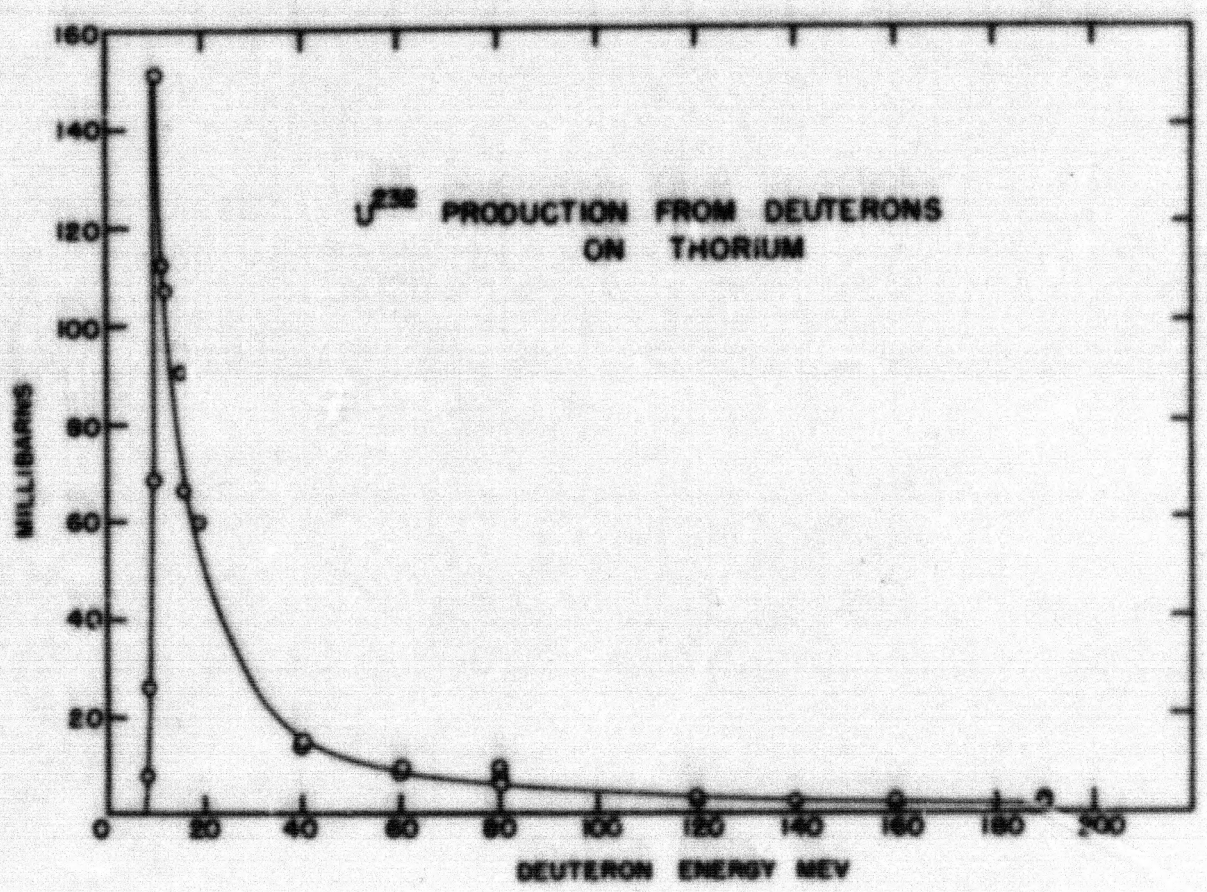

FIG. 5

UCRL 3246

DECLASSIFIED

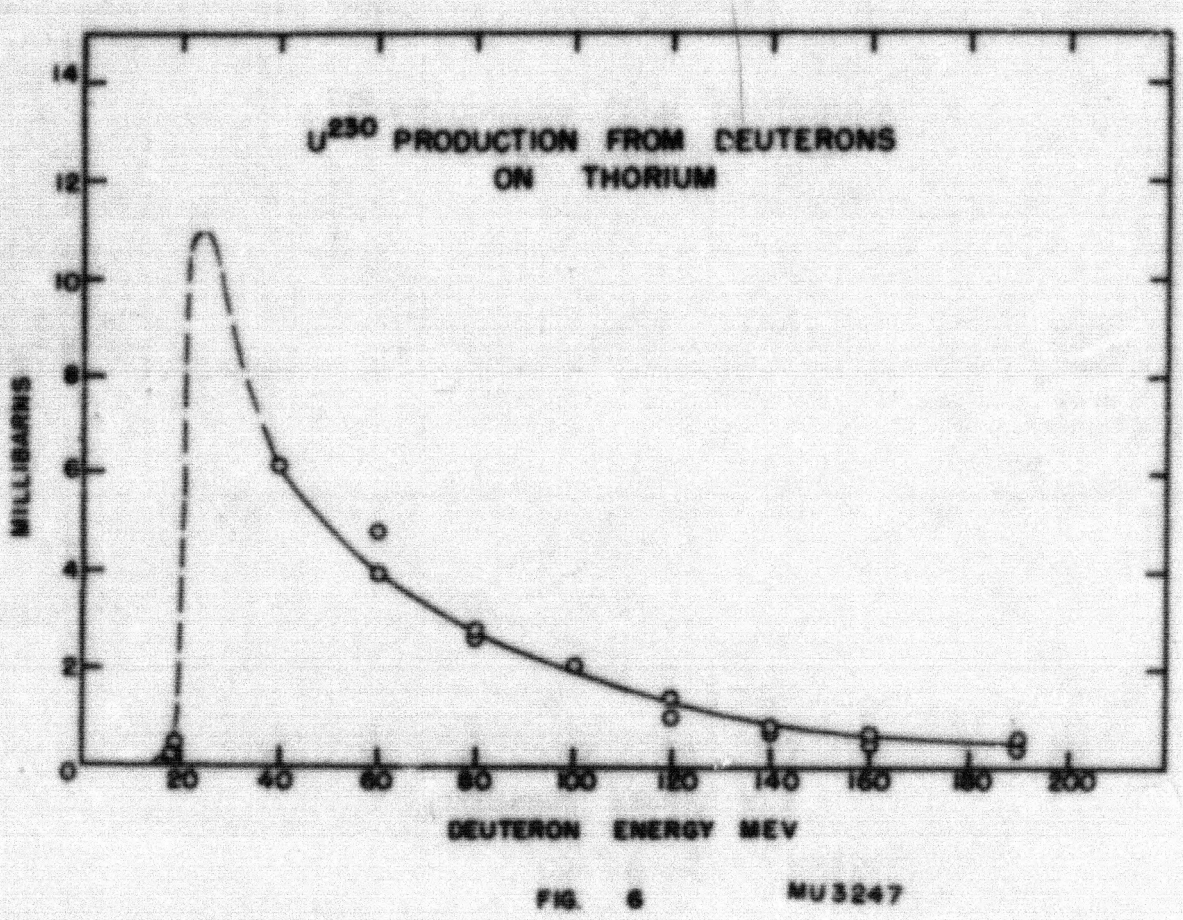

FIG. 6 MU3247

DECLASSIFIED

14. MTA CHEMICAL PROCESSING

Process Research

T. E. Hicks, W. H. McVey, F. C. Dietz, S. J. Horn, A. Ottenberg,
F. J. Brutschy, R. H. Gercke and K. L. Mattern
CRDC

D. Heisig
UCRL

Stability of Ferrous Iron and Pu(IV) in Uranyl Nitrate Solution

Both the Purex process (tributyl phosphate extraction system) and the TTA process (thenoyltrifluoroacetone chelate extraction system) require plutonium in the plus four oxidation state for optimum extraction and decontamination of plutonium. At present, both processes involve the addition of ferrous sulfamate to reduce the plutonium to the plus three state followed by a nitrous acid oxidation of plutonium to the plus four state.

Current investigations show that whereas ferrous iron is stabilized for long periods of time by the presence of sulfamic acid, it is stable for a sufficiently long period of time without sulfamic acid to effect quantitive reduction of any Pu(VI) which may be present. The oxidation of ferrous iron by nitric oxide or nitrous acid has been found to be auto-catalytic with a very rapid oxidation following a reasonably long induction period. Hence, the ferrous iron will be at nearly full reducing strength up to the moment of its disappearance. Initial measurements indicate that the induction period is proportional to the square of the ferrous concentration, inversely proportional to the hydrogen ion concentration, and inversely proportional to the third power of the nitrate ion concentration. Table I gives an indication of the time of the induction period.

Table I

Fe^{++} (M)	H^{+} (M)	UO_2^{++} (M)	NO_3^{-} (M)*	Induction Time (Min)
0.0755	0.000	1.74	3.48	80
0.0755	0.156	1.74	3.79	10
0.0755	0.234	1.74	3.79	6
0.0755	0.312	1.74	3.79	4.5
0.0755	0.624	1.74	4.10	1
0.0755	0.780	1.74	4.26	2
0.0755	0.936	1.74	4.42	1

* $LiNO_3$ added in some experiments

UNCLASSIFIED

Any Pu(III) produced is oxidized by the nitrous acid normally present.

It is know that plutonium can be produced quantitively in the plus four state from any combination of oxidation states simply by the addition of dilute ferrous iron, preferably ferrous perchlorate in the laboratory. Whether this may be true in large scale process equipment must be verified.

Complexing of Plutonium with Trichloroacetic Acid

None of the anions of the common acids are completely satisfactory in the solvent extraction of plutonium, due to the plutonium complex ions found in the aqueous phase. Therefore a study of trichloroacetic acid was initiated, and its complexing of plutonium(IV) was measured. K_1 for the following reaction was found to be 5.7,

$$Pu(IV) + HA \overset{K_1}{=} PuA^{+3} + H^+$$

using the value $K_2 = 0.2$ for the reaction

$$HA \overset{K_2}{=} H^+ + A^-$$

where HA represents trichloroacetic acid.

Plutonium Chelates

A new chelating agent was tried with plutonium(IV)--4,4,5,5,5,6,6,6, heptafluoro - 1(3,4) ortho-dichlorophenyl-hexane 1,3 dione (DII) a homologue of TTA. The constant for the reaction

$$Pu(IV)_{aq} + 4\ HK_{org} \overset{K}{=} Pu\ K_{4\ org} + H^+_{aq}$$

was found to be 1.5×10^6 when using ortho-dichlorobenzene as a solvent. This is almost the same value found when TTA is used. The solubility of Pu(DII) in ortho-dichlorobenzene is 0.02 M; however, solutions of greater than 0.1 M were obtained readily which gave no precipitation on standing overnight. This may be compared with the solubility of $Pu(TTA)_4$ in ortho-dichlorobenzene of 0.008 M. This work was designed to explore the possibilities of improved chelating agents to supplant TTA in the chelate process for plutonium recovery.

Zirconium Extraction with TTA

The extraction of zirconium from 2 M UNH solutions with TTA was measured as a function of added acid. In the range of 0.1 M to 0.7 M added nitric acid, the ratio Zr_{org}/Zr_{aq} showed an inverse 2.5 power dependence on the added acid.

DECLASSIFIED

Process Development

T. E. Hicks, W. H. McVey, B. Rubin, L. M. Guenther,
R. W. Robinson, J. Jost, Jr. and A. L. Lindsay, Jr.
CRDC

Plutonium Recovery

Since the limiting fission product activity in the decontamination of plutonium from Hanford dissolver solution by the use of TTA in o-dichlorobenzene is the niobium-95 which grows from zirconium-95 during the zirconium's transit time in the re-extraction column, it was decided to remove zirconium-95 before extracting plutonium. In this way there would be no zirconium in the re-extraction column, and therefore no niobium. The flow scheme shown in Figure 1 has been tested using mixer-settlers with the flow rates and solution compositions of Table II.

Table II

Stream	Flow Rate (ml/min)	Composition
ZF	25	2.15 M UNH, 0.025 M H^+ (Pu, F.P.s)
ZX	10	0.283 M TTA in o-dichlorobenzene
ZS	5	Recycle from IW
ZW	10	ZX plus Zr
IF	29	1.85 M UNH, 0.27 M H^+ (Pu, F.P.s)
IX	15	0.100 M TTA in o-dichlorobenzene
IS	4	1.80 M H^+, 1.00×10^{-4} M $K_2Cr_2O_7$
IW	25	1.85 M UNH, 0.27 M H^+, (F.P.s)(No Pu)
IIF	15	0.100 M TTA in o-dichlorobenzene (Pu)
IIX	5	3.00 M H^+, 1.98×10^{-4} M $K_2Cr_2O_7$
IIW	15	Recycled to IX
IIP	5	3.00 M H^+, 1.98×10^{-4} M $K_2Cr_2O_7$ (Pu)

The composition used for the ZF stream serves reasonably well as a synthetic Hanford dissolver solution since zirconium extracts better than plutonium, while niobium is poorer. Thus, there are two elements which bracket plutonium in this system and a demonstration of a plutonium cut can be shown. Detailed data from this run will be reported later.

DECLASSIFIED

Since the TTA-o-dichlorobenzene is stripped clean, it is recycled in this scheme. Any industrial installation would, of course, have a TTA clean-up inserted in the recycle.

The I column must be split as o-dichlorobenzene is lighter than the IF stream but heavier than the IS stream.

The purpose of feeding an IW cut to the Z column is to scrub plutonium from the ZW stream. As the IW stream contains no plutonium, it is quite satisfactory for this purpose and it is also heavier than the ZX stream, eliminating the problem of density inversion found in the I column.

The IS stream from the top half of the I column is fed back to the Z column to insure the proper H^+ concentration for zirconium extraction.

U-233 Recovery from Synthetic Neutron Irradiated Thorium

A synthetic "23" solution was contacted in a batch counter-current contactor according to the flow scheme of Fig. 2. The compositions of the streams are shown in Table III.

Table III

Stream	Unit Volume per Unit Time	Composition
IF	1	1.25 M TNT, 0.0025 M UNH, 0.0 M H^+
IX	1.8	5 percent TBP/CCl_4
IS	0.2	1.6 M HNO_3
IW	1.2	1.04 M TNT, ~ 5×10^{-6} M UNH
IIS	0.2	H_2O
IIW	1.8	5 percent TBP/CCl_4
IIP	0.2	0.0125 M UNH, ~ 4×10^{-4} M TNT

This represents a recovery of 99.98 percent of the uranium with a purity of 97 percent; the 3 percent impurity being thorium.

Thorium Recovery

Both counter-current batch and pulse column runs have been tested on thorium nitrate, TNT, solutions using 60 percent TBP by volume in CCl_4. End feed column runs indicate that 99 percent TNT recovery can be achieved with no difficulty. No information on the decontamination of TNT under these conditions is available at present.

Miniature Mixer-Settler

The glove box and shield, power supply and control box, and the

DECLASSIFIED

miniature mixer-settler bank itself have been completed. The entire unit will be complete when the pumps are finished. They are at present being assembled.

Fission Product Contaminants (P. L. Auer, CRDC at ANL)

An investigation has been started of fission product contaminants from A-12 targets which might be potential trouble makers in a Purex-type process. Studies of the behavior of radio-tin from the Clinton pile have been made in a TBP, CCl_4 aqueous system but no definite conclusions are available at present.

Purex Program (R. A. Lewis, CRDC at ORNL)

Studies have continued at Oak Ridge to develop the Purex process for uranium, plutonium and fission product processing which apply to uranium loaded A-12 lattice.

Hydroxylamine sulfate is proposed as a reductant in the IB column of the Purex process instead of ferrous sulfamate to eliminate iron from the waste streams. This should permit a greater reduction of the waste volume. Reduction of the volume to the second plutonium cycle is also proposed and a volume reduction factor of 25 is expected over the two cycles. The addition of ion exchange after the second cycle is expected to give another volume reduction factor of 15, bringing the over-all reduction factor from dissolver feed to resin bed eluate of 375. The ion exchange column also permits final removal of uranium from the plutonium.

Pulse Column Studies (R. A. Lewis, CRDC at ORNL)

The use of pulse columns as contactors in the Purex system has continued with some progress. Approach to square wave operation will net a relative reduction in the IA column uranium loss by roughly a factor of six compared with operation with harmonic pulse wave operation; however, flooding occurs at a lower frequency.

A free area in the plates of the IB pulse column scrub section has been changed from 23 percent free area in an attempt to make the scrub section diameter the same as the extraction section diameter. Five percent, 10 percent and 15 percent free area plates were tried with the 15 percent free area plates giving the best results. A combination of square pulse wave and the scrub section 15 percent free area plates resulted in one-tenth the uranium losses to the TBP that occur with 23 percent free area plates and harmonic pulse.

Process Design

L. R. Michels, H. Schneider, D. L. Fry, J. Unverferth,
M. L. Feldman and K. G. Steyer
CRDC

The major effort of the group has been devoted to intitiating process designs on a thorium separation plant.

Thorium Processing

To guide research and development programs, economic studies are

DECLASSIFIED

being made of the cost of recovering thorium from irradiated fuel and the cost of purchased virgin thorium make-up for comparison. The economics of various methods of processing Pu^{233} and U^{233} are also under investigation to enable a decision as to whether it is preferable to separate Pu^{233} during processing or allow it to decay, allowing for increased lag storage capacity.

Preliminary calculations were completed on the distillation separation of the Thorex solvent for recycle of the tributyl phosphate and kerosene components.

Plutonium Processing

A schematic drawing was started on equipment necessary for the Purex process plus necessary feed solution preparation, product and solvent purification equipment.

Pilot Plant

Preliminary process design studies were completed on a concentration and packaging installation for high level beta-gamma wastes from the Livermore pilot plant. The use of 15 ton concrete blocks, each encasing 40 gallons of waste, is envisioned.

Design continues on specific equipment and facilities for the pilot plant proper.

Hazard Report

The report defining hazards to the public associated with operation of A-12 chemical separations processes has been completed.

General

Messrs. M. Feldman and K. Steyer have reported to the Chemical Technology Division of the Oak Ridge National Laboratory where they have been assigned to the Unit Operations and Arco Process design groups, respectively.

270 115

DECLASSIFIED

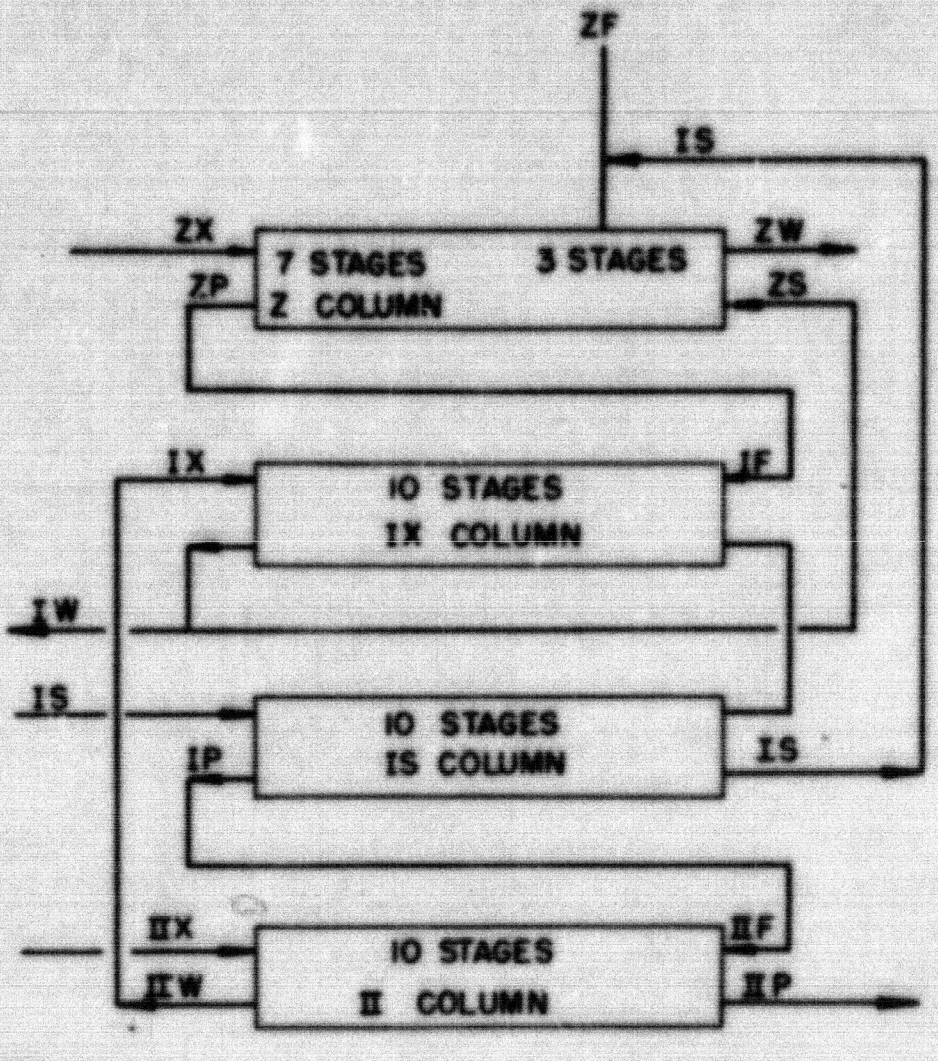

FIG. 1

MU 3240

27C 116

DECLASSIFIED

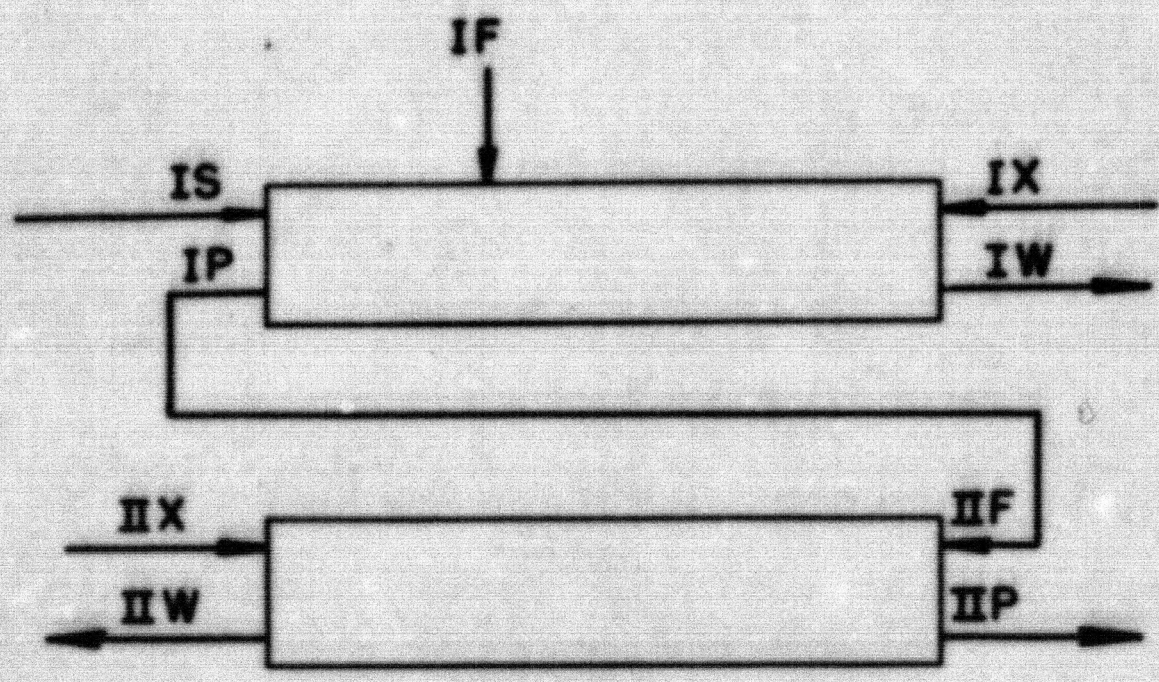

FIG. 2

MU 3241

2TC 117

DECLASSIFIED

15. THEORETICAL STUDIES

David L. Judd
UCRL

Cloverleaf Cyclotron

The major theoretical efforts in connection with this program during the period of this report have been outgrowths of the graphical orbit plotting work of the magnet design group. Briefly, the order of events was as follows: (1) The magnetic group found that an empirical modification of the most obvious step-to-step plotting method was needed to correctly reproduce the calculated orbits supplied by the fourth-order perturbation theory. (2) A theoretical analysis of the plotting method problem showed that this modification should not yield correct orbits. (3) The fourth order orbit equations were reviewed and found to contain errors, resulting from lack of higher order terms, large enough to explain the discrepancy. To remove these, rather lengthly calculations of fifth and sixth order terms were made, and small empirical corrections representing the effects of even higher order terms were inserted in the orbit equations. (4) The resulting orbits now appear to be reproduced empirically, within the field-plotting and orbit-plotting errors, by the unmodified and theoretically correct plotting method. (5) To carry out the orbit theory to higher orders in a consistent way, additional small terms in the magnetic field were found necessary. The effects of these terms on axial and radial stability of the orbits were calculated, using the differential analyzer methods developed earlier for this purpose. It was found to be even more difficult than before to maintain axial stability at large radii while avoiding a radial resonance effect until the design energy of 300 Mev is reached. A decision was made to proceed on the new electron model magnetic shims using a set of magnetic parameters which preserves axial stability but allows the radial resonance effect to occur at a velocity corresponding to a deuteron energy of the order of 275 Mev, in order to be able to study the nature and seriousness of this resonance effect empirically on a model scale.

The importance of this resonance effect can be estimated theoretically only by solving a non-linear differential equation with periodic coefficients. This is so because the linearized equations for small radial oscillations predict exponential growth of the oscillation amplitude in the resonance region, characteristic of unstable Mathieu equation solutions; if non-linear effects are strong, this growth will be quickly checked, and vice versa. As no theory of such non-linear equations exists, recourse must be had to simplifying approximations or to numerical solutions. Programs involving both methods are now under way.

A report is to be issued summarizing the theoretical and empirical work on orbit plotting methods.

During the period of this report a topic of interest has been the study of various rf accelerating systems. While the bulk of this work is being carried on by mechanical and electrical engineering groups, some theoretical estimates of axial stability and other aspects of specific proposals

DECLASSIFIED

been made. This work is still in progress.

Other Theoretical Work

A considerable portion of the group's computing facilities continue to be devoted to target studies, which are being reported elsewhere. In addition, design studies on the Mark II linear accelerator are being carried on in collaboration with CRDC personnel; this work is summarized from time to time in their reports.

DECLASSIFIED

16. ELECTRON MODEL THOMAS CYCLOTRON

Elmer Kelly
UCRL

Improvement of Equipment and Apparatus.

The trimming coil current controls have been replaced by a new arrangement that gives direct and independent adjustment of the sum and difference currents supplied to each pair of coils. Thus for a pair of orbit coils one knob varies the sum of the two currents and hence the resonance condition while another varies the difference of the currents and hence the median plane condition. These controls are mounted in a cabinet on wheels that can be rolled up to the tank enabling the operator to adjust coil conditions while watching the effect on the beam. Also the current for these coils is now supplied by two Kobatrons which seem just as steady as the old storage battery supply and much more convenient.

A portable manual phase control has been added to the rf supply so the operator can now adjust phase, main magnetic field, and trimming coils while seated at a tank window.

The rf phase servo system (for details see UCRL-1484) has been considerably improved. The 180° injector source was brought into operation but beam definition was disappointing and this source has been discarded. A satisfactory source has been developed by replacing the electron emitter of our standard source (see Fig. 2 of the previous Quarterly, Report, UCRL-1573) with a snouted synchrotron source emitter. This source works very well between 2 in. and 3 in. radii where it is usually operated.

"Bump" coils having a radial extent of 2 in. and an azimuthal extent of 30° were installed, centered along the hill lines, consisting of 4 pairs in all. Each pair, one upper and one lower, was connected in series and supplied through its own control circuit. It was hoped that these coils could provide a greatly improved magnetic field by empirical correction of the magnetic bumps that had unintentionally been built into the present poles.

Design and shop work on the new electron model (300 Mev deuteron equivalent) has been going ahead as fast as pole contour design data have permitted. The earliest date at which it can be ready for operation now appears to be May 1, although this could be improved some if a higher priority should be assigned to the project.

Beam Studies at Large Radii

A radial run using a current probe covered with three layers of foil leaf (0.45 mg/cm^2) indicated the beam current was essentially constant from 8 in. to 15 in. However, the amount of beam current at 15 in. was about twice as much as that measured with a similar probe covered with 1/2 mil Al foil (3.5 mg/cm^2). To test whether this might be the result of a

DECLASSIFIED

multi-energy beam, the three hill probes were used simultaneously. It was found that the beam measured on the current probe was well centered and cut off sharply when the probe at any hill was pushed in slightly. This was true for either the leaf covered probe or the 1/2 mil foil covered probe. In addition, the ratio of circulating beam at 15 in. or 16 in. on a hill to the spill beam was the same for either of these two probes. Thus one can feel fairly confident that the beam has the proper energy. The observed current differences probably arise from the difference in transmission of the two absorbers used. An attempt was made to measurethe transmission of these probes directly by use of a high voltage d.c. source of electrons. It was soon evident that the accuracy we wanted would require more time and equipment than the answer was worth and the work was stopped.

Beam Studies at Small Radii

The snouted source used in conjunction with the two radial flag slippers to define the axial extent of the first two or more beam turns made it possible to see individual turns of the beam and hence to study the actual beam path quite accurately. It was found that with the source at the 3 in. radius on the 0° hill, the beam could be brought out to 8-1/2 in. on the 120° hill and it then blew up radially. See Fig. 1. Using the three hill probes it was found that the beam was well centered out to 5-1/2 in.; then successive turns (7th through 14th) on the 240° hill fell one on top of the other while on the other hills the turns increased steadily in radius. Thus the orbit center began to move at the 7th or 8th turn until at the 14th turn it was 1-1/2 in. off the magnet center causing the beam to become radially unstable. The same effect occurred if the source was at 240° and 3 in. Graphical orbit plotting showed that a reasonable localized magnetic bump in the field produced just such an effect. Iron added to the poles externally at 5 in. radius and 60° azimuth was found largely to alleviate this difficulty. The bump coils could also be used to improve the beam pattern but were no better than the external iron and were considerably less convenient. The best external iron shim found was a 2-1/2 in. x 2-1/2 in. x 12 in. piece at 5-1/2 in. and 50° on the top pole only. This is now a fixed addition to the machine.

In a check of beam pattern sensitivity to dee alignment it was found that the dee alignment was not at all critical. A 1/2 in. extension to the radial edge of one side of one dee either on the top surface or on the bottom surface produced no appreciable change in the beam or in the operating conditions.

Further examination of the beam pattern showed the frequency of axial oscillation between 4 in. and 6 in. to be 1/6 or 1/7 that of the rotational frequency. See Fig. 1. By adjusting the flag clippers the amplitude of axial oscillation could be increased or decreased, indicating a particle oscillation and not a median place motion. Also by changing the rf dee voltage the radial extent of an axial oscillation could be varied but the number of electron beam turns remained the same, indicating the restoring force was magnetic and not electrostatic. Taking into account the trimming coil adjustments used, this observed value of ν_z is quite consistent with the theoretical value calculated by Judd.

276 121

DECLASSIFIED

Improved Performance

The overall performance achieved has been very gratifying. Using the sharply defined source mentioned above it has been possible to get a spill beam with no loss to the top or bottom of dees or ground sheets. In addition, the beam turns were separate and distinct out to 8 in. or more. See Fig. 2. This could be accomplished with a peak rf dee voltage anywhere between 500 volts and 60 volts.

The 60 volts represents a new low in threshold dee voltage indicating the beam made at least 350 turns in getting out. The 60 volts threshold corresponds to a gain per turn of 650 kv on the full scale deuteron machine.

It should be noted that all of the operation described in this report was done with three 60° solid dees operating at 3 phase and 60 megacycles.

270 122

DECLASSIFIED

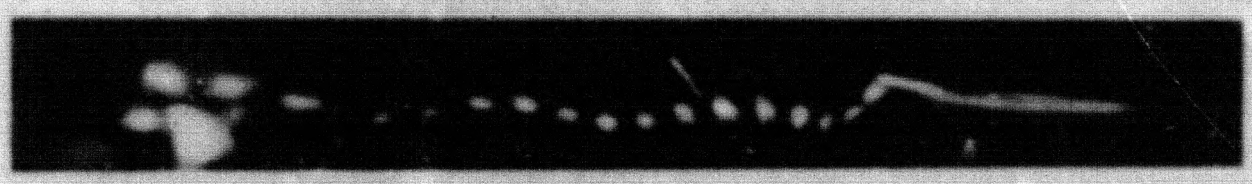

FIG 1

RADIAL BEAM PATTERN

ZN 206

DECLASSIFIED

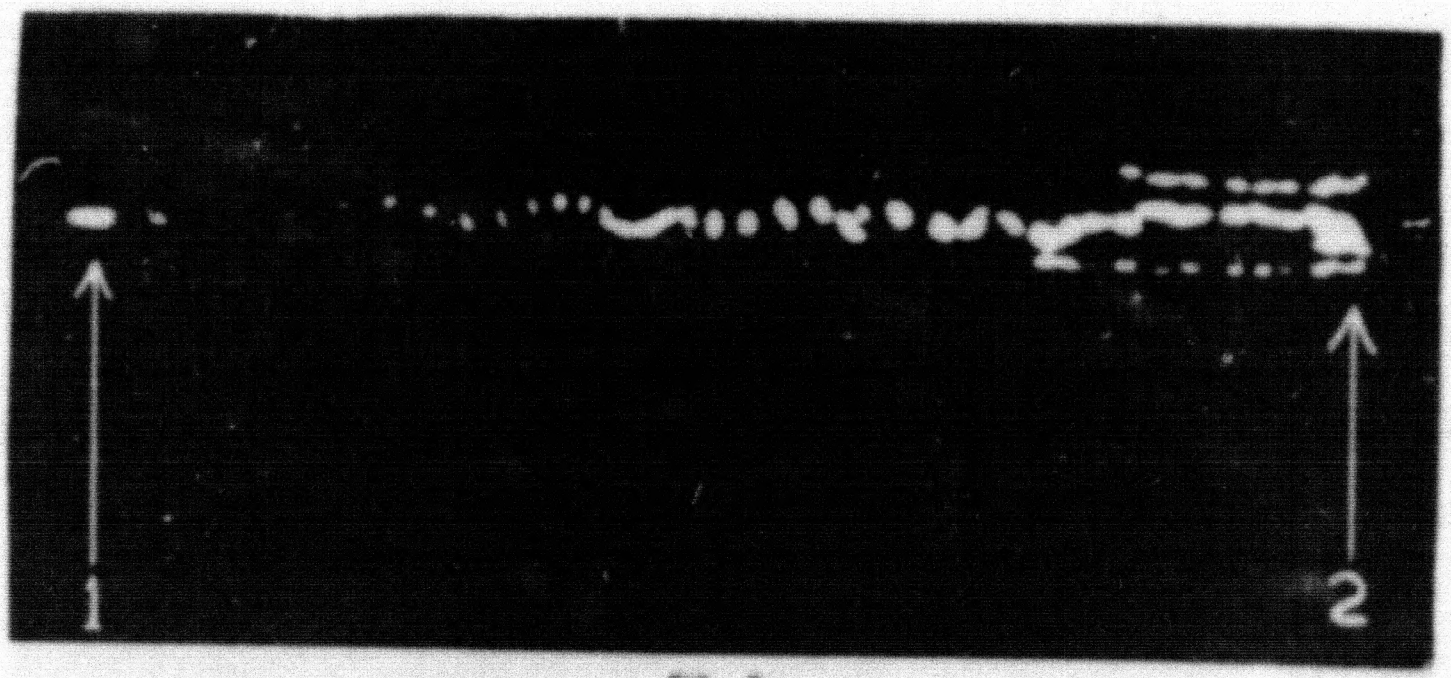

FIG. 2

RADIAL BEAM PATTERN

ARROW NO. 1 INDICATES THE FIRST TURN AT A 3" RADIUS
ARROW NO. 2 INDICATES THE EDGE OF THE PALE
THE SPILLBEAM IS CAUGHT ON A CURRENT PROBE, AND SO IS NOT VISIBLE.

ZN205

17. 20-INCH CYCLOTRON PROJECT

M. Heusinkveld, M. J. Jakobson and L. Ruby
UCRL

In this quarter the dee phase servo system was developed to the point where sustained experiments with the beam could be done. The beam was worked up to better than 2 mils at the full radius, corresponding to 1 Mev protons. Various source geometries were tried, and the radial distribution of the beam was measured. Some experiments were attempted with acceleration at triple the resonant frequency but these were inconclusive.

During the period of this report, several changes in the rf system were made. In each of the final amplifier stages, a 10 KW RCA A-2505 tetrode was installed to replace the 20 Kw Eimac 20,000A tube previously used. Only one tube failure has since occurred, a grid-cathode short of uncertain origin. However, some additional protective equipment was also added.

With the development of the phase servo system, it has been possible to cut back the rims which were mounted around each dee to decrease the inter-dee coupling. The tips of the dees, which are tilted slightly toward the median plane, are now entirely exposed. It has also been possible to extend the tips to within 1/2 inch of center without excessive additional coupling. (See Fig. 1.) New 20kv variable capacitors have been added to the dee stem. These have increased range, 100 micromicrofarads, and a five speed coupling to the servo motors to obtain variable time constant of response. A controllable electronic delay has been added to replace the delay lines between the oscillator and the amplifiers. There are now five servos; the CA and BA dee stem phase servos which correct the C and A stem capacitors, the A plate-grid amplifier efficiency servo which corrects the A stem capacitor, and the CA and BA amplifier grid phase servos which correct the electronic delay. The system is described in detail in UCRL-1484. This three phase servo system now operated very satisfactorily.

The radial distribution of the beam in the three-phase positive sequence mode with hydrogen is typified by the following table:

Hydrogen Ion Beam with 23-1/2 KV Peak RF Voltage

Beam Current	Probe Radius
23.5 mils	1 inch
15	2
9.0	3
5.0	4
3.4	5
2.1	6
1.8	7
1.6	8
1.3	8-1/2

The beam is seen to fall-off rapidly out to about four inches where the fall-

UNCLASSIFIED 276 125

off becomes much more gradual. We have obtained over two mils at eight and a half inches with and open arc source and 30 kv peak dee voltage. Magnetic cones were added which increased the median plane magnetic field at the center by four percent. These did not produce any significant change in the beam versus radius distribution.

Protons may be accelerated in other modes by simultaneously doubling or tripling the phase differences between dees and the rf frequency. To investigate the latter "3 omega" mode, all three dees were tied together at the center and the magnetic field dropped to one third value. The source was set at two inches radius facing a feeler on one of the dees. A beam tuned in to the extent of about a mil at seven inches radius. Since the gain per turn in this mode is increased by two, whereas the energy at a given radius is decreased by nine, the total number of turns is decreased by a factor of eighteen, or to two turns at the full radius. Because of this limitation it was concluded that definitive experiments could not be performed in this mode of operation.

In the three phase "1 omega" mode, several source geometries were tried with the source at the center of the machine. These included an open arc, a ring shaped arc surrounding a grounded post, a hooded arc with three slits, and the latter with three accelerator slits one sixteenth of an inch away with up to two kv d.c. voltage. The open arc source proved most successful although after several modifications the accelerator system is nearly as good. The open arc is usually run at about two amperes arc current with a 3/32 inch arc aperture.

The three dee cyclotron has several interesting properties which affect the beam fall-off with radius. Among these are the fact that if only the positive or negative sequence rf mode is present, ions of the same magnitude of e/m but of opposite sign will not be accelerated simultaneously. Also, for the proton resonant magnetic field and frequency, other ions may be accelerated merely by changing the rf phase sequence. A separate report on these characteristics is now being prepared. Since other sequences are never entirely eliminated, some multiple beam acceleration is always possible. In any case, for a fraction of a turn, any ion might be expected to gain energy. Another effect which is large at the center is phase selection. In addition, beam can be lost by electrostatic and space charge de-focusing. A calculation of the latter effect at large radii where the magnetic focusing can be estimated indicates the space charge and magnetic restoring forces to be of the same order of magnitude. It is not known to what extent the space charge is neutralized.

276 126

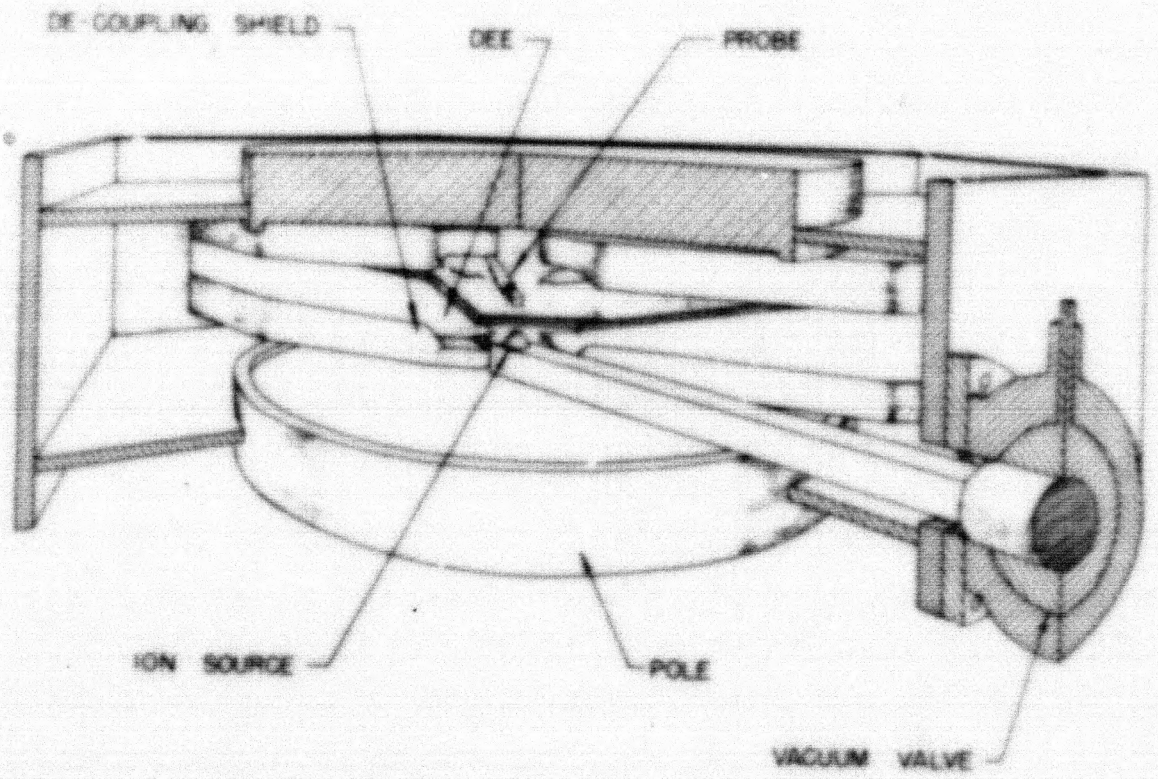

THREE "DEE", TWENTY INCH CYCLOTRON

DECLASSIFIED

END